ASSESSMENT OF ANTIMONY AS A PRIORITY POLLUTANT AND EXPLORATION OF ANTIMONY REMOVAL FROM AQUATIC ENVIRONMENT

A THESIS SUBMITTED TO
THE GRADUATE SCHOOL OF NATURAL AND APPLIED SCIENCES
OF
MIDDLE EAST TECHNICAL UNIVERSITY

BY

ÖZGE YÜCEL

IN PARTIAL FULFILLMENT OF THE REQUIREMENTS
FOR
THE DEGREE OF MASTER OF SCIENCE
IN
ENVIRONMENTAL ENGINEERING

SEPTEMBER 2017

Approval of the Thesis:

ASSESSMENT OF ANTIMONY AS A PRIORITY POLLUTANT AND EXPLORATION OF ANTIMONY REMOVAL FROM AQUATIC ENVIRONMENT

submitted by **ÖZGE YÜCEL** in partial fulfillment of the requirements for the degree of **Master of Science in Environmental Engineering Department, Middle East Technical University** by**,**

Prof. Dr. Gülbin Dural Ünver _____
Dean, Graduate School of **Natural and Applied Sciences**

Prof. Dr. Kahraman Ünlü _____
Head of Department, **Environmental Engineering**

Assist. Prof. Dr. Derya Dursun Balcı _____
Supervisor, **Environmental Engineering Dept., METU**

Examining Committee Members:

Prof. Dr. Ülkü Yetiş _____
Environmental Engineering Dept., METU

Assist. Prof. Dr. Derya Dursun Balcı _____
Environmental Engineering Dept., METU

Prof. Dr. İpek İmamoğlu _____
Environmental Engineering Dept., METU

Assoc. Prof. Dr. Tuba Hande Bayramoğlu _____
Environmental Engineering Dept., METU

Assoc. Prof. Dr. Niğmet Uzal
Civil Engineering Dept., AGÜ _____

Date: September 7, 2017

I hereby declare that all information in this document has been obtained and presented in accordance with academic rules and ethical conduct. I also declare that, as required by these rules and conduct, I have fully cited and referenced all material and results that are not original to this work.

Name, Last name: Özge Yücel

Signature:

ABSTRACT

ASSESSMENT OF ANTIMONY AS A PRIORITY POLLUTANT AND EXPLORATION OF ANTIMONY REMOVAL FROM AQUATIC ENVIRONMENT

Yücel, Özge

M.S., Department of Environmental Engineering

Supervisor: Assist. Prof. Dr. Derya Dursun Balcı

September 2017, 130 pages

Antimony is a metalloid element that has adverse health and environment effects at high concentrations. In this study, the antimony mining site located in the Yeşilırmak River Basin is considered as a point source and removal of antimony from aquatic environment was explored. Results indicated that surface waters in the downstream of antimony reserve are susceptible to antimony pollution. Samples collected near vicinity of the antimony mining site have exceeded Environmental Quality Standards (EQS) of antimony more than 200 times. The most effective treatment methods for antimony in aqueous environment were explored and most effective processes were identified as adsorption, membrane processes and coagulation/flocculation. In this study, natural zeolites were utilized to remove antimony ions by adsorption. Clinoptilolite originated from Gördes, Manisa deposit was investigated in its natural form for its effectiveness in removing antimony from aqueous solutions. Throughout this work, equilibrium and kinetic studies were performed with zeolite that has approximately 40 m^2/g surface area. The results of equilibrium studies revealed that zeolite adsorption capacity for Sb ions increases as pH of the sample decreases. Maximum capacities attained were 2.02 mg/g for 50 mg/L initial Sb concentration. At lower initial Sb concentrations, adsorption capacities observed for zeolite was found significantly lower. For the optimum conditions, the highest removal efficiency for

antimony removal achieved as 85 % by zeolite adsorption. Due to low adsorption capacity of zeolite, membrane processes were also investigated. With nanofiltration (NF270 membrane), removal efficiency was higher than 80 %, and it was possible to reach 99 % removal with Reverse Osmosis (SW30 membrane). Moreover, as an alternative method, coagulation/flocculation processes were studied with two common conventional coagulants, ferric chloride and aluminum sulfate. It was seen that 99% removal was achieved via conventional coagulation and flocculation process with ferric chloride. On the other hand, only 44% removal was achieved with aluminum sulfate.

Keywords: antimony, river basin, removal, zeolite, adsorption,

ÖZ

ANTİMONUN ÖNCELİKLİ KİRLETİCİ OLARAK DEĞERLENDİRİLMESİ VE SUCUL ORTAMDAN ANTİMON GİDERİMİNİN İNCELENMESİ

Yücel, Özge
Yüksek Lisans, Çevre Mühendisliği Bölümü
Tez Danışmanı: Yrd. Doç. Dr. Derya Dursun Balcı

Eylül 2017, 130 sayfa

Antimon yüksek konsantrasyonlarda insan ve çevre sağlığına karşı olumsuz etkileri olan metaloit bir elementtir. Bu tez kapmasında, Yeşilırmak Havzasında yer alan antimon madeni noktasal kirlilik kaynağı olarak ele alınmış ve antimonun sucul ortamdan giderilebilmesi için çeşitli yöntemler incelenmiştir. Çalışma sonuçlarına göre, antimon sahalarının bulunduğu havzalardaki nehirlerin antimon kirliliğine maruz kalma ihtimalleri yüksektir. Antimon maden sahası deşarj noktası yakınından alınan numunelerde antimon konsantrasyonu yönetmelikte verilen yıllık ortalama Çevresel Kalite Standardı (ÇKS) limitlerinin 200 katının üzerine çıktığı gözlenmiştir. Antimonun sucul ortamdan giderimi için etkili yöntemler irdelenmiş ve adsorpsiyon, membran prosesleri ve koagülasyon-flokülasyon prosesleri arıtılabilirlik çalışmalarına dahil edilmiştir. Bu çalışmada, adsorpsiyon ile antimon giderimi için doğal zeolit kullanılmıştır. Manisa, Gördes bölgesinden elde edilen Klinoptilolit, antimon giderimi üzerindeki etkisinin incelenmesi açısından doğal formunda araştırılmış ve yaklaşık 40 m^2/g yüzey alanına sahip zeolit ile denge ve kinetik çalışmalar gerçekleştirilmiştir. Yapılan çalışmalar ile ortamın pH'ı düştükçe zeolit adsorpsiyon kapasitesinin arttığı gözlemlenmiştir. En yüksek zeolit adsorpsiyon kapasitesi, 50 mg/l Sb giriş konsantrasyonu için 2,02 mg/g olarak hesaplanmıştır. Uygun koşullarda elde edilen en yüksek antimon giderimi ise %85 olarak bulunmuştur. Zeolit ile elde edilen düşük adsorpsiyon kapasitelerinden dolayı membran prosesi ile de antimon giderimi araştırılmıştır. Nanofiltrasyon amacı ile kullanılan NF270 membran ile yapılan

çalışma ile %80 üzeri antimon giderimi elde edilirken ters ozmos için tercih edilen SW30 membran ile %99 giderime ulaşmak mümkün olmuştur. Koagülasyon-flokülasyon yöntemleri de yaygın olarak kullanılan ferrik klorür ve alüminyum sülfat ile antimon giderimi için alternatif bir metot olarak değerlendirilmiştir. Geleneksel koagülasyon ve flokülasyon yöntemlerinde demir klorür kullanarak %99 giderim elde edildiği görülmüştür. Fakat alüminyum sülfat kullanıldığı zaman sadece %44 giderim sağlanmıştır.

Anahtar kelimeler: antimon, nehir havzası, arıtım, zeolit, adsorpsiyon

ACKNOWLEDGMENTS

First and foremost, I would like to express my sincere appreciation and gratitude to my supervisor Assist. Prof. Dr. Derya Dursun Balcı for her invaluable guidance, knowledge, continuous support and friendship throughout this study.

I also would like to thank principal investigator of our project and my thesis committee member Prof. Dr. Ülkü Yetiş and other committee members Prof. Dr. İpek İmamoğlu, Assoc. Prof. Dr. Tuba Hande Bayramoğlu and Assoc. Prof. Dr. Niğmet Uzal for their valuable feedbacks and suggestions on this thesis.

I would like to especially thank Assoc. Prof. Dr. Niğmet Uzal since she provided an opportunity me to work in her laboratory during my study at Abdullah Gül University. I also thank Central Laboratory and Metallurgical and Materials Engineering Department of METU since they enable me to perform my analyses.

I would like to express my deepest thanks to my friends; Kumru, Zeynep, Emre, Ruken, Cansu, Hale, Sena, Mert, Burcu and Ghazal for their continuous support and morale. This study became easy and fun with them.

Finally, I must express my very profound gratitude to my parents and my brother for providing me with unfailing support and continuous encouragement through my entire life.

This study was supported by The Scientific and Technological Research Council of Turkey (TUBITAK) through Project No: 115Y013.

TABLE OF CONTENTS

LIST OF TABLES

TABLES

LIST OF FIGURES

FIGURES

CHAPTER 1

INTRODUCTION

Antimony (Sb) is a metalloid element that has properties of both metal and non-metals. It has similar chemistry as well as toxicity to Arsenic (As). Antimony can occur in the environment as a result of natural sources such as soil runoff, rock weathering. Furthermore, anthropogenic sources of antimony include fossil fuel combustion, smelting and mining activity and superphosphate fertilizers applied for agricultural purposes (Nash et al., 2000). Due to the toxic effects of antimony to human and environment, its removal from water has a great importance. Therefore, by "United States Environmental Protection Agency" (USEPA, 2014) and "European Union" (European Commission, 1976) antimony was considered pollutants of priority interest (Ungureanu et al., 2015). Today, antimony is still among the priority list of USA. And it is specific pollutants for Belgium, Cyprus, Czech Republic and Slovenia. Recently, antimony was also listed among the specific pollutants of Turkey (Yerüstü Su Kalitesi Yönetmeliğinde Değişiklik Yapılmasına Dair Yönetmelik, 2016).

1.1 General Information

Antimony and its compounds have been known since ancient times by humans (Multani et.al., 2016). Early chemists named antimony sulfide as "wolf of metals" since antimony dissolves and destroys all type of metals except gold. Description of antimony and its chemistry by Basil Valentine, in the fifteenth century in his book "*Triumph Wagen des Antimonii"*, is accepted as first important mention for antimony. And then, Agricola (1559) and Biringuccio (1550) expressed liquation of antimony ores in their studies. A scientific treatise *"Traité de l'antimoine"* written by French chemist Nicolas Lemery includes his specific studies about properties and preparations of antimony mineral. His studies are accepted as first major scientific progresses on antimony (Li, 2011). An ancient cosmetic named as "Kohl" is traditionally made by the most common form of antimony stibnite (Sb_2S_3). It was

commonly used by ancient women for black eye makeup as eyeliner and mascara in Africa, South Asia and Middle East (Ben-noun, 2016).

From ancient times to the present day, antimony also has strategic importance and has found all manner of applications. These days, antimony is intensively used to alloy with lead and other metals to improve their hardness and strength. This lead antimony alloy is very commonly used in batteries. It is also used as semiconductor in the electronics industry. Moreover, antimony compounds, antimony trioxide (Sb_2O_3), are mainly used to make flame-retardant materials, in glass and pigments and as a catalyst in PET manufacture (Multani et al., 2016).

Antimony is seen as an "emerging" pollutant but the information about toxic effect of antimony on the environment and human health are very limited. Health effects in humans and animals have been observed as a result of inhalation, oral and dermal exposure. Studies show that exposure to several antimony compounds have been caused to "respiratory effects", "cardiovascular effects", "dermal effects" and "gastrointestinal effects" on human and animals. But evidence on carcinogenic effect of antimony in humans is still insufficient (Agency for Toxic Substances and Diseases Registry, 2017).

1.2 Motivation of the Study

This study was conducted as a part of TÜBİTAK project (115Y013) on "Management of Point and Diffuse Pollutant Sources in Yeşilirmak River Basin". Since the antimony mining site located in the Yeşılırmak Basin is considered as a point source for antimony pollution, removal and management of antimony draw significant attention. The details of the project can be seen in section 2.2.1.

Several projects prior to our TÜBİTAK project are conducted to identify and to decrease the effect of hazardous pollutants in different regions of Turkey. A project named as KIYITEMA (2012-2014) was conducted in pilot areas; İzmit Gulf, İzmir-Nemrut and Aliağa Gulfs, İskenderun Gulf and Samsun Port in order to determine specific pollutants and EQS and discharge standards for these pollutants. Antimony

was determined almost all pilot regions except İskenderun Gulf. As a result of these studies, antimony was listed in specific pollutant list of Turkey and it is also demonstrated that antimony pollution is an important issue in different regions of Turkey.

1.3 Aim of the Study

Antimony is found at very low concentration naturally, but due to anthropogenic sources and natural processes, the amount of antimony in the environment is increasing. Increasing antimony amounts have led to negative effects on human health and environment. It can cause some health problems such as cardiovascular diseases, problems related with lungs, diabetes and other health issues (Mubarak et al., 2015). In the last century, heavy metal pollution draws attention of many people due to numerous severe industrial and environmental accidents occurred. Especially in the last decades, antimony as a specific pollutant has started to get significant consideration among researchers and authorities and antimony pollution has been identified as a critical issue in many studies (Ungureanu et al., 2015).

Water Framework Directive (2000/60/EC) includes determination of river basin "specific pollutants" and identification of EQS for these specific pollutants and meet EQS in all water bodies. Since Turkey is in harmonization process with the European Union, compliance with Water Framework Directive, and as a result, management of specific pollutants including antimony has become crucial.

In Turkey, by the regulation called "Regulation on the Surface Water Quality" (Yerüstü Su Kalitesi Yönetmeliğinde Değişiklik Yapılmasına Dair Yönetmelik, 2016), antimony was indicated as specific pollutant. Moreover, based on the results of previous studies, Environmental Quality Standards (EQS) for antimony were determined as 7.8 µg/l (annual average) and 103 µg/l (maximum) for rivers/lakes and 4.5 µg/l (annual average) and 45 µg/l (maximum) for coastal/transitional waters within this regulation.

Although antimony has been listed among the specific pollutants of Turkey, there is not much information related to the management and the removal of antimony from the aquatic environment. Studies on treatment of antimony from the aquatic environment are limited and not much information is available regarded on management and removal of antimony in Turkey. Also, there is very limited information about the antimony concentration in aquatic systems around main antimony mining sites of Turkey. Hence this thesis mainly aims to fill the knowledge gap in this area and shed light on antimony removal.

The aims of this study are:

- To evaluate antimony levels in Turkey based on available data
- To explore the antimony removal methods from aquatic environment
- To investigate the removal of antimony via zeolite adsorption, coagulation-flocculation and membrane processes
- To compare the removal efficiency of antimony by conventional and advance treatment methods

CHAPTER 2

LITERATURE REVIEW

2.1 Antimony

2.1.1 Properties of Antimony

Antimony (Sb) located in the group 15 (VA) of the periodic table is a metalloid element. It has silver-white color, easily breakable and solid crystalline structure and also has very weak electrical and thermal conductivity. The atomic number of Sb element is 51 and atomic weight is 121.76 and density of antimony is 6.697 g/cm^3. The boiling and melting points are 1380 °C and 630 °C, respectively (Anderson, 2012).

Antimony compounds can be found in four different oxidation states which are -3, 0, +3 and 5. In the environment, it is mostly distributed as Sb(III) and Sb(V) (Filella et al., 2002b). Oxidation state of antimony determines the toxicity of antimony species. Generally, Sb(III) is ten times more toxic than Sb(V) and inorganic antimony compounds are more toxic than organic forms (Ungureanu et al., 2015).

According to the Goldschmidt's classification, antimony is among the chalcophile elements, which have low affinity for oxygen and prefer to bond with sulfur. In nature, it mainly exists as stibnite (Sb_2S_3) and antimony trioxide (Sb_2O_3) which is transformation form of stibnite (Filella et al., 2002a) . Studies showed that Sb is insoluble in water. However, compounds of Sb are soluble in water. The solubility of diantimony trioxide and stibnite are 2.76 mg/l. and 1.75 mg/l in water, respectively (Agency for Toxic Substances and Diseases Registry, 2017).

2.1.2 Antimony Reserves

The amount of antimony in the earth crust has been found to be between 0.2 and 0.3 mg/kg and much higher concentrations have been observed in rocks. Minerals are the source for antimony but it can be also found in copper, lead and silver ores in small amounts (Diantimony Trioxide Risk Assessment Report, 2008).

China has the highest antimony production amount in the world and they continue to dominate this market for more than 100 years. In 2014, global mine production of antimony was declined by 3 % and compared to 2011 which is the historical peak for global antimony production; the production of antimony was reduced 16 %. Today, about 77 % of antimony production is provided by China and followed by Russia (6 %) and Australia (4 %). Although the production of antimony in Australia, Bolivia, Russia, and Turkey has increased, the decrease observed in Burma, Canada, China, and South Africa caused to decline of total worldwide antimony mine production. Antimony mine production between 2010 and 2014 is given in below table (USGS, 2016a).

Table 1. Antimony mine production by country (USGS, 2016a)

	Production amount (metric tons)				
Country	**2010**	**2011**	**2012**	**2013**	**2014**
Australia	1106	1577	2481	3275	5800
Bolivia	4980	3947	5088	5081	5500
Burma	4700	5600	5900	7200	3300
Canada	5700	5800	4100	148	-
China	150,000	150,000	136,000	120,000	120,000
Kyrgyzstan	700	1500	1200	1200	1000
Mexico	71	100	169	294	270
Russia	6000	6348	7300	8700	9000
South Africa	3239	3175	4500	5300	1600
Tajikistan	2000	4500	4248	4675	4700
Thailand	738	56	-	-	-
Turkey	1400	2400	7300	4600	4500
TOTAL	180,000	185,000	178,000	160,000	156,000

2.1.3 Antimony Reserves in Turkey

In Turkey, main antimony mineral reserves are mostly located in Western Anatolia. In this region, there are large number of antimony deposits within the boundaries of Kütahya, Balıkesir, İzmir, Manisa, Aydın, Uşak and Bilecik. Active tectonic structure and volcanic activities in this region play an improtant role in this situation. Other important regions in terms of antimony mining reserves are Tokat and Niğde provinces (Devlet Planlama Teşkilatı, 2001). In Figure 1, Turkey's antimony reserve map is given. The label of the basins was given on the map and also circles on the symbols show the size of reserves. Detailed information about the reserves is given in Table 2.

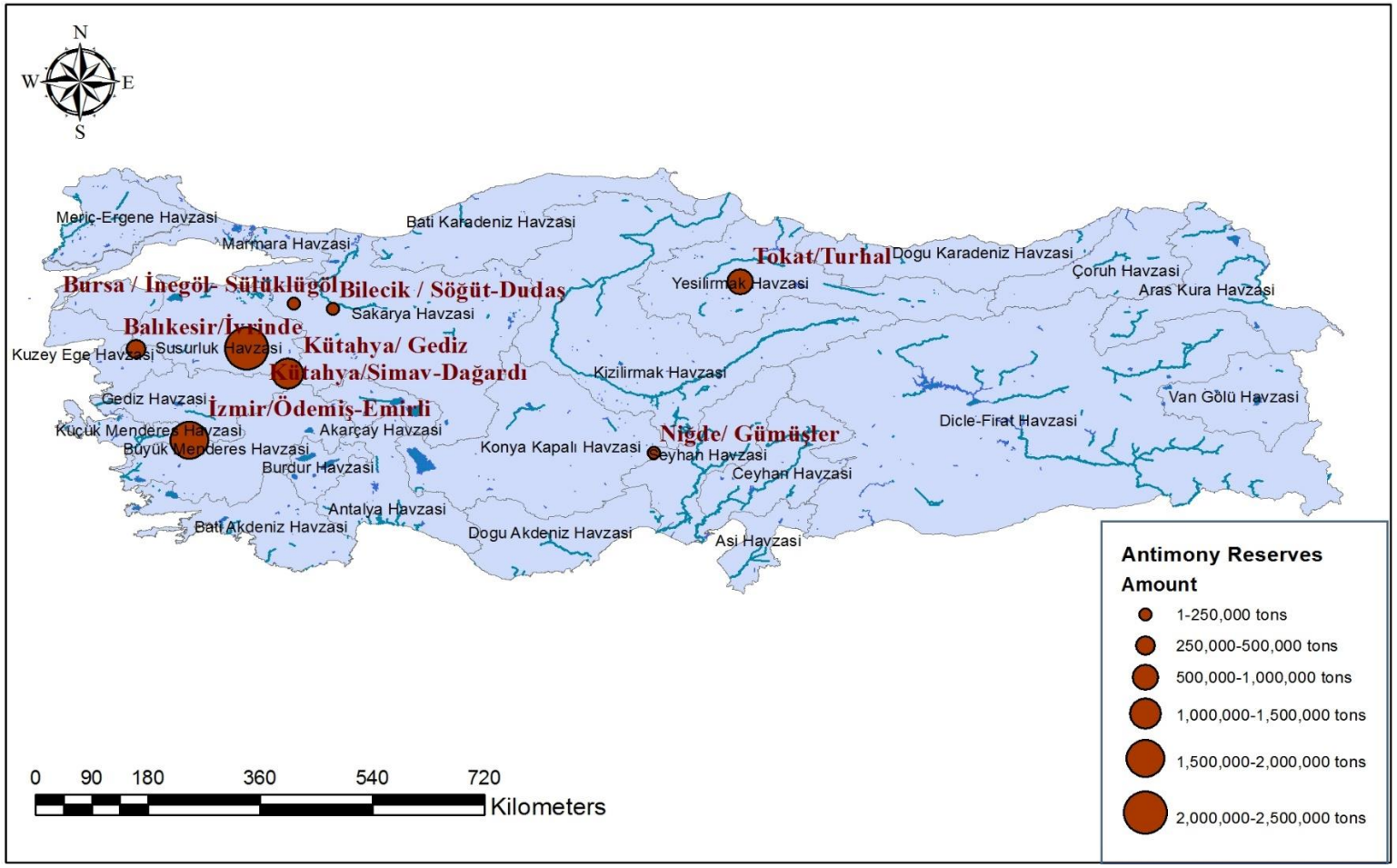

Figure 1. Antimony reserves in Turkey

Turkey's antimony potential is about 6,672,000 tonnes which corresponds to 330,000 tonnes of metal content. Antimony reserves in Turkey are given in Table 2.

Definitions of the some mining terms are given in this paragraph. According to these definitions, information about the antimony reserves is given in below paragraphs. The concentration of a metal in a mine ore is called as the ore grade. The reserves are classified in terms of their probability of recoverability. If there is a reasonable certainty that the reserve is commercially recoverable, it is called proved reserve. Moreover, if statistical data are employed, it is expected that there should be at least 90 % possibility for the recovery of the mine. If the presence possibility of the mine ore is greater than 50 %, the reserve is called as probable. However, if the possibility is only greater than 10 % and mineralization is not sampled enough to accurately estimate its tonnage and grade the reserve is classified as possible (Engler, n.d.).

With regard to antimony resources, only 11 % of antimony reserves have been classified as proved. It is shown that 4 % of total reserve is in proved + probable category and about 17 % is in probable category. The remaining 68 % is defined as a possible reserve.

As it is seen, Turkey has a considerable amount of antimony ores and it is among the World's main antimony producers. On the other hand, since exploration activities are not enough, it is difficult to give a number of producible reserves. Because of the nature of the antimony mineralization, determination of reserve with normal exploration works is not possible. Moreover, since antimony mining areas are operated by small capital companies and they cannot provide sufficient fund for exploration works, the studies on reserves of antimony is limited (Devlet Planlama Teşkilatı, 2001). According to U.S. Geological Survey report named as "The Mineral Industry of Turkey", there is considerable increase (37 %) in antimony production of Turkey in 2013 (USGS, 2015).

The antimony mining in Turkey has been maintained on the antimony deposits that have been known and operated for a long time. The large parts of these reserves are operated by small companies and it is not possible to find reliable information about the production number of these reserves.

In some mining deposits, the amount of ore produced up to now is above the amount of reserves known for this site. Accordingly, development of some antimony mining sites is possible since it is likely to have higher amount of antimony reserves than our knowledge. However, it is not likely to say much about this issue since there is not enough information on this area. According to MTA (Mineral Research and Exploration Institute) reports, reserve detection studies about the known mining sites are done in the past and nowadays there are not any exploration works. For the development of antimony mining, this subject should be studied comprehensively and the country's antimony potential, the ore properties of the reserves and exploration opportunities should be revealed (Devlet Planlama Teşkilatı, 2001).

Table 2. Antimony reserves in Turkey (Devlet Planlama Teşkilatı, 2001)

			Reserves (tons)				
	Location	**Grade (Sb%)**	**Proved**	**Probable**	**Possible**	**Total**	**Metal content (tons)**
Balikesir	Susurluk-Demirkapı	1.16	-	-	11,250	11,250	130
	İvrindi-Korucu-Taşdibi	6.0	47,850*	-	235,600	283,450	17,007
	İvrindi-Korucu-B. Yenice	6.0	1,370	17,805	26,000	45,175	2,800
	İvrindi-Kayapa-K. Yenice	6.0	5,120	8,000	91,350	104,470	6,268
Bilecik	Söğüt-Dudaş	2.0	-	-	10,000	10,000	200
Bursa	İnegöl-Sülüklügöl	6.5	-	15,000**		15,000	975
İzmir	Ödemiş-Emirli	4.8	575,331	1,015,291	-	1,596,622	76,349

**Proved + Probable*

***Probable + Possible*

Table 2 Cont'd. Antimony reserves in Turkey (Devlet Planlama Teşkilatı, 2001)

			Reserves (tons)				
	Location	**Grade (Sb%)**	**Proved**	**Probable**	**Possible**	**Total**	**Metal content (tons)**
Kütahya	Gediz-Dereköy	2.0	-	-	364,000	364,000	7,280
	Gediz-Göynük	1.2	-	-	924,000	924,000	11,088
	Simav-Dağardı	6.4	-	-	2,584,440	2,584,440	165,404
Niğde	Gümüşler-Canyarığı	38	-	2,350	-	2,350	893
	Gümüşler-Örendere	4.5	-	-	100,000	100,000	4,500
Tokat	Turhal-Çamlıca	4.0	200,000*	-	-	200,000	8,000
	Turhal-Elalmış	12	124,000	-	-	124,000	14,880
	Turhal-Özdemir	4.0	43,000	111,000	150,000	304,000	12,160
	Turhal-Sütlüce	23.5	3,900*	-	5,780	9,680	2,274

**Proved + Probable*

***Probable + Possible*

2.1.4 Usage of Antimony

Antimony and its compounds have been used for different purposes such as ingredient of cosmetic products by humans at least for 6000 years. Until 4000 BC, antimony ores were used to decoration of vessels by the Chaldeans. And by 3000 BC, it was being used as covering on copper products by Egyptians (Butterman & Carlin, 2004). Moreover, Shortland (2002) analyzed over 150 different glasses from Malkata and Amarna and identified different antimonate colorants used in these early glasses of the second millennium BC. A peat from Swiss bog also affirmed that significance of antimony is extending back to Roman times. It shows that antimony which is originated from anthropogenic sources have exceeded natural ones for more than 2000 years (Shotyk et al., 1996). As it is seen, antimony application has been continued over the ages and used as a material for accessories, jewelry and alloys (Multani et al., 2016).

Due to its hardness and brittleness, these days antimony is especially used in lead and tin based alloys to improve their strength and hardness rather than using as a metal by itself. Lead based antimony alloys are the most common ones and formed by adjusting the composition of antimonial lead. Antimony ratio in these alloys may reach up to 25 percent. Some form of antimony lead alloy is used in batteries, cable covering and other applications. Also, antimony is used as a component of some tin based alloys, such as pewter, britannia metal, white bearing metal and tin antimony silver solder. The most important commercial form of antimony is antimony trioxide (Sb_2O_3) used mainly in flame retardants, in polyvinyl chloride (PVC) and other plastics as heat/UV stabilizers and for the production of polyethylene terephthalate (PET) as a catalyst (Butterman, & Carlin, 2004).

Currently, majority of antimony is used in flame retardants and in lead alloys, mainly in batteries (Figure 2). In addition to these usage areas, chemicals, ceramics, paints and glasses are the major industries that use antimony. Most commonly consumed antimony is in four different forms; antimony trioxide mainly used for flame retardants, antimony lead alloys mainly used in batteries, refined antimony mostly used in LA (lead-acid) batteries and sodium antimonate used in glasses (Butterman,

& Carlin, 2004). Estimated worldwide antimony usage in 2014 is shown in Figure 2. Worldwide antimony consumption was about 182,000 ton in 2014 (USGS, 2016b).

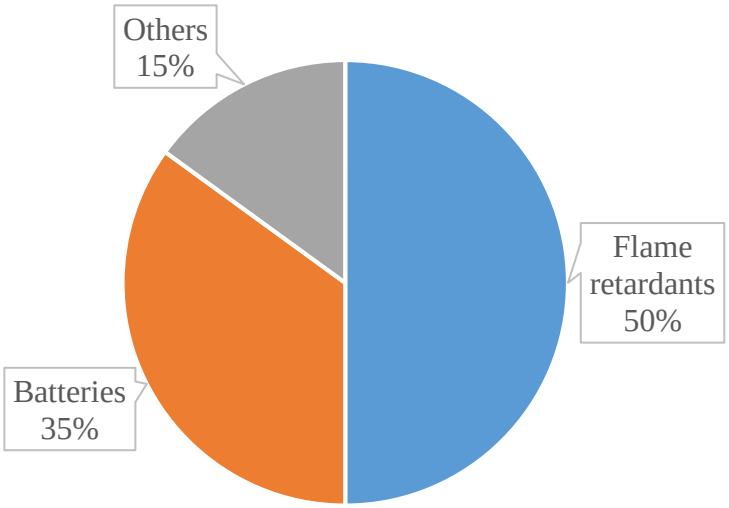

Figure 2. Worldwide antimony usage in 2014 (USGS, 2016b)

2.1.5 Effects of Antimony

Naturally, antimony is found at very low levels in the environment, so low that it cannot be measured sometimes. The amount of antimony in rivers and lakes is also very low. However, due to the increment of anthropogenic sources, antimony concentrations are measured above the natural levels in some areas. Antimony enters the environment during the mining and processing of antimony ores and in the production of antimony metal, alloys, and antimony oxide. As a result, humans can be exposed to antimony by breathing air, drinking water, and eating foods that contain it. Also, skin contact with soil, water, and other substances that contain antimony can cause antimony exposure (Agency for Toxic Substances and Diseases Registry, 2017).

2.1.5.1 On Human

Whether antimony can cause cancer, birth defects or reproduction problems for humans is not known clearly. But studies performed on laboratory animals showed that antimony cause lung cancer on animals inhaled dust containing antimony and also

irritation of the eyes, skin, lungs, and stomach as a result of long exposure to antimony (Fay et al., 1999).

Rats exposed to high level of antimony for several days had damage in their liver, heart, lung, and kidney; while, rats breathed very low antimony level for a long time have some problems such as eye irritation, hair loss and lung damage. In another study, breathing low levels of antimony for a long time caused heart problems in dogs and rats. In rats, breathing exceeding levels of antimony for a couple of months, fertility problems have been observed. Furthermore, in some studies, rats breathed high concentration of antimony, lung cancer has been observed (Fay et al., 1999).

Moreover, recent studies showed that antimony can cause lung effects and cardiovascular problems on people. Especially myocardial damage and change in electrocardiogram (EKG) readings have been observed in humans (Agency for Toxic Substances and Diseases Registry, 2017).. Vomiting, nausea, ulcers and abdominal pain also have been seen on antimony workers. In some studies, lung cancer have been seen on workers. Two study conducted on antimony workers have found an increase in lung cancer deaths. However, due to the lack of studies observed effect of antimony on human health, antimony has not been classified as a carcinogen by EPA, International Agency for Research on Cancer (IARC) or Department of Health and Human Services (DHHS). On the other hand, , IARC has classified antimony trioxide as possibly carcinogenic to humans in group 2B (Agency for Toxic Substances and Diseases Registry, 2017).

IARC report published in 1989 states that although there were sufficient evidence on the carcinogenicity of antimony trioxide and antimony trisulfide in experimental animals, the number of evidence were not adequate for humans. Considering the time and research conditions of the evaluation, from then to today, increased number of studies and development in technology will lead to improved evaluation. Moreover, due to the increase of anthropogenic antimony sources and antimony discharges, it is safe to say that the evaluation results are expected to differ in today. In 1999, Fay et al indicated that the potential damage of antimony to human is a known fact (Fay et al., 1999).

2.1.5.2 On Environment

Antimony is naturally occurring in environment in low concentrations but it is released to environmental systems in high levels due to anthropogenic sources. In unpolluted waters, dissolved antimony concentration is typically at nanogram levels. However, when samples are taken from nearby anthropogenic sources, concentrations can be measured as close to 100 times of natural levels (Filella et al., 2002a).

Several studies have been conducted in order to determine the effect of antimony on aquatic life. In a study, influence of Sb(III) was observed on aquatic organisms such as "*Oryzias latipes (Japanese rice fish), Simocephalus mixtus (crustacea), Moina macrocopa (crustacea) and Pseudokirchneriella subcapitata (green algae)"*. It was seen that the presence of antimony, inhibited survival of Oryzias, larval fishes. As Sb(III) concentration increases, survival of larval fish percentage dramatically reduces. Moreover, to see the effect of Sb(III) on early stage development of fishes, fertilized eggs were exposed to antimony. Abnormality development was observed in some of embryos. Studies showed that *Moina macropa* and *Simocephalus mixtus* were more sensitive to presence of Sb than other organisms. Therefore, *Simocephalus mixtus* may be a better indicator of antimony pollution since it is the most sensitive one to presence of Sb in environment (Nam et al., 2009).

Fu et al. (2010) investigated effect of antimony in fish and algae samples collected from the Xikuangshan, the largest mining site in China. Results showed that serious Sb contamination is exist in the aquatic environment. Average Sb concentration in fish was measured as 218 ± 113 μg/kg dry weight. When distribution of Sb examined in fish organs, higher Sb concentration was observed in fish gills. It may be related with ionic exchanges and mucus production in gills serve as a binding area to capture metals. Moreover, in algae Sb concentrations were higher than the average concentrations studied earlier in freshwater and marine algae. As a result of the study, Sb is mostly accumulated in fish gills and liver but extent of accumulation can change according to different fish species.

Duran et al. (2007) studied accumulation of antimony on some type of macroinvertebrates in Yeşilırmak River. Aquatic invertebrates take trace elements

directly from water and transferred to higher food chain organism such as fish and birds. Two different sampling sites were investigated; before the antimony mining site (non-affected site) and mine-affected site. It is pointed that before the mining site, the antimony concentration was found to be below the detection limits on "*Asellus aquaticus*, *Hydropsyche pellucidula*, *Leucorrhinia dubia*, and *Gammarus pulex"*; however, on the mine-affected site, the antimony concentration significantly increased on these macroinvertebrates. Another finding was that the taxonomic diversity was considerably lower on the mine-affected site compared to before mining site. The diversity was decreased from 76 to 36. This change on the taxonomic diversity was linked to the negative effect of the antimony mine on aquatic systems.

In another study, effects of antimony on microbial activity was investigated in organisms; "*Escherichia coli*, *Bacillus subtilis* and *Streptococcus aureus"*. At different Sb concentrations; 25, 50 and 100 mg/l, growth of the *Bacillus subtilis and Streptococcus aureus* were significantly inhibited. At 100 mg/l, *Bacillus subtilis* growth is completely inhibited. The EC 50 for inhibition of specific growth were 555, 18.4 and 15.8 mg Sb/l for *E. coli, B. subtilis, and S. aureus*, respectively. It is seen that microbial growth is negatively affected in all test organisms. And *S. aureus* is the most sensitive one to Sb pollution than other organisms (An & Kim, 2009).

2.1.6 Fate of Antimony in Water

In order to understand dissolution and distribution mechanisms of antimony species within aqueous environment, investigation of solubility properties of antimony is vital. Temperature, pH and redox potential (Eh) of the environment are important parameters effecting solubility and specification of antimony (Herath, et.al, 2017).

The mobility and transport of antimony is affected by changes in redox status of aquatic environment. Redox reactions of Sb, involve oxidation and reduction under aerobic and anaerobic conditions. In this scope, identifying redox processes of Sb is important to understand fate of antimony species in aquatic environment (Filella et al., 2002a).

2.1.6.1 Aerobic systems

Sb(V) in the form of $[Sb(OH)_6^-]$ is dominant specie in oxic waters but presence of thermodynamically unstable Sb(III) is also determined in the presence of oxygen. Most studies point out biological activity as the reason of unstable Sb(III) presence in aerobic conditions. However, there is not much evidence to confirm this hypothesis (Filella et al., 2002a). Sb primarily exists as Sb(V) in oxygen rich water system that can be correlated with oxidation effect of iron and manganese oxyhydroxides or low speed kinetics of reduction by dissolved sulfides (Chen et al., 2003).

Antimony species oxidation/reduction behavior can be seen in redox potential (Eh) vs pH diagram. Redox potential is a measure of how easily a chemical substance will be reduced or oxidized by give up or retain its electrons (Kjaergaard, 1977). According to the diagram in Figure 3, Sb is found as soluble $[Sb(OH)_6^-]$ form in oxic waters and soluble $Sb(OH)_3$ form in anoxic waters at wide pH range. Under reduction conditions and presence of sulfur, solid Sb_2S_3 specie is formed at lower pH values and SbS_2 specie is formed at higher pH values (Filella et al., 2002b). These results indicate that Sb(III) gets oxidized to Sb(V) at lower Eh values and so Sb(V) is very stable when compared to Sb(III) in oxic systems (Mitsunobu et al., 2006).

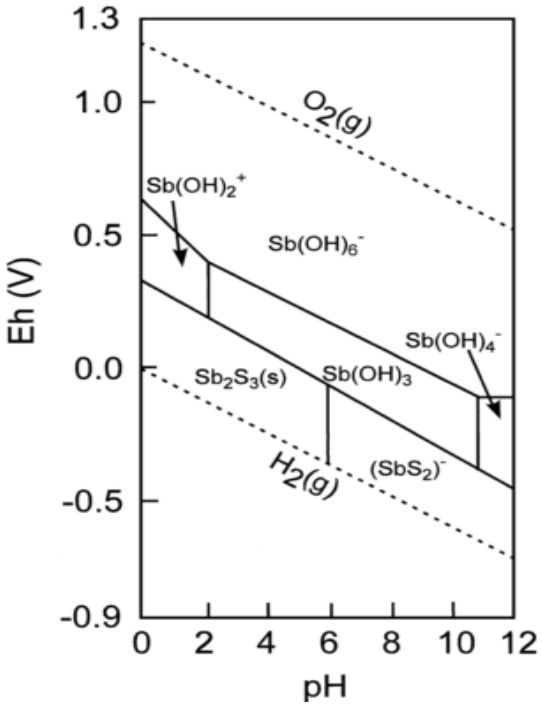

Figure 3. Potential (V) & pH diagram of the antimony in water systems (Filella et al., 2002b)

On the other hand, chemical equilibrium of antimony species in aerobic conditions is controlled by Reaction 1. The below equation shows that at pH 7, concentration ratio of Sb(V) in the form of $[Sb(OH)_6^-]$ to Sb(III) in the form of $Sb(OH)_3$ is $10^{18.4}$ in oxic aquatic system. So this equation also show that Sb(V) should be dominant specie in oxic systems (Kang et al., 2000).

$$Sb(OH)_3 + 3H_2O \rightarrow Sb(OH)_6^- + 3H^+ + 2e^- \qquad \textbf{Reaction 1}$$

In a study conducted by Chen et.al. (2003) on the distribution of antimony in lakes, the importance of iron and manganese on behaviour of Sb particles has been revealed. Presence of iron and manganese oxyhydroxides, O_2 and H_2O_2 enhance the oxidation of toxic Sb(III) to less toxic Sb(V) in aquatic environment. This oxidation reaction of Sb(III) is highly pH dependent and favored at pH range 3 to 5.9 (Reaction 2) (Herath et al, 2017).

$$2Fe(OH)_{3(s)} + Sb(OH)_{3(aq)} \rightarrow 2Fe(OH)_{2(s)} + H_3Sb_{4(aq)} + H_2O_{(l)} \qquad \textbf{Reaction 2}$$

Moreover, the oxidation processes of Sb(III) by O_2 and H_2O_2 is also highly pH dependent but the rate of these reaction are slower than the Reaction 2. Oxidation process of Sb(III) in the presence of H_2O_2 is given in Reaction 3,4 and 5 (Herath, et al, 2017).

$$H_2O_{2(aq)} + H^+_{(aq)} \leftrightarrow HO^-_{2(aq)} \text{ pKa=11.6} \quad \textbf{Reaction 3}$$

$$Sb(OH)^-_{4(aq)} + H_2O_{2(aq)} \leftrightarrow Sb(OH)^-_{6(aq)} \quad \textbf{Reaction 4}$$

$$Sb(OH)_{3(aq)} + HO^-_{2(aq)} + H_2O_{(l)} \rightarrow Sb(OH)^-_{6(aq)} \quad \textbf{Reaction 5}$$

2.1.6.2 Anaerobic systems

The specification of antimony in anoxic systems is not certain yet. According to thermodynamic calculations, dominant specie is Sb(III) in the form of $Sb(OH)_3$ in anoxic waters. Sulfur acts as reducing agent and enhance the reduction of less toxic Sb(V) to high toxic Sb(III) specie (Reaction 6) (Herath et al, 2017).

$$H_2S_{(aq)} + Sb(OH)^-_{6(aq)} + H^+_{(aq)} \rightarrow Sb(OH)_{3(aq)} + 1/8\ S_{8(s)} + 3H_2O_{(l)} \quad \textbf{Reaction 6}$$

Moreover, recent studies showed that Sb(III) also can be oxidized to Sb(V) by sulfur as shown in Reaction 7.

$$Sb(III)_{aq} + S^{2-}{}_{n(s)} + H^+_{(aq)} \rightarrow Sb(V)_{aq} + HS^-{}_{aq} + S^{2-}{}_{(n-1)(s)} \quad \textbf{Reaction 7}$$

As can be seen from this reaction, the transformation of insoluble sulfur (S^{2-}) into polysulfide compounds (HS^-) could be of particular concern for surface and groundwater systems which are especially used for drinking purposes (Herath et al., 2017).

Microbial redox processes can also affect the speciation, mobility and transport of Sb species in the environment. Several studies show that antimony oxidizing bacteria such as *Stibiobacter senarmontii, Stenotrophomonas, Hydrogenophaga taeniospiralis, Pseudomonas, Agrobacterium tumefaciens*, etc. play a critical role in oxidation of toxic Sb(III) to less toxic Sb(V) species in different environmental

system. These type of microbial species have a significant effect in controlling the redox transformation and mobility of Sb in different environmental systems such as aqueous solutions, fresh water sediments, mined soil and sediments (Herath et al., 2017).

2.1.7 Regulations on Antimony

Antimony and its compounds are considered as specific pollutants. Considering the abundance of antimony in environment due to anthropogenic sources, limit values are critical in groundwater and surface waters.

The safe drinking water act (SDWA) was introduced as a national law in 1974 to protect drinking water and its sources quality in USA. Under the SDWA, USEPA determines the limit values for contaminants in drinking water below which adverse health effects are not likely to occur. These limit values are called as maximum contaminant level goal (MCLG). The MCLG for antimony has been set by EPA as 6 µg/l or 6 ppb. Moreover, maximum contaminant level (MCL) as an enforceable regulation has been set at 6 µg/l or 6 ppb for antimony. MCL are set close to MCLG by considering some factors such as cost, efficiency and applicability to water treatment systems to remove contaminants. Furthermore, individual states can set stricter limit values for antimony than USEPA for any system, product, etc. For instance, in some New York Counties, antimony in toys and children's products has been banned. In Albany County, Westchester County and Rockland County according to their local laws, the sale of children's products containing antimony are prohibited ("A Local Law to Protect Infants And Children From harmful Health Effects Of Unnecessary Exposure To Toxic Chemicals," 2014) ("Local Law-Proposed amendment-Prohibiting the sale of children's products containing certain chemicals," 2015).

In European Union countries, quality of drinking water is determined according to the Council Directive 98/83/EC on "the quality of water intended for human consumption". In this directive, antimony level in drinking water in order to protect human health against the adverse effects of antimony is set as 5 µg/l (European

Commission, 1998). Moreover, in Basel convention aiming to protect human health and the environment against adverse effects of hazardous wastes and other wastes, antimony is listed as hazardous substance under Article 1, paragraph 1 (a) ("Basel Convention on the Control of Transboundary Movements of Hazardous Wastes and Their Disposal Adopted By the Conference of the Plenipotentiaries on 22 March 1989," 1992). This means that its risk of damaging to human health and environment are known fact and people started to be aware of this situation. In United Kingdom(UK), for antimony same standard with EU Drinking Water Directive is approved and applied as 5 µg/l maximum concentration in drinking water ("The Water Supply (Water Quality) Regulations," 2016)

China, has the largest reservoir of antimony in the world, set limit values for antimony as 5 µg/l in their Standards for Drinking Water Quality.

In Turkey, there is a regulation called as Regulation on Water Intended for Human Consumption ("İnsani Tüketim Amaçlı Sular Hakkında Yönetmelikte Değişiklik Yapılmasına Dair Yönetmelik", 2013) to manage the principles and procedures regarding the quality standards of waters. According to this regulation, limit value of antimony for drinking water is set to 5 µg/l which is same with the limit value of EU, UK and China for drinking water standards.

Moreover, as it is mentioned before, by the regulation called "Regulation on the Surface Water Quality" (Yerüstü Su Kalitesi Yönetmeliğinde Değişiklik Yapılmasına Dair Yönetmelik, 2016), antimony is indicated as specific pollutant in Turkey. Environmental Quality Standards (EQS) for antimony are identified as 7.8 µg/l (annual average) and 103 µg/l (maximum) for rivers/lakes and 4.5 µg/l (annual average) and 45 µg/l (maximum) for coastal/transitional waters within this regulation.

2.2 Antimony Pollution in Aquatic Environment

Turkey has a number of antimony reserves within boundaries of Kütahya, Balıkesir, İzmir, Tokat, Manisa, Aydın, Uşak, Bilecik and Niğde as mentioned in section 2.1.3. Vicinity of these reserves can be susceptible to antimony pollution due to discharges

originated from the mine processing activities in these areas. There are some studies indicate that the high antimony concentrations in aquatic systems near the antimony mining sites in the world. For example, in China, the largest antimony producer in the world, measured antimony levels were between 2 and 6384 µg/l in rivers around Xikuangshan which is the biggest antimony mining area. The measured concentration level of antimony was very high when compared to average antimony concentration of the rivers in the world being 1 µg/l (Wang et al., 2011). In Alaska/USA, antimony concentration was found as 720 µg/l due to historic mining activities in Kantishna Hills mining district. High concentrations of antimony were measured more than 8 km downstream of the mining site (Ritchie et al., 2013). Another study showed antimony contamination found at Pezinok mining site in the Slovak Republic. Antimony measurement results was up to 7500 µg/l and it was mainly sourced from stibnite dissolution (Flakova et al., 2012). In Italy, antimony occurrence and dispersion in aquatic system around the Sarrabus-Gerrei mining district were evaluated. Even after mine site was closed, due to the contact of water with the slag materials, Sb concentration in downstream of the mine was measured up to 1500 µg/l concentration. Contamination extends several kilometers downstream of the mine and affects the Flumendosa river which is used for irrigation and domestic purposes. In this river, Sb concentration also exceeds 5 times the Italian standard for drinking water (5µg/l) (Cidu et al., 2012).

Currently in Turkey, data about antimony concentration in the aquatic environment close to mining sites are very limited. In a study conducted by Targan et al. (2013), the antimony concentration of the sample taken from Karaçay on Gediz river was found as 559 µg/l. It is above the average antimony concentration of the rivers in the world. There is not any evaluation about the reason of the high concentration but it may be sourced from antimony reserves found in Gediz region. Moreover, result of another project called "Control of Hazardous Material Pollution" (Tehlikeli Madde Kirliliğinin Kontrolü, TMKK) showed that antimony levels were detected above the EQS in Ergene, Susurluk and Konya Basins.

In a study conducted in surface waters around Gümüşköy Silver Mine in Kütahya, antimony was detected in all of sampling points. Moreover, the results of the Sb measurement at two sampling points from streams formed by direct leakage from

waste pools, and Ephemeral stream located downstream of mine site and Perennial stream affected by mine wastes exceeded EQS. Sb concentrations were measured as 39.5, 33.3, 14.8 and 14.0 µg/l in these points, respectively. As it is mentioned in section 2.1.2, antimony can be found in silver ores. These results can be related with mining activities in this region as well (Arslan & Çelik, 2015).

Gemici & Tarcan (2007) evaluated some pollutants around untreated abandoned Türkönü mercury mine in Ödemiş/İzmir. Three water samples were gathered from the mining area; one of which was from adit water and the remaining two were taken from puddles located on waste rocks. Antimony concentrations on these samples were measured as 0.6, 168.9 and 418.6 µg/l, respectively.

Based on the information gathered from Yeşilırmak River Basin, antimony concentrations were measured around 1650-1750 µg/l at Tokat/Turhal antimony mining site. These measurement results are above the average antimony concentration in the world and all the limit values related to antimony in the previously mentioned regulations.

All of these results indicate that antimony pollution due to the mining activities is a significant problem that cannot be ignored. Even closed mining site, the antimony concentration is much higher than the limit values which causes to environmental contamination. The discharge of the mining sites to rivers used for domestic purposes can cause health and environmental problems.

2.2.1 Yeşilırmak project

The European Union (EU) Water Framework Directive (WFD) was put in effect on 23 October 2000. The primary purpose of WFD is to improve the status of degraded ground and surface waters. Within the scope of WFD, The Turkish Ministry of Water Affair and Forestry is conducting River Basin Management Plans (RBMP). In this extend, a TUBİTAK has awarded a project named as "Management of Point and Diffuse Pollutant Sources in Yeşilirmak River Basin", in short Yeşilırmak project. The main objective of this project is to prepare RBMPs for Yeşilırmak river basin.

With this project, it is aimed to identify and manage point and diffuse pollutant sources and identify specific pollutants in this basin. One of the tasks in this project is to evaluate possible treatment methods that could be applied in wastewater treatment plants (WWTP) for identified specific pollutants.

There is an antimony mining site in Tokat-Turhal region located in the Yeşilırmak River Basin. This mining site is among the important antimony reserves of Turkey. Based on initial onsite measurements, this mining site can be regarded as a point source and antimony should be considered as a specific pollutant for this basin. Results of monitoring studies performed in the Yeşilırmak River Basin are given in section 4.1

2.3 Removal of Antimony

Today, there is a global water crisis due to lack of access to clean and safe drinking water. As a result of fast industrialization and urbanization, wastewater from industrial processes has been discharged into water bodies and soils. Impact of these discharges on ecosystems and humans can be toxic and poisonous because of its contents such as cationic and anionic ions, organics, inorganics, oil, etc. (Wang & Peng, 2010). Considering toxic effects and allowed legal limit values, removal of antimony originated from natural and anthropogenic sources is necessary (Ungureanu et al., 2015). For the removal of antimony from aqueous systems various methods have been proposed and compared.

2.3.1 Removal in Conventional Urban Wastewater Treatment Plants

In order to evaluate different removal methods for antimony, understanding fate of Sb in wastewater treatment plants (WWTP) is important. Although, there are numerous studies about removal and fate of metals such as copper, zinc, iron, lead and mercury through wastewater processes, knowledge about the fate of the other metals such as antimony, silver, barium, and titanium are very limited and they are not monitored regularly within the WWTP (Hargreaves et al., 2016).

Yoshida et al. (2015a) investigated fate of 32 elements including antimony in a conventional WWTP. Metal concentrations measured in influent and effluent of the WWTP and historical data between 2006 and 2010 is compared and they provide consistent trends. Based on the results of the study conducted in a conventional WWTP in Denmark, the Sb was divided equally to sludge and effluent as a result of wastewater treatment process. According to mass fraction, about 50 % of Sb is measured in effluent water, nearly 20 % in primary sludge and 30 % in secondary sludge. Moreover, based on the analysis of sludge sent to anaerobic digestion, 40 % removal of Sb was observed during anaerobic process.

In another study, particularly fate of antimony and mercury was investigated and efficiency of primary and secondary treatment processes on removal of Sb was evaluated at a urban WWTP in United Kingdom. In this plant, primary sedimentation tank is followed by activated sludge process for the secondary treatment. According to the study, 16.3 % removal of antimony was achieved by the primary treatment. However, at the secondary treatment stage -28.9 % negative removal was observed for Sb. According to the authors, as an explanation for this negative Sb removal result, it was suggested that complexation formed by Sb and extracellular polymers is weak. So during activated sludge treatment, oxidation of polymers will cause the releasing of Sb back to the effluent and Sb concentration will increase throughout the treatment. The same situation was observed for arsenic and cadmium removal but more examination on the subject is required to confirm this presumption about Sb removal (Hargreaves et al., 2016).

A study conducted by Choubert et al. (2011) focused on removal of 23 metals and metalloids in a WWTP. Particulate and dissolved metals include antimony is measured in each treatment step. In secondary treatment, most metals have removed with a high rate (> 70 %) except some elements such as antimony, arsenic, and vanadium because of their low adsorption capacities. Furthermore, with experimental tertiary treatments (rapid chemical settler, polishing pond, ozonation) removal efficiency for antimony was obtained below 30 %.

2.3.2 Treatment Methods

Literature researches showed that most commonly applied treatment methods for antimony removal are adsorption, coagulation-flocculation, filtration-ultrafiltration, ion exchange, reverse osmosis and electrolysis processes (Ungureanu et al., 2015).

2.3.2.1 Adsorption

Adsorption is a surface phenomenon in which molecules of a substance accumulate on the surface of another substance. This process occurs as a result of interaction between adsorbents and adsorbate molecules and adsorbent became attached to the solid surface in the form of an adsorbed layer. Relation between the amount of adsorbed on the surface of adsorbate at a given temperature and equilibrium concentration of the substrate is known as adsorption isotherm and used to describe adsorption process (Sharma, 2012).

Adsorption can be categorized into two groups as chemisorption and physisorption. Chemisorption is a chemical interaction between adsorbate and adsorbent. In this type, adsorption takes place through chemical bond formation, electron exchange or chemical precipitation. The process is not always reversible. Physorption is interaction of adsorbents and adsorbate through Van der walls forces which are weak forces. Therefore, it is characterized as relatively low adsorption energy and the process is reversible (Sharma, 2012).

Among the methods for metal removal, adsorption is seen as one of the most common and effective processes for antimony removal (Abdel & Mohamed, 2013). Adsorption has various advantages over the other removal methods due to its simple design, fastness, low initial and operation cost, high efficiency and simple operation (Abdel & Mohamed, 2013; Yang et al., 2015). Besides its many advantages, the success of adsorption mainly depends on discovery and usage of an adsorbent that could remove antimony efficiently (Abdel & Mohamed, 2013). The summary of studies performed to find efficient and low-cost adsorbents and optimum treatment conditions are given in below paragraphs.

Yu et al. (2014) investigated efficiencies of granular activated carbon (GAC) and ferric chloride-modified activated carbon (FAC) on Sb(III) removal at different experimental conditions. Batch experiments were performed with 1.5 mg/l Sb(III) initial concentration to see the effect of several factors including different temperatures (15-45 °C), pH values (2-10) and adsorbent dosages (0.2-1.0 g/l). The highest adsorption capacties for GAC and FAC was found as 0.54 mg/g and 2.64 mg/g, respectively at pH 7 and temperature 25 °C with 1.0 g/l adsorbent.

Jia et al. (2013) performed a study to compare adsorption effects of different adsorbents which are three types of activated carbon (AC) and a kind of machine made coal. With 1 mg/l initial antimony concentration at 3.6 pH and 25 °C, machine made coal shows the highest removal efficiency as 52.4 %. And the other adsorbents coconut AC, coal based AC and apricot stone based AC have removal efficiency as 42.6 %, 31.3 % and 24.6 %, respectively.

Another study focused on adsorption effect of freshly prepared ferric hydroxide (FeO_xH_y) towards Sb(III) and Sb(V). The initial antimony concentration was between 12 and 360 µg/l and adsorbent FeO_xH_y dose was 80 mg/l as Fe. After 5 minute contact time, FeO_xH_y has 75 % and 83 % removal efficiency towards Sb(III) and Sb(V) at pH 5 respectively. After 30 and 120 minutes, 88 % and 95 % removal efficiency was observed for Sb(III). Freundlich model was better than Langmuir to describe the adsorption of Sb(III) and maximum adsorption capacity of Sb(III) and Sb(V) was found as 1.55 and 1.24 mg/g, respectively (He et al., 2015).

Abdel & Mohamed (2013) studied treatment of antimony by using multi walled carbon nanotube (MWCNT) at different experimental conditions. Effect of contact time, adsorption dose, pH, and temperature were observed in this study. At pH 7 and 25 °C with initial 4 mg/l Sb(III) concentration and 200 mg MWCNT, adsorption process has the highest removal efficiency. The rate of the Sb(III) removal was 58 % after 1 minute contact time and it reached to 80 % after 30 minute contact time. And then it stayed constant until the end of the experiment (120 minutes). Moreover, the adsorption capacity of MWCNT is found as 0.32 mg/g under these conditions.

Leng et al. (2012) suggested graphene as an adsorbent for the removal of Sb(III). Adsorption effect of graphene was studied under different conditions. Batch experiments were performed by using 10 mg graphene for the initial Sb(III) concentrations between 1 and 10 mg/l. According to the experiments, it was found that pH was an important parameter affecting adsorption process and the highest removal efficiency was achieved at pH 11. Their results indicated that the increase of the adsorption onto graphene with decreasing pH might not be controlled by electrostatic factors. These findings were based on van der waals interactions which possibly dominate electrostatic interactions. The result of equilibrium experiments were fitted to Freundlich and Langmuir isotherms. It was stated that Freundlich isotherm described the equilibrium adsorption data better than Langmuir isotherm. Moreover, the maximum adsorption capacity was found as 7.46 mg/g under optimum conditions.

Zhou et al. (2015) studied with synthetic beta zeolite supported by nanoscale zero valent iron (NZVI) to remove Sb(III). According to the BET (Brunauer–Emmet–Teller) analysis, the surface area of the NZVI-zeolite was determined as 392.37 m^2/g. Batch experiments were studied for antimony removal for the different initial Sb(III) concentrations ranging from 20 to 220 mg/l. 40 mg NZVI-zeolite was added to each of the 200 ml Sb(III) solutions. Adsorption equilibrium was achieved at 30 minutes and 80 % antimony removal efficiency was observed by 3 g/l NZVI zeolite. The equilibrium data fitted to Langmuir and Freundlich isotherms. The data fitted better to Freundlich model better than Langmuir model with respect to the correlation coefficient ($R^2 > 0.95$ for Freundlich). Additionally, the maximum adsorption capacity was calculated as 7.65 mg/g.

Antimony adsorption on kaolinite was investigated by Xi et al.(2014). According to the BET analysis, surface area of the kaolinite was 15.8 m^2/g. For the batch experiments, 500 mg kaolinite was added to each of the 20 ml Sb(III) solutions. Initial Sb(III) concentrations were between 0.05 and 3 mg/l at pH 6.5 in the temperature range from 10 to 45 °C. The adsorption data were successfully fitted to Langmuir ($R^2 > 0.95$) and Freundlich ($R^2 > 0.95$) models. The maximum adsorption capacity was calculated as 0.42 mg/g and adsorption of Sb(III) is higher at low temperatures.

Sb(III) and Sb(V) simultaneous adsorption on ferrihydrite was investigated by Qi & Pichler (2016). According to the study, the simultaneous presence of Sb(III) and Sb(V) species did not have any impact on Sb(III) adsorption but Sb(III) presence significantly affect Sb(V) adsorption adversely. Presence of Sb(III) has inhibitory effect on Sb(V) adsorption. Batch experiments were carried out at neutral pH and room temperature. For the 2 mg/l initial Sb(III) concentration and 40 mg/l adsorbent dose, the adsorption capacity of Sb(III) on ferrihydrite was found about 35 mg/g.

Watkins et al. (2006) studied the adsorption of Sb(III) on synthetic goethite (α-FeOOH). Batch experiments were performed at 25 °C. The sorption process was fast and equilibrium of the sorption is achieved within 15 minutes. The adsorption data were fitted to Langmuir ($R^2 > 0.83$) and Freundlich ($R^2 > 0.99$) models. For the initial Sb concentration ranged from 4.79 μg/l to 47.93 μg/l, the maximum adsorption capacity was found as 33 mg/g.

2.3.2.2 Coagulation-Flocculation

Coagulation-flocculation is also another treatment method commonly used for metal removal. Although this method is not a specific process to remove antimony, limited available studies on this subject show that conventional coagulants provides considerable success on antimony removal (Ungureanu et al., 2015). For water and wastewater treatment, iron and aluminum based coagulation-flocculation processes are among the most common treatment technologies for hazardous elements elimination due to its low cost and easy applicability. In order to simulate coagulation-flocculation process, jar testing method is used as a pilot scale test. By this test, general information about which coagulant will work best, the required amount of chemicals for treatment and proper system pH for the highest removal efficiency can be determined (Satterfield, 2005).

The common coagulants can be classified as iron and aluminum based ones. When the coagulants are added to water, they form charged metal-hydrolysis species and precipitate as floc particles. The efficiency of hydrolysis species depends on mixing, pH and coagulant dosage. These reactions consume alkalinity and decrease pH of the

solution (IWA, n.d.). Some examples of the antimony removal studies via coagulation-flocculation are given in below paragraphs.

Guo et al. (2009) worked on removal of antimony compounds from drinking water via Coagulation-Flocculation-Sedimentation (CFS) process. The removal efficiency of CFS process has been investigated with respect to initial Sb(III) and Sb(V) concentration, coagulant type and dosage, pH and other ions present in the solution. For 50, 100, and 500 μg/l initial antimony concentrations, 0.1, 0.2 and 0.3 mM alum and ferric coagulants were prepared to determine optimum coagulant dose and type. With ferric chloride (FC), while effective removal is observed for Sb(III) within the pH range from 4 to 10, for Sb(V) it is determined at pH 4.5-5.5. Although 99 % high removal efficiency of FC coagulant, removal efficiency with aluminum sulfate was about 25 %, so it is not proper coagulant for antimony removal. Moreover, while the presence of humic acid and phosphate influence the removal of Sb(V), they do not have any important effect on Sb(III) removal.

Du et al. (2014) developed a combined coagulation–flocculation–ultrafiltration (CF–UF) process for Sb(III) removal. Ferric coagulant dose, pH, and initial Sb(III) concentration were arranged in order to optimize the process. In this system, during coagulation hydrous ferric oxide (HFO) particles are formed and Sb(III) is adsorbed on these particles. Then, the formed complex compounds are removed from the water by ultrafiltration. According to the conducted experiments, at 28 °C, pH values between 7.1 and 9, with 30-158 μg/l initial antimony concentration 90 % removal is achieved by using 0.4 mM ferric coagulant for this hybrid process.

In another study, coagulation process was investigated to remove antimony in surface water and groundwater. For the study, ferric sulphate ($Fe_2(SO_4)_3$) was used as a coagulant to optimize coagulation process. The experiments performed by using real sample taken from antimony containing surface water and groundwater. For the surface water sample, 40 mg/l ferric sulphate was dosed to decrease initial 29.4 μg/l antimony concentration to below 5 μg/l, drinking water limit value of Slovakia. The experiments performed with groundwater sample required 150 mg/l ferric sulphate to decrease 66.8 μg/l antimony concentration to below 5 μg/l. The process was

successful in removal of antimony, but decrease of pH to 3.2 and increase in Fe content in treated water are the disadvantages of this process (Barloková et al., 2012).

Kang et al. (2003) studied removal of antimony species by coagulation method, comparing efficiencies of polyaluminium chloride (PACl) and ferric chloride (FC) usage as coagulant. In the scope of the study, effect of system pH, coagulant dose and prechlorination on antimony removal was handled to be able to reduce the antimony concentration below the standard antimony level of South Korea which is 2 μg/l. Jar test results show that removal of Sb(III) by using FC has higher removal efficiency than that of PACl. For 6 and 40 μg/l initial concentrations, FC removal efficiency was found above 90 % at optimum pH 5, however with PACL only 40 % removal efficiency was achieved for the same conditions. Also, it was concluded that chlorination of Sb(III) solutions before coagulation affects the removal of antimony negatively. It decreases the ability of FC coagulant to remove Sb(III).

2.3.2.3 Membrane Processes

Membranes are semipermeable barriers that can be used in separating two phases. Membrane permeability depends on their pore sizes. Very small pores inside the membrane allow the passage of materials through the membrane which are smaller than pores and block the ones larger than the pores (Servos, 2014).

Membranes used in water and wastewater treatments are categorized in two main groups as porous and nonporous membranes. Porous membrane separation based on sieving mechanism or size exclusion. On the other hand, non-porous membranes separate molecules based on solubility differences. Molecule penetration to the permeate side happens by diffusion of the molecule to the other side when it is dissolved in membrane. While microfiltration (MF) and ultrafiltration (UF) membranes are among the porous membrane, Reverse Osmosis (RO) is a typical nonporous membrane. Nanofiltration (NF) is between RO and UF and their separation based on sieving and solution diffusion (Shirazi et al., 2010).

Properties of the most common used membrane MF, UF, NF and RO are given in Table 3. There are number of studies on effective removal of arsenic which has similar chemistry to antimony, by membrane processes. However, research on the antimony removal with membrane processes are very rare and not much information about these studies are found in the literature (Ungureanu et al., 2015).

Table 3. Properties of typical membranes used in water and wastewater treatment (Shirazi et al., 2010)

Membrane	**Pore size (nm)**	**Operating Pressure (kPa)**	**Applications**
MF	50-2000	10-50	Separate particles and bacteria from other smaller solutes
UF	2-50	50-200	Separate colloids from solutes such as sugar or salts
NF	< 2 or nonporous	200-1000	Separate multivalent salts, pesticides, herbicides, etc., from water
RO	nonporous	1000-10,000	Separate monovalent salts, small molecules and solvents, etc., from water

Limited availability of studies on antimony removal are given in below paragraphs.

Kang et al. (2000) worked on antimony removal efficiency of reverse osmosis membranes and identified effect of solution pH on the process. According to result of the membrane experiments, removal of Sb(V) is higher than Sb(III) in pH range 3-10. For Sb(V) species removal efficiency was larger than 80 % on the other hand for Sb(III) removal was about 60 %. Also, the results show that both Sb(Ill) and Sb(V) removal are nearly constant at pH range 3-10. So, it can be concluded that removal of Sb compounds does not depend on solution pH which can be explained by oxidation state of antimony changes from Sb(III) to Sb(V) within short periods of time.

In a project conducted by USEPA, antimony removal in drinking water was studied by using Point-of-Entry (POE) Reverse Osmosis (RO) Coupled with Dual Plumbing Distribution instead of conventional reverse osmosis. In influent water, antimony concentration ranged from 8.6 to 13.2 µg/l and was mainly present in soluble form. Evaluation of the performance after reverse osmosis system shows that 99 % removal efficiency was observed. The POE-RO system reduced antimony concentration from 10.8 to below 0.1 µg/l in filtrate water. The reject water was the only residual of this treatment system. The reject water was corresponds to 60 % of feeding water to the system and contains 17.7 µg/l of antimony (Wang et al., 2011).

2.4 Zeolite

Zeolites are three dimensional, crystalline solids that contain aluminosilicate framework, exchangeable cations and zeolitic water. Various types of zeolites have been determined in nature. The most common forms are clinoptilolite, analcime mordenite, stilbite, chabazite, phillipsite, and laumontite. In addition to these types, paulingite, barrerite, offretite and mazzite are rarely found in the world. Clinoptilolite, most abundant natural zeolite has wide applications for many different purposes (Wang & Peng, 2010).

Zeolites have been used in different sectors with increasing interest since 1980 in Turkey. In 1971, analcime occurrences were detected in the vicinity of Bilecik/Gölpazarı and Bolu/Göynük. Then, analcime and clinoptilolite deposits were found in the west of Ankara. These two types are the most commonly observed types of zeolite in Turkey. Moreover, deposits of different type of zeolite species such as chabazite, phillipsite, mordenite and erionite are also found in Turkey. The most significant zeolite deposits are located in Manisa/Gördes and Balıkesir/Bigadiç. The zeolites obtained from these locations can be easily processed for further uses. It is estimated that total zeolite reserve in Turkey is nearly 50 billion tons (Kırşan, 2004).

According to the study of MTA, the clinoptilolite deposit in Manisa/Gördes is 2 billion. Due to high clinoptilolite content and absence of undesirable substances such

as boron, the raw material in this region is more favorable (Kırşan, 2004). High quality zeolites mainly composed of clinoptilolite and heulandite are mined in Manisa/Gördes region. Both of them have same structure but different chemical and physical properties. Clinoptilolite has richer silica content than heulandite and is more heat resistance (Bilgin & Kokturk, n.d.). The zeolite ore mined from Gördes region is shown in Figure 4.

Figure 4. Gördes zeolite (Bilgin & Kokturk, n.d.)

Turkey's zeolite deposits map is given in Figure 5. The latitude and longitude coordinates of the zeolite reserves are taken from Kırşan (2004) to create the map given below.

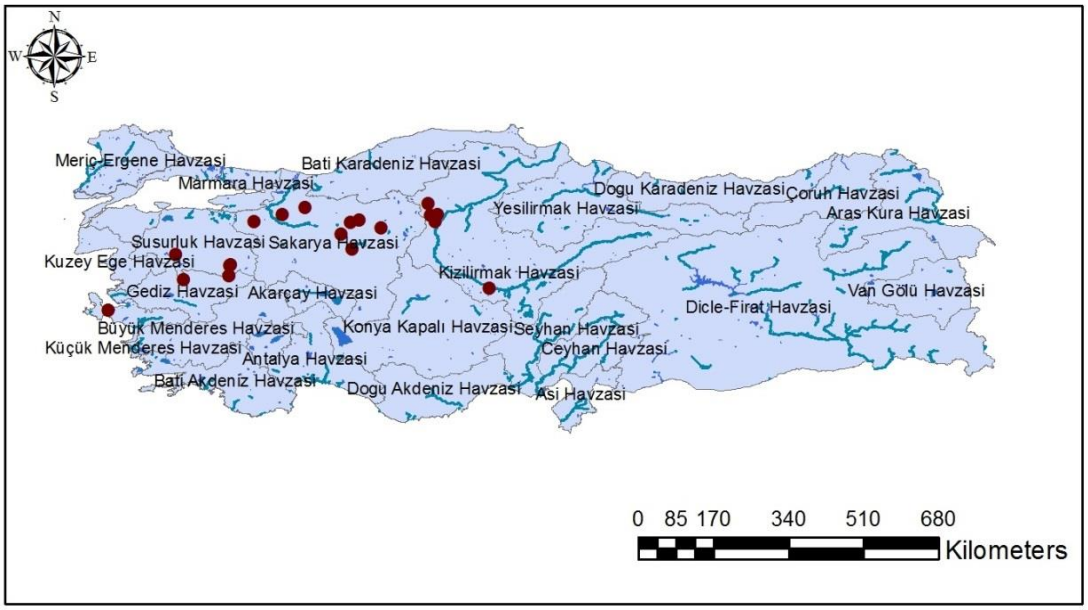

Figure 5. Turkey's zeolite deposits map

2.4.1 Properties of Zeolite

The general formula for zeolite is $M_{2/n}$ O*Al_2O_3*xSiO_2*yH_2O ; where M is ion balancing any alkali or alkaline element such as Na^+, K^+ and Ca^{2+} etc., n is the charge of metal cation, x for the number of Si tetrahedron between 2 and 10 and y for the number of water molecules between 2 to 7 (Jha & Singh, 2016).

The silicon $(SiO_4)^{4-}$ and aluminum $(AlO_4)^{5-}$ atoms are tetrahedrally joined by shared oxygen atoms located at corners of each tetrahedron (Elaiopoulos, Perraki, & Grigoropoulou, 2010). Aluminosilicate framework is stable part, identifies the structure type and contains pores, voids and channels. Cations commonly Na^+, K^+ and Ca^{2+} balance this negative charge on the framework. Furthermore, the water molecules (zeolitic water) are present in the pores, channels and voids and bonded between the framework and the cations (Wang & Peng, 2010). The crystalline structure built from $(SiO_4)^{4-}$ and $(AlO_4)^{5-}$ and shared oxygen atoms located at corners of each tetrahedron showed in Figure 6.

Size and great number of the cavities and channels in the structure shows that zeolite has a high surface area, and so it can absorb large amounts of substances not just water. These channels make easy float of the ions and molecules into and out of the structure.

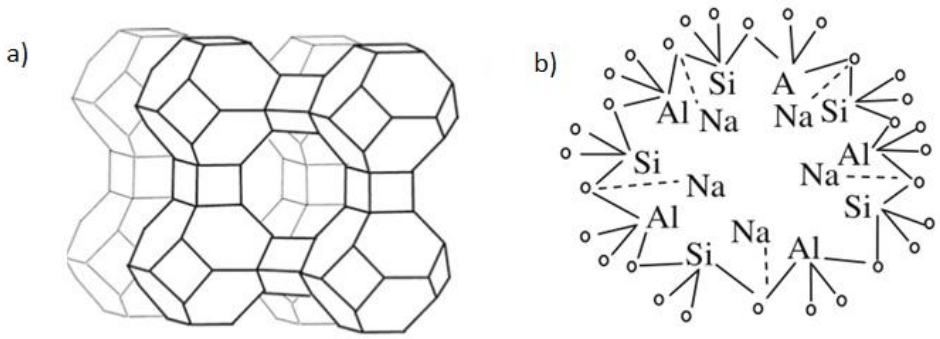

Figure 6. a) Schematic view of the crystal structure of zeolite and b) $(SiO_4)^{4-}$ and $(AlO_4)^{5-}$ atoms in a ring of sodium zeolite (Jha & Singh, 2016)

2.4.2 Zeolite as an Adsorbent

High adsorption capacity, low cost, ecofriendliness and easy management are the key features of an effective and economical adsorbent. As the most common adsorbent, active carbon has been used for removal of any organic pollutants due to its high surface area and removal capacity. Despite of its high effectiveness on removal of organic matters, it is not as good as at removal of heavy metals and other inorganic pollutants (Abd El Maksod et.al., 2016). Moreover, due to its high production and maintenance cost, the use of active carbon is not suitable especially in developing countries. On the other hand, because of zeolites' porous structure, molecular sieving and sorption properties, abundance in many regions and low cost, use of natural zeolite as an adsorbent has gained importance among researchers (Wang & Peng, 2010).

Existence of negatively charged, small sized pores and channels on zeolites surface, provide them having high adsorbent and absorbent properties. Moreover, they are called as "molecular sieves" that enable cation exchange during adsorption (Jha & Singh, 2016). As a result of its thermal stability, acid resistance, and sieve framework structure, zeolite has wide range of usage area such as ion exchange, removal of heavy metals, catalysis, agriculture, gas separation, etc. (Gevorkyan et al., 2002).

The cations on zeolite structure are available for exchange with cations in solution such as Pb^{+2}, Cu^{+2}, Fe^{+3}, and Cr^{+3}. Since the zeolite exchangeable cations are relatively harmless, they are particularly suitable to remove certain heavy metals from wastewater (Erdem et al., 2004). Due to its mentioned properties and characteristics

and availability in large deposits, zeolites are considered as effective adsorbent for removal of contaminants from water and wastewater. Some of the examples for zeolite use for contaminant removal are given in below studies.

Zanin et al. (2017) studied on adsorption effect of natural zeolite (clinoptiolite) to remove copper, chromium and iron in graphic industry wastewater. For the experiment, 0.5 grams zeolite with a particle size in the range of 0.4 to 1 mm was added to 100 ml solution. Results showed that zeolite has high removal effect on these metals. Removal rate were 96 %, 95.4 % and 85.1 %, respectively for copper, iron and chromium at 25 °C and pH 4. And for copper and chromium, adsorption mechanism followed pseudo first order kinetic model and iron followed pseudo second order model. Moreover, zeolite did not show any toxic effect on treated effluent.

Another study was conducted to examine adsorption of Cd^{+2}, Pb^{+2}, Ni^{+2} and Cu^{+2} by pretreated clinoptilolite. Surface area of the zeolite used in experiment was 13 m^2/g and after pretreatment with hydrochloric acid it increased to 78 m^2/g. For the study, 0.5 grams clinoptilolite with a range of 0.125 to 2 mm was added to 200 ml synthetic solutions. Then the samples were shaken separately with 10-800 mg/l initial concentrations of Pb^{+2}, Ni^{+2} and Cu^{+2} and 1-80 mg/l of Cd^{+2}. As a result of batch studies, maximum adsorption capacity of zeolite was determined as 4.22 mg/g for cadmium at 80 mg/l initial concentration and 27.7, 25.76 and 13.03 mg/g for lead, copper, and nickel, respectively at 800 mg/l concentration. The founded capacities are not the ultimate zeolite capacities for these elements, many studies evaluated sorption capacity of zeolite but the results are considerably different form each other (Sprynskyy et al., 2006).

Vivacqua et al. (2013) studied adsorption effect of clinoptilolite on zinc removal. Experiments were carried out in a slurry bubble column filled with 100 grams of zeolite. The diameters of zeolite particles are between 0.3 and 1.4 mm. Experiments were conducted at 15 °C for 1 hour. According to results, adsorption capacity increased with decreasing clinoptilolite particle diameter. For the particle size range between 0.3 and 0.5 mm, maximum adsorption capacity was found as 10.49 mol/kg.

In another study, clinoptilolite treated with cetylpyridinium surfactant were used for adsorption of zearalenone. Batch experiments were conducted with 6 mg of adsorbent in the pH range between 2 and 12. Each of the 10 ml sample with initial zearalenone concentrations ranged from 1 to 4.5 mg/l was shaken for 30 minutes. At pH 7, highest adsorption capacity was achieved as 6.98 mg/g for clinoptilolite treated with cetylpyridinium (Dakovi et al., 2017).

Yousef et al. (2011) investigated natural zeolites as adsorbents for removal of phenol. The experiments were conducted at pH 4 for the initial phenol concentrations ranged from 10 to 100 mg/l. For batch method, 50 ml samples were shaken at 150 rpm at temperature between 25 and 55 °C. Results showed that adsorption capacity was found to increase as initial phenol concentrations increases. After reaching equilibrium in 24 hours, maximum adsorption capacity was found as 34.5 mg/g at 25 °C.

Morali (2006) used clinoptilolite to remove zinc and lead from aqueous solutions in the scope of thesis study. Experiments were conducted with raw clinoptilolite and conditioned one. Conditioning is performed with NaCl to replace cations on zeolite structure with cations which are easily undergone to ion exchange process. Maximum adsorption capacities for zinc are 0.14 meq/g (raw clinoptilolite) and 0.39 meq/g (conditioned) and for lead 0.51 meq/g (raw clinoptilolite) and 1.10 meq/g (conditioned). Experimental results were fitted successfully to Langmuir isotherm model. Results showed that more effective removal for lead was achieved and even for lower zinc adsorption capacities conditioning improve capacity of clinoptilolite.

In another thesis study, removal of copper and nickel ions by clinoptilolite were investigated. Experiments were also conducted with raw clinoptilolite and conditioned one. Experiments indicated that pH 5 and 4 are optimum for copper and nickel removal, respectively and contact time is required as 48 hours to reach equilibrium. Maximum adsorption capacities for copper are 0.31 meq/g (raw clinoptilolite) and 0.5 meq/g (conditioned) and for nickel 0.32 meq/g (raw clinoptilolite) and 0.43 meq/g (conditioned). Experimental results were well fitted to Langmuir isotherm model than Freundlich model. Results of the exploration of the exchangeable cations showed that both of copper and nickel ions have highest preference on sodium ions (Çağın, 2006).

CHAPTER 3

MATERIALS AND METHODS

3.1 Set up

The stock solution of Sb(III) was prepared by dissolving Potassium antimony (III) oxide tartrate trihydrate ($K_2(SbO)_2C_8H_4O_{10}*3H_2O$; Merck Grade) in deionized water. Among different antimony species, Sb(III) was used for experiments since trivalent Sb species is described more toxic than pentavalent forms (Filella et al., 2002a). Moreover, NaOH and HNO_3 solutions were used to adjust pH of used solutions.

All the chemicals used for the experiments were analytical grade reagents. Deionized water was used for the preparation of solutions for experimental studies.

Antimony measurements were conducted by using Perkin Elmer AAnalyst 400 Atomic Absorption Spectrometry (AAS). For the antimony measurement, specific Lumina hollow cathode 2"lamp-Sb was used. Atomic Absorption Spectrometry was calibrated before each measurement by at least five points calibration. For the calibration, atomic absorption standards were prepared with commercially provided 1000 µg/l concentration of antimony analytical standard (VHG-PSBH-100). The calibration curve is given in Appendix A. Additionally, Hach-HQ40D portable multi meter was used for the pH and temperature measurements and the multi meter was calibrated weekly by using buffer solutions.

All glass materials, bottles, and pipets used for the experiments and analyses were washed with HNO_3 solution and rinsed with distilled and deionized water before every usage.

3.2 Adsorbents-Zeolite

Zeolite (clinoptilolite) samples used in the experiments were directly supplied from Gördes Zeolite Company. According to the data sheet provided by the company, the properties of the zeolite are summarized in Table 4. Other properties and detailed information about the zeolite sample are given as technical data sheet in Appendix B.

Table 4. Properties of the zeolite used in experiments

General Technical Specifications	
Chemical Name	Hydrated sodium-potassium-calcium-alumino-silicate
Chemical family	Natural zeolite
Chemical abstract name	Clinoptilolite
Chemical formula	$Na_{0.5}K_{2.5}Ca_{1.0}Mg_{0.5}Al_6Si_{30}O_{72}*24H_2O$
Main Mineral Content	
Clinoptilolite Group	80-90 %
Main Chemical Composition	
SiO_2	64.7 %
Al_2O_3	11.2 %
Fe_2O_3	1.4 %
Physical Characteristics	
Specific gravity	2 g/cm^3
Thermal stability	Stable up to 840 °C
Porosity	~35 %
Surface area	40.79 m^2/g

Zeolite samples were washed with distilled and deionized water about 10 times and dried at oven at 105 °C for 24 hours. It was stored in a desiccator until its use. The washed zeolite samples before (left side) and after (right side) drying at oven are given in Figure 7.

Figure 7. Zeolite samples before (left) and after (right) drying

3.3 Zeolite Characterization

Natural zeolite was characterized with Brunauer–Emmett–Teller (BET), Scanning Electron Microscopy (SEM) and X-Ray Diffraction spectrum (XRD) analysis. BET is a commonly used valid method to determine specific surface area of solids. Surface areas are measured by employing BET theory to nitrogen adsorption isotherms at 77 K (Walton & Snurr, 2007). SEM is a type of microscope uses focused beam of electrons to produce signals on the surface of sample. The signals are used to characterize the topography of surfaces and generate information about texture and structure of the sample (Swapp, 2014). For the analysis, zeolite samples were covered with a thin layer of gold and two samples of zeolite before and after antimony adsorption were examined under Scanning Electron Microscopy in order to see effects of adsorption on zeolite structure. XRD pattern is a plot of the X-Ray intensity scattered at different angles by the sample. This analysis were applied to get information on the crystalline components present in the sample (Speakman, n.d.)

BET and XRD analyses were carried out in Central Laboratory of METU and SEM analysis was performed in Metallurgical and Materials Engineering Department of METU.

3.4 Batch Kinetic Tests

Batch kinetic experiments were performed by adding 5 grams of zeolite in 250 ml antimony stock solutions at initial antimony concentrations of 5, 10, 20, 30, and 50 mg/l. Initial antimony concentrations were prepared by dissolving $K_2(SbO)_2C_8H_4O_{10}*3H_2O$ at proper amounts. The prepared solutions at 500 ml Erlenmeyer flasks were shaken by orbital shaker (ZHWY 200B, Zhicheng) at different agitation rates, temperatures and pH values. During and at the end of the shaking period, samples were taken and filtered at determined time intervals. Filtration was performed using 0.45 micrometer pores syringe filters to avoid the effect of turbidity on antimony measurement. Then, filtered sample immediately analyzed by AAS for antimony detection.

The equilibrium adsorption capacities of the samples were calculated according to following Equation 1.

$$q_{eq} = \left(\frac{c_i - c_{eq}}{m}\right) * V \quad (1)$$

where,

c_i = Initial antimony concentration (mg/l)

c_{eq} = Equilibrium antimony concentration after 4 hours (mg/l)

m = Mass of the zeolite (g)

V = Volume of the sample (l)

3.4.1 Effect of Initial Concentrations

Effects of initial antimony concentration on adsorption capacity were observed by changing all the parameters; pH, temperature and agitation. For different pH values, temperatures and agitation rates, samples' antimony concentrations were adjusted to 5, 10, 20, 30, and 50 mg/l. When determining minimum initial concentration in the experiments, detection limit of atomic absorption spectrometry which is 0.06 mg/l was considered.

3.4.2 Effect of pH

The pH effect on adsorption process was evaluated at different pH values for five initial antimony concentrations by keeping temperature and agitation at a constant value. The desired pH was adjusted using 0.1 M NaOH and 0.1 M HNO_3 at a negligible amount. For the experiments, pH values were set to 3, 5, 7, 9, and 10. Initial conditions of the pH experiments are given in Table 5.

Table 5. Initial conditions for the pH experiments

pH	Initial Sb concentrations (mg/l)	Temperature (°C)	Agitation rate (rpm)	Zeolite amount (g)
3, 5, 7, 9, 10	5, 10, 20, 30, 50	25	140	5

3.4.3 Effect of Temperature

The effect of temperature on adsorption capacity of zeolite was studied. At a particular temperature, five antimony solutions of different initial concentrations were prepared. For constant pH and agitation rate, temperature was adjusted to 20 °C, 25 °C, 30 °C, and 35 °C. For the temperature experiments, initial conditions are given in Table 6. During the experiments, temperature was measured in every 30 minutes and kept constant by cooling down or heating up by setting temperature controller of the shaker.

Table 6. Initial conditions for the temperature experiments

Temperature (°C)	Initial concentrations (mg/l)	pH	Agitation rate (rpm)	Zeolite amount (g)
20, 25, 30, 35	5, 10, 20, 30, 50	3	140	5

3.4.4 Effect of Agitation

Agitation effect on adsorption was observed in batch experiments at five different speeds which are 100, 120, 140, 180, and 200 rpm. During the experiment sets for different speeds, pH and temperature were kept constant, and only initial antimony concentrations were changed. For the shaking experiments, initial conditions are given in Table 7.

Table 7. Initial conditions for the agitation experiments

Agitation rate (rpm)	**Initial concentrations (mg/l)**	**Temperature (°C)**	**pH**	**Zeolite amount (grams)**
100, 120, 140, 180, 200	5, 10, 20, 30, 50	25	3	5

3.5 Adsorption Isotherms

To evaluate the concentration dependency of adsorptive capacity, commonly used conventional Langmuir and Freundlich isotherm models were used. Results were fitted to these conventional sorption models and best fitted equation was used to identify this adsorption equilibrium. For these equilibrium studies, initial antimony concentrations of 5, 10, 20, 30, 50 and 100 mg/l were investigated at pH 3 and 25 °C for 140 rpm agitation speed.

3.5.1 Langmuir Isotherm

Langmuir isotherm is theoretically derived a single layer model. Basic assumptions for the model are;

- There is homogeneous **monolayer** process between the adsorbate and adsorbent.
- Adsorption energy is uniform on the surface,
- All adsorption sites are identical,

- There is not any interaction between sorbent species,
- Sorbent molecules only interact with the site (Sarı et al., 2010; Xi et al., 2011a).

Because of the monolayer assumption, the model is more commonly valid for low concentration. This model can be written in non-linear form as given in the below Equation 2.

$$q_e = \frac{q_m * K_L * C_e}{1 + K_L * C_e} \quad (2)$$

where,

q_e = equilibrium amount of solute adsorbed per gram of adsorbent (mg/g)

C_e = equilibrium solute concentration in the solution (mg/l)

K_L = Langmuir adsorption constant (l/mg)

q_m = theoretical maximum amount of solute adsorbed (mg/g)

3.5.2 Freundlich Isotherm

Freundlich isotherm is a commonly used empirical model. Basic assumptions for the model are;

- There is a heterogeneous adsorption surface,
- Adsorption energy is not uniform on the surface,
- It is a **multilayer** adsorption,
- Adsorbed adsorbate concentration increases as concentration of adsorbate increases (Hamdaoui & Naffrechoux, 2007; Zanin et al., 2017).

Due to mentioned assumptions, this model is generally appropriate for high concentrations. This model can be written in non-linear form as given in the below Equation 3.

$$q_e = K_F * C_e^{1/n} \quad (3)$$

where,

q_e = equilibrium amount of solute adsorbed per gram of adsorbent (mg/g)

C_e = equilibrium solute concentration in the solution (mg/l)

K_F = Freundlich adsorpstion constant (l/mg)

1/n = Constant for adsorption intensity (dimensionless)

3.6 Coagulation - Flocculation

Ferric chloride and aluminum sulfate (alum) which are two widely used coagulants in water and wastewater treatments were selected for antimony removal in the study. Stock solutions of ferric chloride and alum were prepared by dissolving $FeCl_3*6H_2O$ and $Al_2(SO_4)_3*18H_2O$ in deionized water.

In order to investigate optimum coagulant type, dosage and pH of the solution, jar tests were performed in six beakers. Jar test is the simulation of the real coagulation-flocculation process in a lab scale. Jar tests were conducted with two coagulants at different initial antimony concentration. During the tests, temperature was kept constant at 25 ºC and pH was adjusted between 3 and 10. The jar test equipment used in the coagulation-flocculation experiments are given in Figure 8.

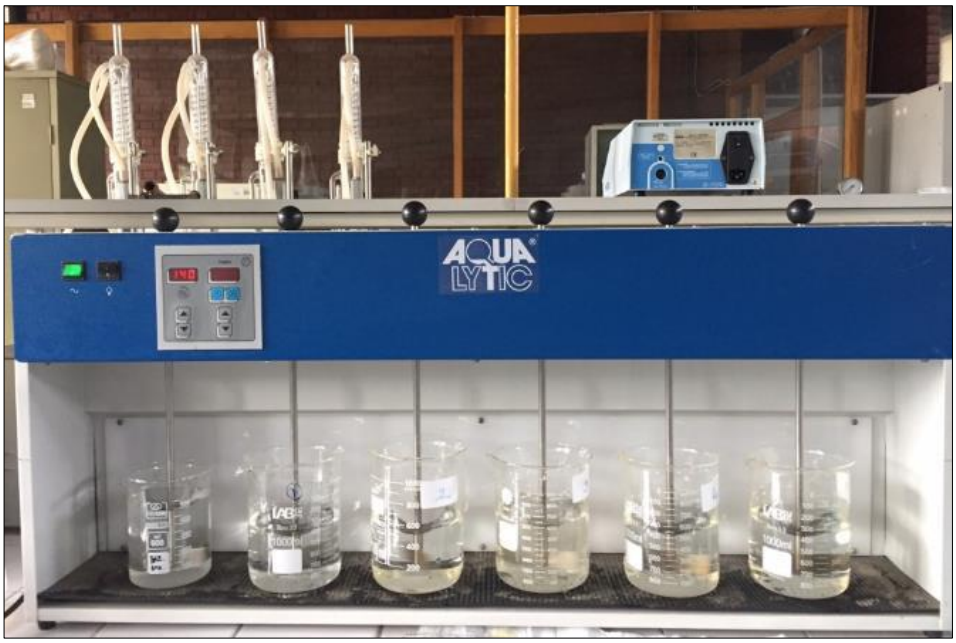

Figure 8. Jar test equipment

For these experiments, each jar was filled with 500 ml solutions at different initial concentrations and dosed with different amount of coagulant. For each test set, one of the beakers is chosen as control and coagulant was not added to see the effect of coagulant addition on antimony removal during the tests. Jar tests consist of three parts namely; rapid mixing, slow mixing and settling period. The samples were first mixed for 3 minutes at 140 rpm, followed by the slow mixing performed for 20 minutes at 40 rpm. Initial rapid mixing provides sufficient contact between coagulant and the contaminant particles by dispersing coagulant throughout each solution. Moreover, slow mixing helps promotion of floc formation. Then, after 30 minutes of the settling period was completed, flocs are settled to bottom and supernatant of the solutions were collected and filtered for the analysis. Filtration was performed using 0.45 micrometer pores syringe filters to avoid the effect of turbidity on antimony measurement. Jar test was carried out several times to find the optimum parameters for effective removal. The design parameters for the experiments are summarized in Table 8.

Table 8. Experimental design for coagulation-flocculation

Coagulant type	Initial Sb concentrations (mg/l)	pH	Coagulant dosage (mg/l)
Ferric chloride ($FeCl_3$*$6H_2O$)	5, 10, 20, 30, 50	3,7, 10	100, 200, 300, 400, 500
Alum ($Al_2(SO_4)_3$*$18H_2O$)	5, 10, 20, 30, 50	3,7, 10	100, 200, 300, 400, 500

3.7 Membrane Filtration

As an alternative option to adsorption for antimony removal, membrane filtration process was conducted. This method was performed to evaluate whether it is an applicable method or not to treat antimony containing water. The aim of conducting this experiment is to have a general idea about the performance of Reverse Osmosis (RO) and Nanofiltration (NF) membranes on antimony removal. The membrane filtration set-up in Abdullah Gül University was used in this experiment.

A lab scale cross-flow membrane filtration system (Sterlitech SEPA CF-II) was used in order to evaluate the performance of membranes for antimony treatment from aqueous solutions. The picture of the membrane system is shown in Figure 9. In this system, the effective area of flat sheet membranes is 150 cm^2 with dimension of 15 cm (length) and 10 cm (width). Feed tank volume of the system is 3 liters.

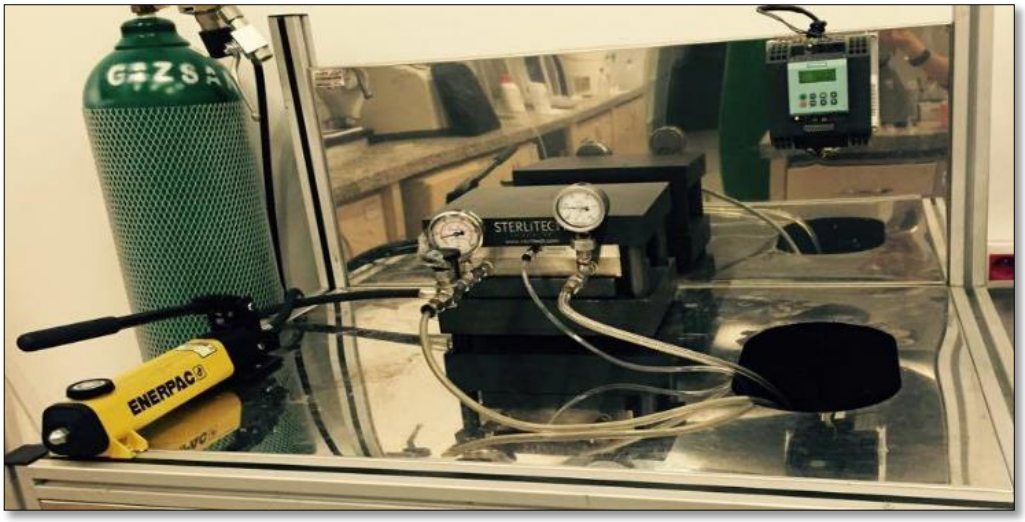

Figure 9. Membrane filtration system used for the experiment

For the reverse osmosis process, SW30 (DOW FILMTEC) RO membrane was used and pressure was kept constant at 15 bar and the temperature was at room temperature (25 ± 3 ºC) during the filtration. For nanofiltration process, NF270 (DOW FILMTEC) NF membrane was used and just as the RO process, pressure was kept constant at 10 bar and the temperature was at room temperature (25 ± 3ºC) during the filtration. The properties of membranes provided by the manufacturer are given in Table 9.

Table 9. Properties of membranes used in the experiments

Membrane	**Minimum Salt Rejection %**	**pH range**	**Maximum Operating Pressure (bar)**
SW30	99.65	2-11	45
NF270	97.00	3-10	41

The performance of membrane filtration is determined according to flux measurements. During the experiments, the system was firstly operated by using clean water until the steady state condition is reached. Initially clean water flux (J_{cw}) is determined and then the feed tank is filled with antimony stock solution. After reaching steady state, the flux of the raw water (J_{rw}) is measured and antimony

concentration at that time was taken as initial antimony concentration in removal calculations. Then, the tank is again filled with clean water and clean water flux after filtration (J_{cws}) is measured.

For the water flux calculation, followed Equation 4 was used.

$$J=\frac{V}{A*t} \quad (4)$$

where,

J = Water flux (l/m^2h)

V = Volume of the permeate (l)

A = Effective area of the membrane (m^2)

t = Time (hours)

The most important disadvantage of membrane systems is the flux decline as a result of membrane fouling. During the filtration of impurities in the water, the membrane gets clogged and loses its efficiency. The cross-flow membrane filtration is effective to prevent fouling by reducing shear on the surface (Choi et al., 2005). Total flux decline during the filtration is calculated according to Equation 5.

$$\text{Flux decline} = J_{cw} - J_{rw} \quad (5)$$

Moreover, the flux decline calculation as a result of fouling is calculated using Equation 6.

$$\text{Flux decline as a result of fouling} = J_{cw} - J_{cws} \quad (6)$$

Besides water flux calculations, antimony rejection is also monitored. For rejection of antimony Equation 7 is used.

$$\text{Rejection } (\%) = 1 - \frac{C_p}{C_f} * 100 \quad (7)$$

where,

C_f = Solute concentration in feed

C_p = Solute concentration in permeate

CHAPTER 4

RESULTS AND DISCUSSION

4.1 Antimony Levels in the Yeşilırmak River

According to results of the monitoring studies performed at four periods, antimony concentration in the vicinity of antimony mining site in Yeşilırmak River Basin exceeds the annual average EQS which is 7.8 µg/l for rivers/lakes. The certain sampling points downstream of Yeşilırmak River show consistent high values in reference to monitoring results. Samples collected at the discharge point of the antimony mining site (Yeşil-62) have very high antimony concentration, nearly 220 times higher than EQS. Moreover, at sampling points (Yeşil-19, Yeşil-21, Yeşil-33, Yeşil-34, and Yeşil-35) downstream of antimony mining site, concentrations were measured as about 5 times of EQS. Results indicate that surface waters in the downstream of antimony reserve are susceptible to antimony pollution. In Table 10, antimony concentrations of the sampling points that exceed EQS and average of the concentrations measured in four monitoring periods are given. Moreover, the locations of the sampling points are shown in Figure 10.

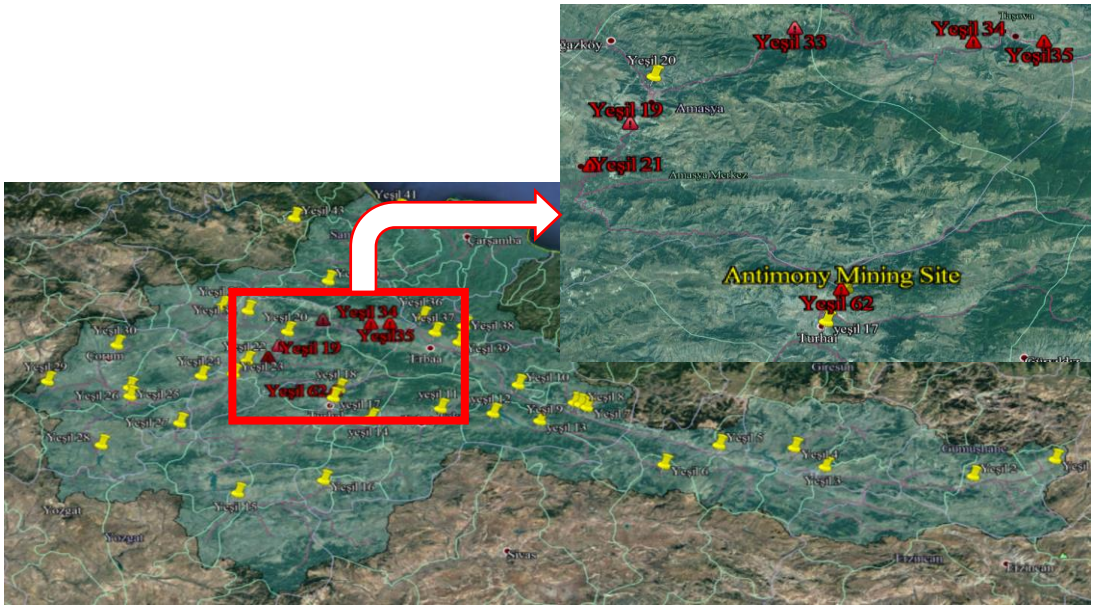

Figure 10. Sampling points in Yeşilırmak Basin

Table 10. Sb concentrations from monitoring studies of the sampling points around antimony mining site exceeding EQS in Yeşilırmak River Basin

Sampling points	Sb (µg/l) (August 2016)	Sb (µg/l) (October 2016)	Sb (µg/l) (February 2017)	Sb (µg/l) (April 2017)	Average Sb conc. (µg/l)
Yeşil-19	19.8	22.3	38.7	16.8	24.4
Yeşil-21	37.9	47.4	37.8	38.3	40.4
Yeşil-33	19.0	23.4	33.2	15.0	22.7
Yeşil-34	15.4	21.4	35.9	12.1	21.2
Yeşil-35	15.5	18.3	24.8	7.1	16.4
Yeşil-62*	-	-	**1694.2**	**1733.8**	**1714.0**

** The mining site discharge point*

As it can be seen from the results, antimony mining site can be evaluated as a point pollution source for antimony contamination. Hence, management of this point source is important to prevent pollution in Yeşilırmak River Basin. If the antimony level at the discharge point of the mining site is controlled via proper treatment methods, antimony pollution problem in the Yeşilırmak River Basin can be minimized.

Sampling points exceeds the EQS were given as bar graphs in Figure 11. It is observed that in winter season, Sb concentrations are relatively higher than other collection dates. In spring season, the concentration decreases significantly; however, measurements were still higher than EQS. In summer and autumn seasons, gradual increase in the concentration was detected. This fluctuation might be the result of the higher spring flow of the rivers due to that spring rains and melting snow increase runoff into the river during the spring season. This increment will cause to dilution of the contaminants. Generally, lake levels tend to decline in the autumn and reaching their lowest point in the late winter. These seasonal water amount variations in the river can be indicated as the reason of the differences in the monitoring results. Moreover, changes in the mine production activities during the year also have effects on these differences.

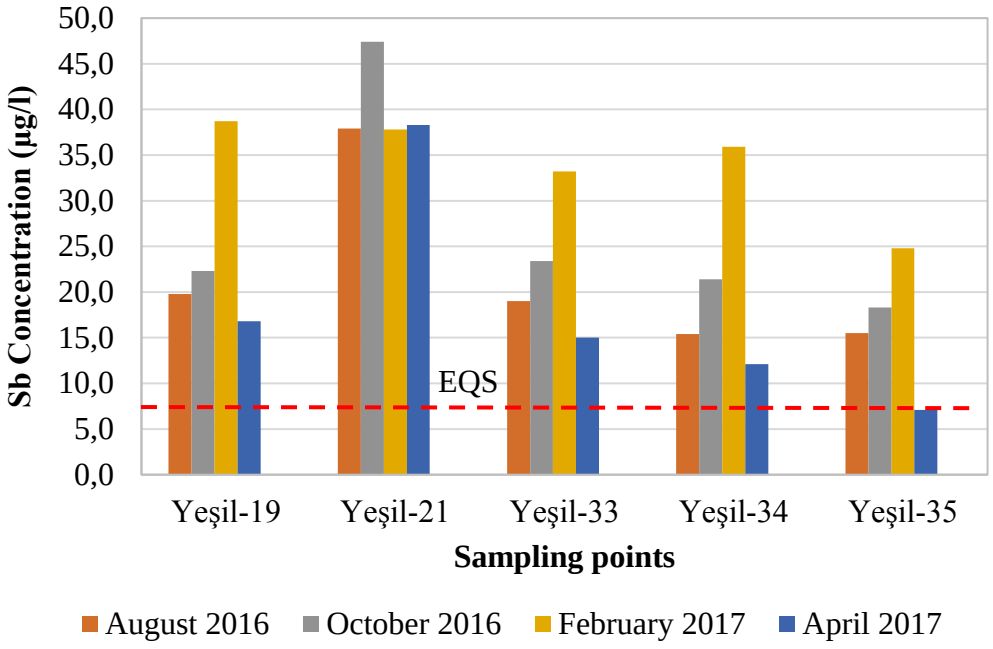

Figure 11. Results from Monitoring studies in Yeşilırmak Basin

4.2 Antimony Levels in Turkey

Antimony concentrations measured in previous studies were gathered and shown on the below map in Figure 12. Numbered locations on the map shows the locations where antimony concentrations were measured above the annual average EQS which

is 7.8 µg/l for rivers/lakes. It is seen that antimony concentrations were exceeds the EQS in the West Anatolia where antimony reserves are mainly located. As stated in the results of KIYITEMA project, points 1, 2 and 3 exceeded the EQS whereas exact concentrations were not stated. Also, in points 4, 5 and 6, the Sb concentrations were above EQS. It can be concluded that in the vicinity of antimony reserves, antimony pollution can be seen. Antimony concentrations on these locations are given on the map, detailed information about these previous studies are given in section 2.2.

Figure 12. Antimony concentrations in Turkey

4.3 Treatment of Antimony via Zeolite Adsorption

Porous structure, molecular sieving and sorption properties, abundance in many regions and low cost make zeolite suitable candidate as adsorbent for removal of wastewater pollutants (Wang & Peng, 2010). As previously mentioned in section 2.4, zeolites are indicated among the promising adsorbents for antimony removal. The use of natural zeolite as an adsorbent has gained interest among researchers; mainly due to that its sorption properties provide a combination of ion exchange and molecular sieve properties which can also be easily modified (Motsi et al., 2009). Moreover, it is quite economical and abundantly found especially in Turkey. And it is also nontoxic and harmless, so can be used for water treatments safely (Kırşan, 2004). The given maps of the antimony and zeolite reserves in Figure 1 and Figure 5, respectively, showed that both of the reserves are located in close regions, so supplying of zeolite will be easier for the treatment application that will be applied in the mining sites.

Also, low efficiency of activated carbon on metal removal has been revealed in other studies (Abd El Maksod et al., 2016). Therefore, for this study, zeolite was selected as the adsorbent for treatment of antimony containing solutions.

4.3.1 Zeolite Characterization

Specific surface area of the zeolite and pore properties were analyzed by the Brunauer, Emmett and Teller (BET) and Barrett–Joyner–Halenda (BJH) method. For BET technique, nitrogen gas was adsorbed to zeolite particles at 77 K. The surface area of the adsorbent was calculated by BET model of adsorption which incorporates multilayer coverage. According to the result of nitrogen multipoint BET analysis, specific surface area of the zeolite particles is found as 39.81 m^2/g. The result is very close to the surface area value provided by the manufacturer as 40.79 m^2/g.

According to the pore analysis performed via t-Method Micropore Analysis (de Boer), any micropore couldn't find for the zeolite sample. Classification done by IUPAC (International Union of Pure and Applied Chemistry) which characterized pores of clinoptilolite as mesopores (20-500 Å) also confirmed this result (Zanin et al., 2017). In Figure 13, pore volume and diameter result found by BJH method were plotted. These results showed that average pore diameter was measured as 27.17 Å which is in diameter range of mesapores.

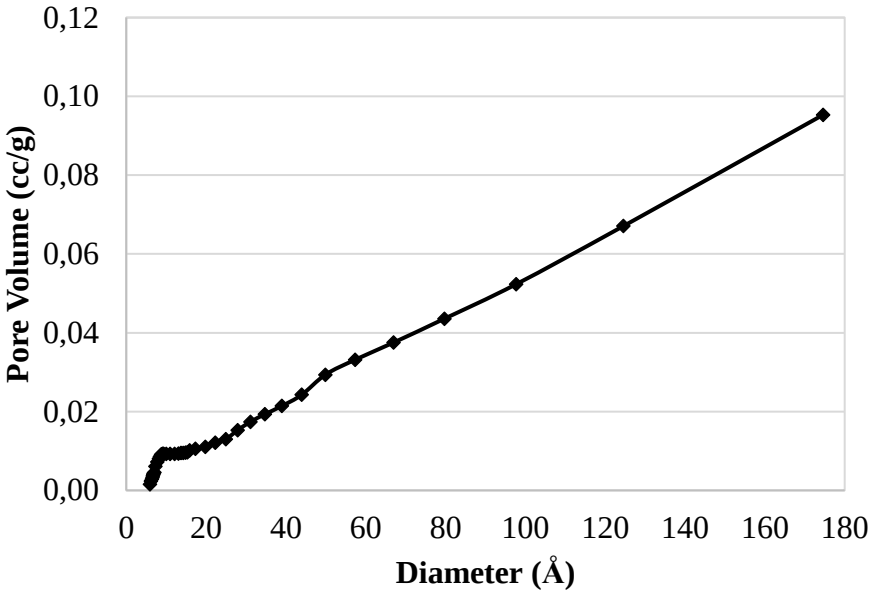

Figure 13. Zeolite analysis result, diameter vs pore volume

In literature search, characterization of zeolite was investigated. In study conducted by Zanin et al. (2017) specific surface area and average pore diameter of zeolite clinoptilolite were found as 59.63 m²/g and 38.72 Å, respectively. In another study, specific surface area of natural zeolite supplied from Turkey was 15.88 m²/g (Motsi et al., 2009). Moussavi et al. (2011) measured BET specific surface area and mean pore diameter of zeolite as 18.4 m²/g and 25.2 nm, respectively. In a study, specific area of the different zeolite samples were measured between the range of 20.4 and 62.8 m²/g (Pavlovic et al., 2013). As it is seen from the different studies, specific surface area and pore diameter of the zeolite change in wide range. As an adsorbent material, zeolite structure feature has an important impact on its adsorption performance; so zeolites with large surface area and total pore volume have better adsorption performance with respect to lower ones. Moreover, these surface properties can be also enhanced chemical treatments that remove impurities found in zeolite structure (Lin et al., 2013).

SEM analyses were conducted to observe differences on the zeolite surface before and after sorption experiments. In Figure 14, analyses results of the zeolite samples before adsorption are given. SEM images of the zeolite at x5000 magnification and x10000 magnification are shown in Figure 14-a and Figure 14-b, respectively. In Figure 15,

analyses results of the zeolite samples after adsorption are given. SEM images of the zeolite at x5000 magnification and x10000 magnification are shown in Figure 15-a and Figure 15-b, respectively.

Figure 14 and Figure 15 shows that noticeable change on the surface of the zeolite was occurred. Before the adsorption (Figure 14), smoother surface morphology was observed when compared to surface of the zeolite after adsorption. Moreover, typical crystal structure of clinoptilolite family can be seen in Figure 14 (Minceva et al., 2008). On the other hand, after adsorption, appearance of zeolite surface became rougher as a result of accumulation of antimony. As it can be seen from the images in Figure 15, in some part of the zeolite surface localization of antimony was observed.

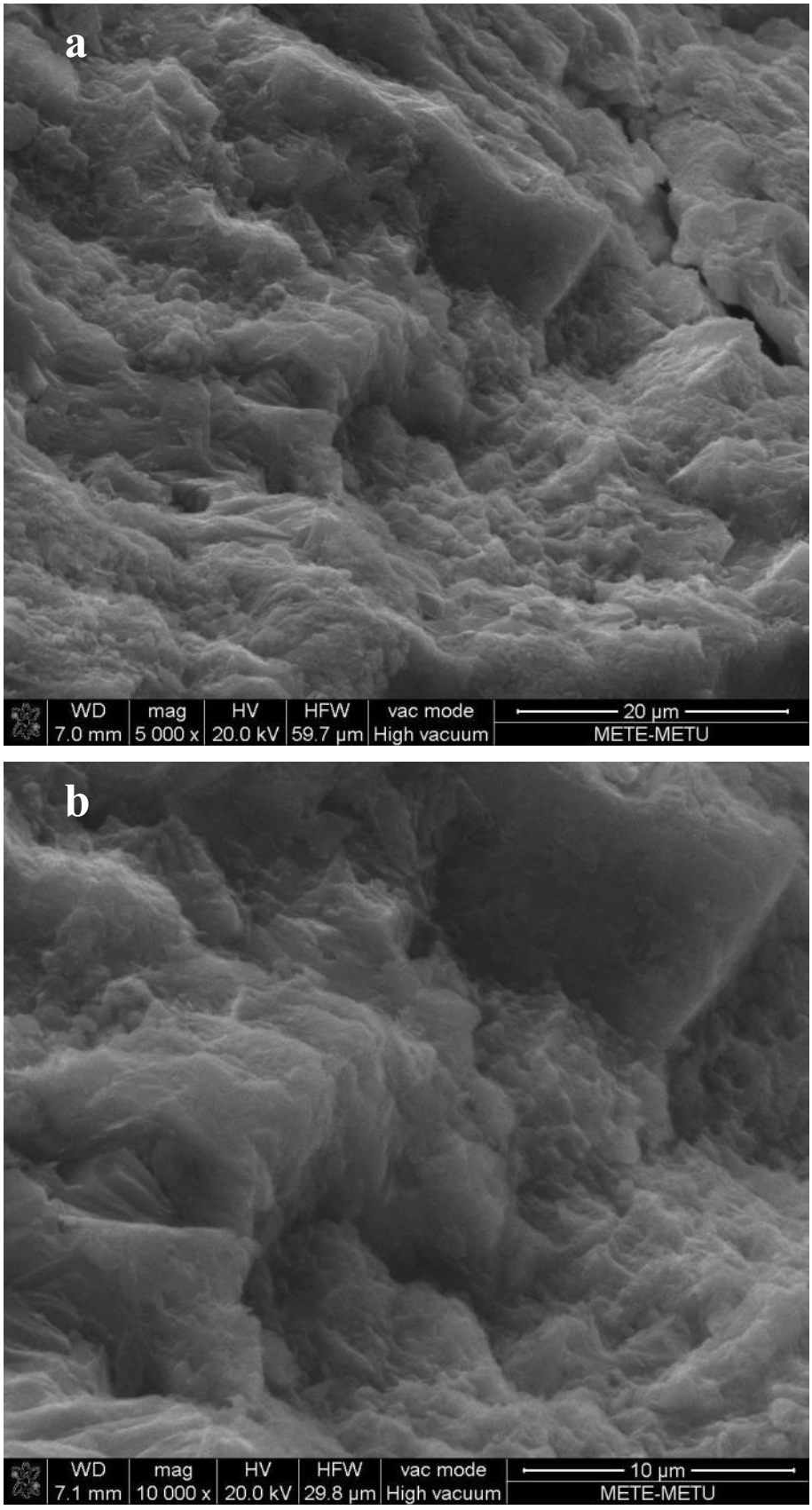

Figure 14. SEM image of zeolite before adsorption for (a) x5000 magnification and (b) x10,000 magnification

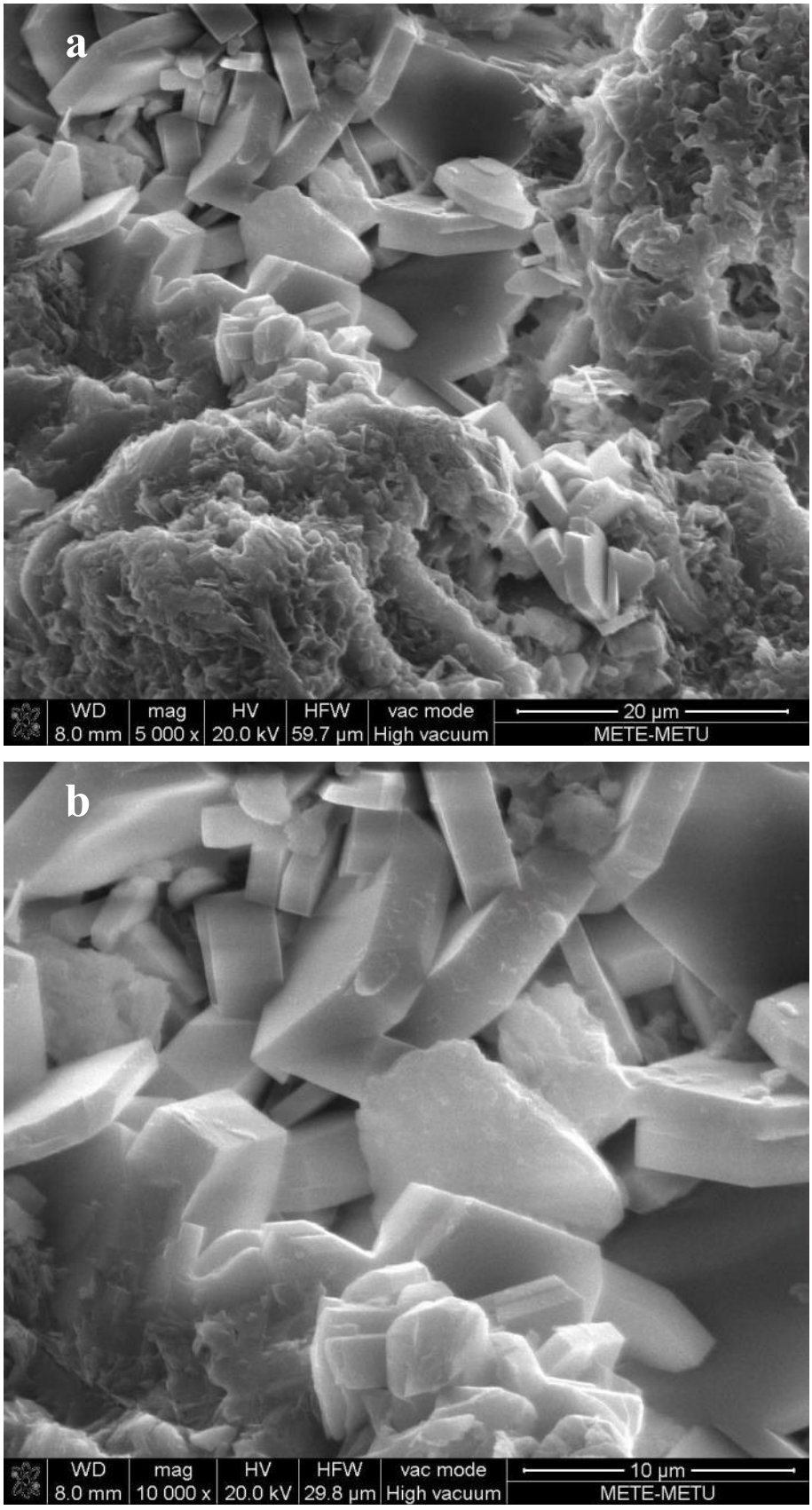

Figure 15. SEM image of zeolite after adsorption for (a) x5000 magnification and (b) x10,000 magnification

Lastly, XRD analysis was performed to determine the mineral composition. Analysis showed that the zeolite mainly consists of clinoptilolite which is about 80 %. And the remaining parts were identified as quartz hp (SiO_2) by XRD analysis. This result was very close to information given by manufacturer about mineral composition of zeolite.

According to the XRD analysis performed in METU Central Laboratory, the chemical formula of the Clinoptilolite was given as $|Na_{1.84}K_{1.76}Mg_{0.2}Ca_{1.24}(H_2O)_{21.36}|[Si_{29.84}Al_{6.16}O_{72}]$. The given plot as XRD analysis result in Figure 16, was also checked from the literature to compare the XRD pattern with the ones given for clinoptilolite (Treacy & Higgins, 2001). Clinoptilolite peaks in the below XRD pattern is similar with the given XRD plots for clinoptilolite in literature.

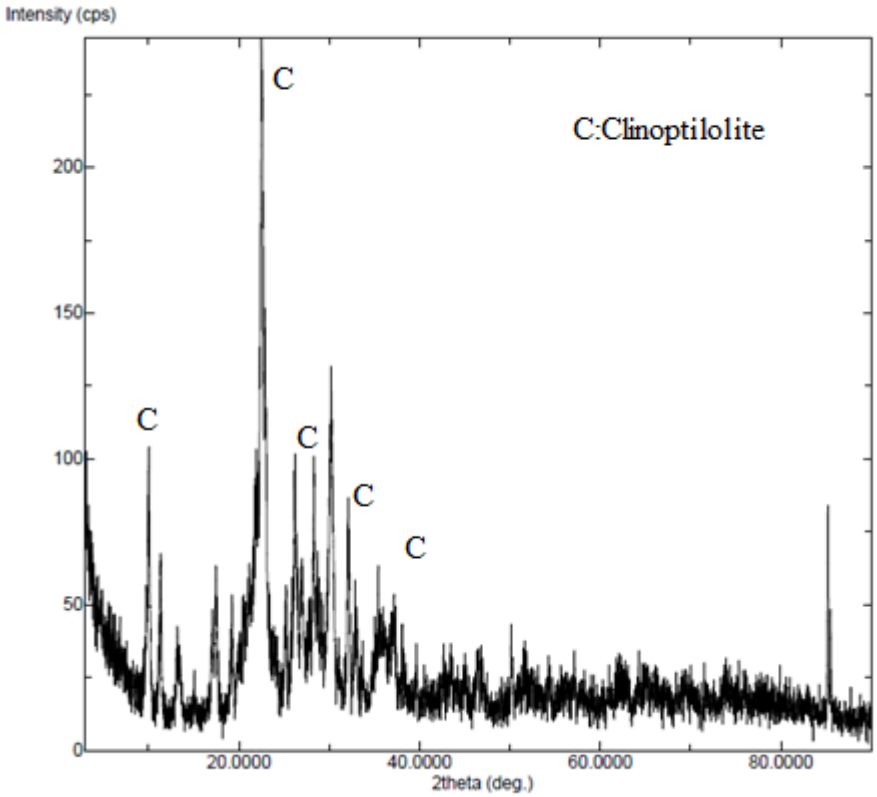

Figure 16. XRD Analysis of zeolite

4.3.2 Batch Kinetic Tests Results

Kinetic experiments were performed to investigate efficiency of zeolite on antimony removal under different conditions. It is seen that the process reaches equilibrium before 4 hours, therefore the batch kinetic experiments were performed for 4 hours to be in the safe side.

4.3.2.1 Effect of pH on Adsorption Capacity

The results of the pH experiments are given for the different pH values separately in Figure 17, Figure 18, Figure 19, Figure 20 and Figure 21. Standard deviation of the results according to duplicate experiments are shown on the graphs as error bars. Results show that adsorption capacity of zeolite decreases with increasing pH. At higher pH, decrease in adsorption capacity can be result of the competition between OH^- ions and predominant $(SbO_2)^-$ species for active sorption sites. As it can be seen from Figure 17, while adsorption capacity for 50 mg/l antimony concentration was found 2.02 mg/g at pH 3, Figure 21 shows that the capacity for the same initial concentration was 1.59 mg/g at pH 10. This trend was also observed for other initial concentrations. 5 mg/l initial concentration results in the least amount capacity for all pH values. The lowest capacity is found as 0.15 mg/g at pH 7 and highest one as 0.20 mg/g for 5 mg/l. Although achieving the lowest adsorption capacity for the lowest initial antimony concentration, removal efficiencies were found as the highest for the lowest initial antimony concentration. The highest removal efficiency was achieved as 85 % and 82 % for 5 mg/l and 50 mg/l initial antimony concentration at pH 3, respectively. Moreover, in order to see the pH effect on adsorption capacities clearly, adsorption capacity vs time graphs of each initial Sb concentrations for the same results were given in Appendix C.

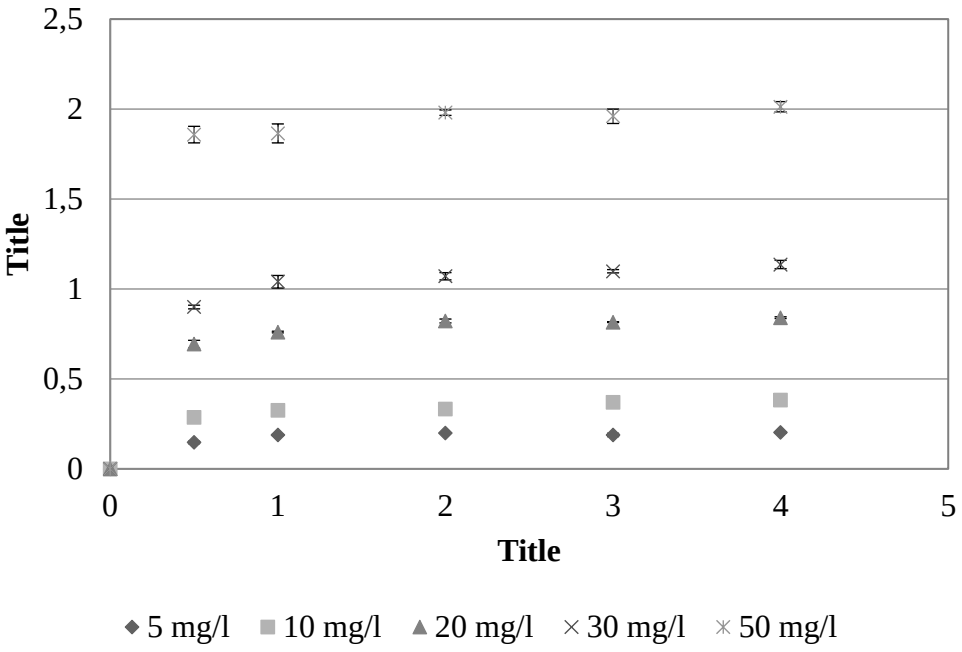

Figure 17. Change of adsorption capacity with time at pH 3

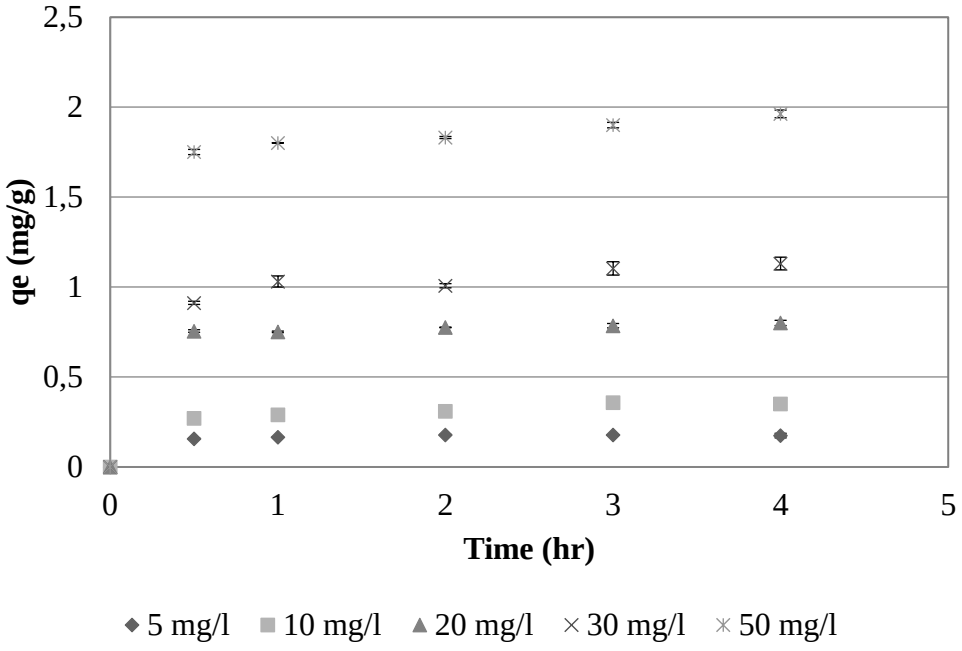

Figure 18. Change of adsorption capacity with time at pH 5

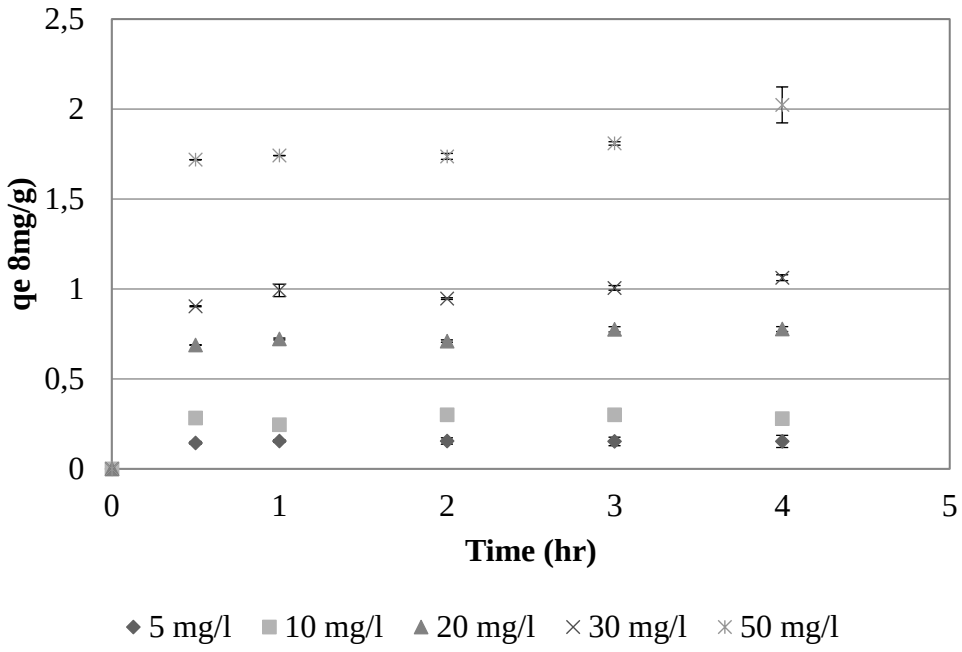

Figure 19. Change of adsorption capacity with time at pH 7

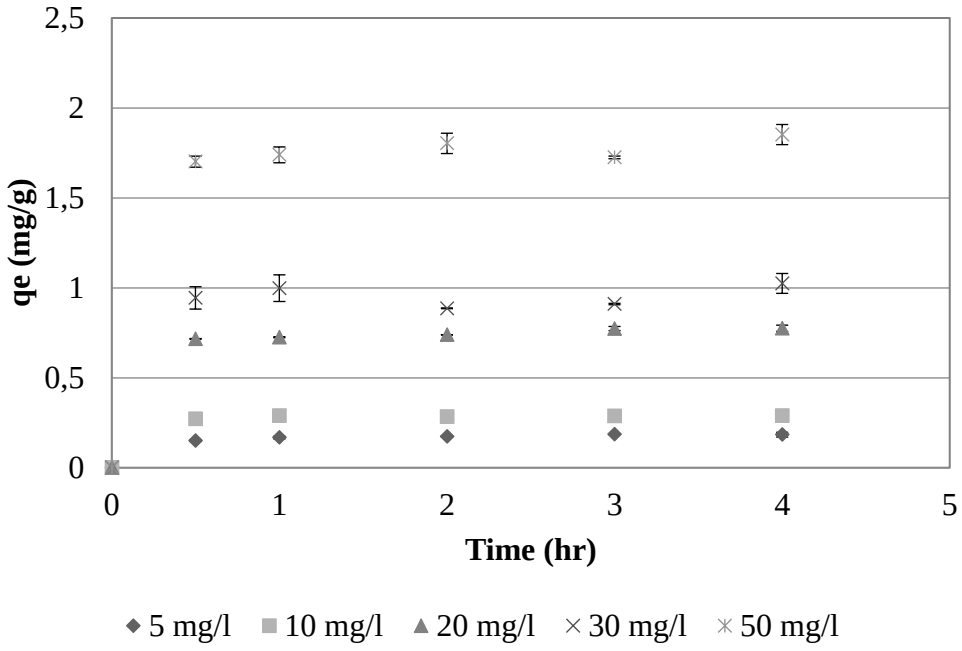

Figure 20. Change of adsorption capacity with time at pH 9

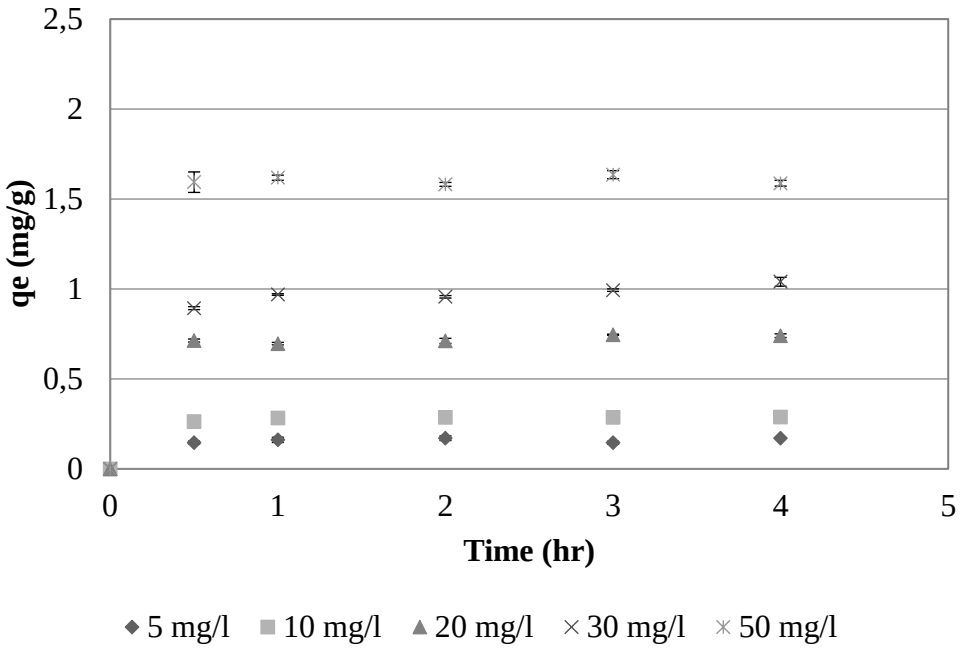

Figure 21. Change of adsorption capacity with time at pH 10

Studies conducted by several researchers for the antimony adsorption showed that pH has a significant effect on adsorption capacity (Watkins et al., 2006; Ilavsk, 2008; Biswas et al., 2009; Uluozlu et al., 2010). As it can be seen from the Figure 22, Sb(III) is found as $(SbO)^{+}$ and $(Sb(OH)_2)^{+}$ forms in aqueous solution if pH lower than 3. For pH between 3 and 10, ($HSbO_2$) and ($Sb(OH)_3$) species are the most common forms and at pH higher than 10, $(SbO_2)^{-}$ is the predominant specie (Watkins et al., 2006).

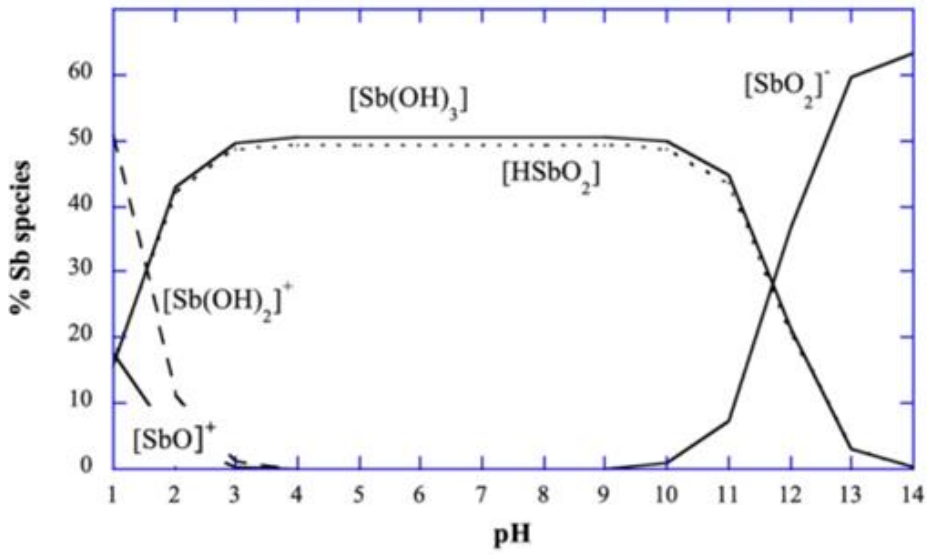

Figure 22. Sb(III) species distribution as a function of pH (Watkins et al., 2006)

pH experiments were conducted in the pH range between 3 and 10. It is due to that in the lower pH values H^+ ions and the higher pH values OH^- ions will compete with antimony ions for available adsorbent sites which will decrease the adsorption efficiency for antimony removal.

The removal mechanism of Sb via zeolite can be achieved by three mechanisms namely ion exchange, adsorption via Van der Waals interactions and precipitation. For this process, since Sb is not found in ionic form in the studied pH range, the removal mechanism is precipitation of Sb as hydroxide.

In Figure 23, the effect of pH on equilibrium adsorption capacities at the end of the 4 hours can be seen. As pH increased from 3 to 7, a slight decrease in the equilibrium adsorption capacities was observed. After pH 7, sharp reduction in the capacity was detected for 50 mg/l. For other concentrations, although the same trend in capacity occurs, the amount of decrease was not as high as 50 mg/l. The batch experiments results showed that highest adsorption capacities were found at pH 3. All of the antimony solutions with five different initial concentrations show the similar tendency that as pH increases from 3 to 10, adsorption capacities decrease. As it is seen in Figure 23, the adsorption capacities of initial antimony concentrations 5, 10, 20, 30 and 50 mg/l at pH 3 were 0.20, 0.38, 0.84, 1.14 and 2.02, respectively and at pH 10 were 0.17, 0.29, 0.74, 1.04 and 1.59, respectively. It is seen that adsorption capacities increase with initial concentrations increase. According to results of the batch experiments with five different concentrations, pH 3 was selected as optimum pH for further applications on removal of antimony by natural zeolite.

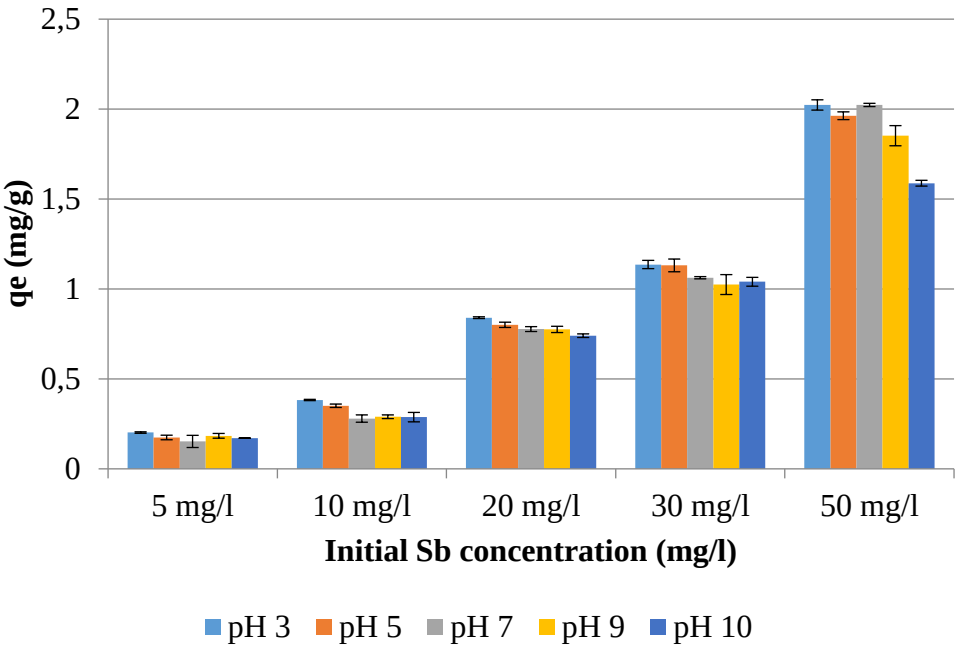

Figure 23. Change of equilibrium adsorption capacity with pH

Effect of pH on antimony adsorption for different adsorbents has been investigated. Yu et al. (2014) studied pH effect on antimony removal via granular acitvated carbon (GAC) at pH range 2 and 10. Adsorption capacity of the GAC decreased as pH was changed from 2 to 7. From pH 7 to 10, a little increase was observed on the adsorption capacity but it was still below the capacity found between pH 2 and 5. For GAC, the optimum pH range is between 2 and 4 which is similar to result of the present study. In another study conducted by Uluozlu et al. (2010), highest Sb(III) sorption on lichen biomass was calculated at pH 3, just as the present study. As pH changes from 3 to 6, removal efficiency decreased. The lowest efficiency was found at pH 8. Moreover, the efficiency calculated at pH 2 was lower than the efficiencies at pH between 3 and 6 which is optimum range for the study. In another study conducted by Sari et al. (2012), adsorption capacities of modified perlite for Sb(III) were evaluated at pH range 2 and 8. The adsorption capacity increase as pH changed from 2 to 4 and after it reached to highest capacity at pH 4, it started to decrease with increase in pH. Therefore pH 4 was selected as optimum pH for this study. The effect of pH on perlite adsorption capacity is similar to effect of pH on zeolite adsorption in the present study (Sari et al., 2012). Similar results have been found also for the antimony removal with different adsorbents such as goethite, activated alumina, Bayoxide E33, GEH, and modified orange waste, etc. All of the adsorption capacities of these adsorbents

decreased with increased pH just as the present study (Watkins et al., 2006; Ilavsk, 2008; Biswas et al., 2009; Uluozlu et al., 2010).

Similar trends for pH effect were observed on removal of heavy metals by clinoptilolite. Removal of Lead (Pb) was accomplished with higher efficiencies in acidic pH. Moreover, decrease in the removal efficiency of Pb and decrease in affinity of zeolite for Pb was observed after pH 7 (Mier et al., 2001).

4.3.2.2 Effect of Temperature on Adsorption Capacity

The temperature experiments were conducted at pH 3 for temperature values 20, 25, 30 and 35 °C. These effects were investigated for five different antimony concentrations. The graphs for the temperature effect on adsorption capacities are given in Figure 24, Figure 25, Figure 26 and Figure 27. The results show that the highest adsorption occurs around at 25-30 °C. The highest capacity is obtained as 2.02 mg/g at 25 °C for 50 mg/l and the lowest one is 0.11 mg/g at 20 °C for 5 mg/l antimony concentration. However, the adsorption capacity does not show a significant change in the experimental temperature range. A little decrease in adsorption capacity was observed at the temperature extremities.

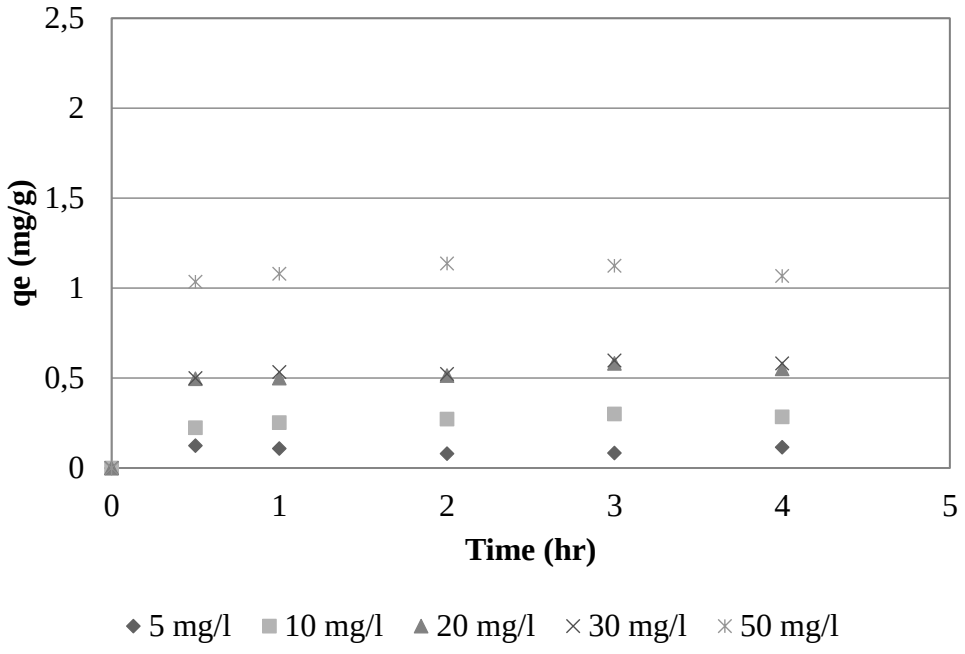

Figure 24. Change of adsorption capacity at 20 °C

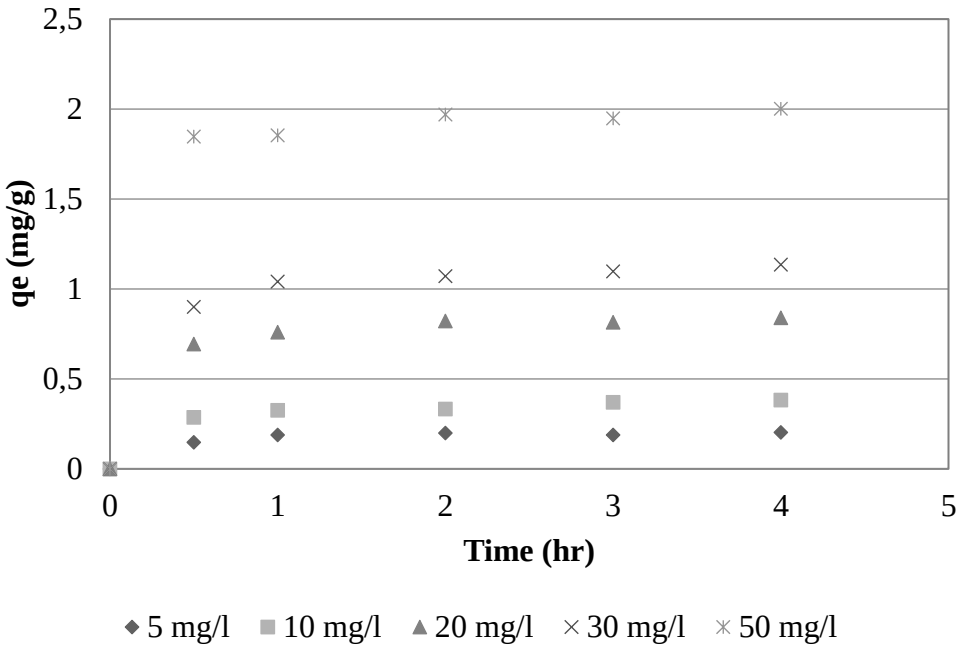

Figure 25. Change of adsorption capacity at 25 °C

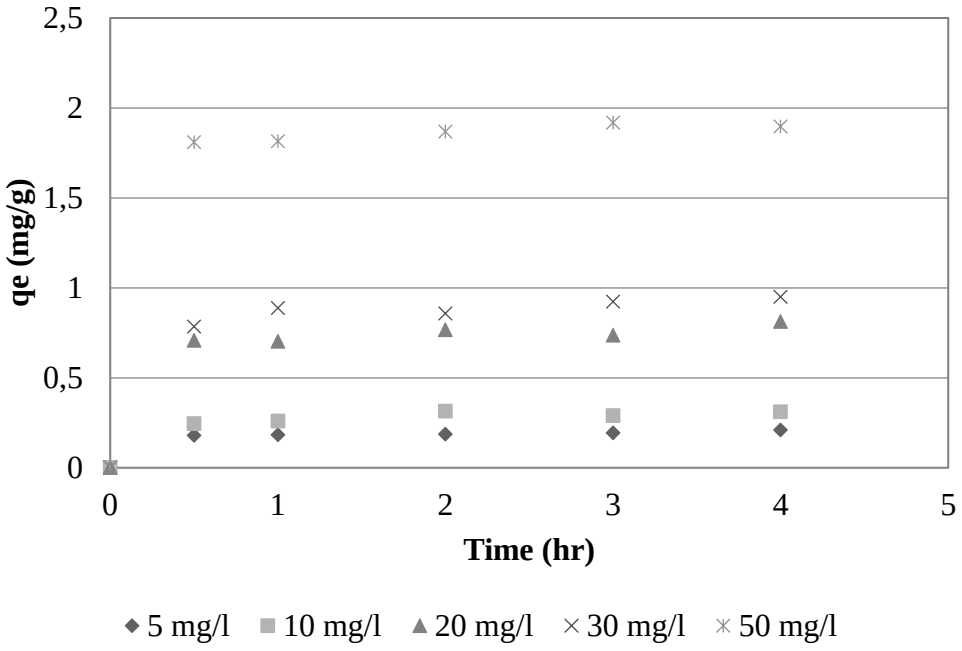

Figure 26. Change of adsorption capacity at 30 °C

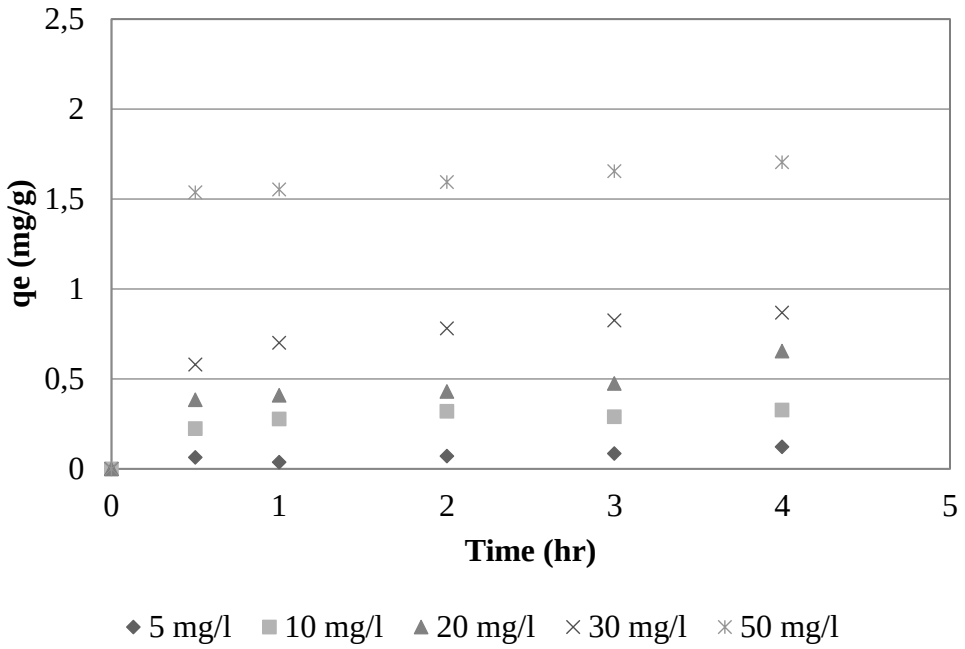

Figure 27. Change of adsorption capacity at 35 °C

In Figure 28, the change in equilibrium adsorption capacities at the end of the 4 hours with respect to temperature is provided. Higher capacities for all the concentrations were obtained at 25 °C and lower ones at 20 °C. The results indicated that adsorption capacity was decreased slightly with an increase in temperature. The highest capacity is obtained as 2.02 mg/g at 25 °C for 50 mg/l. At 20 °C and 40 °C the capacity decreases to 1.07 mg/g and 1.70 mg/g for 50 mg/l, respectively. Similar trends are followed by all experiments concentrations. For 5 mg/l, the highest capacity is obtained as 0.20 mg/g at 25 °C and the lowest one is 0.11 mg/g at 20 °C. According to results of the batch experiments with five different concentrations, optimum adsorption temperature was chosen as 25°C for Sb(III) removal.

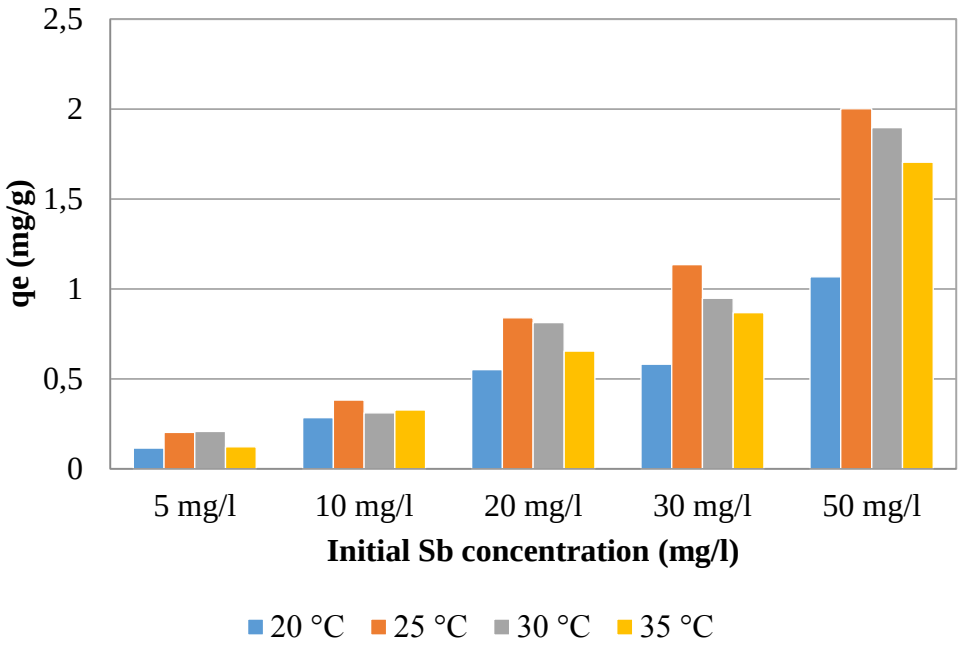

Figure 28. Change of equilibrium adsorption capacity with temperature

Effect of temperature on antimony adsorption for different adsorbents has been explored by several researchers. In a study conducted by Targan et al. (2013), effect of the temperature on adsorption of Sb(III) ions to Erzurum Clay on range of 10 and 35 °C was evaluated. Maximum adsorption capacity was found at 25 °C, similar to the present study. As temperature increases, adsorption capacity decreases slightly. Furthermore, adsorption capacity at 10 °C was found as the minimum capacity. In another study conducted by Xi et al. (2011a) for antimony adsorption on bentonite, temperature effect on Sb(III) removal was investigated. And results showed that similarity to results of the present study. Adsorption of Sb(III) decreases on bentonite, as the temperature increases. This result may be due to the energy release during the adsorption reaction between Sb(III) and bentonite. In this study, change in enthalpy of adsorption (ΔH°) for Sb(III) adsorption is calculated as negative value. (Xi et al.,2011a).

Adsorption capacity decreases as the adsorption temperature increases, due to the exothermal nature of the adsorption process. The result of the batch experiments supports that the adsorption process is exothermic and more favorable at low temperature. The decrease in adsorption capacity may be result of the following reasons: with increasing temperature, the attractive forces between the zeolite surface

and antimony are weakened, and then sorption decreases; destruction of the some active sites on zeolite surface because of the bond ruptures; and increase in escape of antimony ions from solid phase to bulk phase (Uluozlu et al., 2010).

4.3.2.3 Effect of Agitation on Adsorption Capacity

The agitation experiments were performed at pH 3 and 25 °C for agitation speed of 100, 120, 140, 180 and 200 rpm. The effect of agitation rate was investigated for five different antimony concentrations. The results showing the change of adsorption capacity with time are given at Figure 29, Figure 30, Figure 31, Figure 32 and Figure 33. The results show that the highest adsorption occurs around at 140 rpm. The highest capacity is obtained as 2.02 mg/g at 140 rpm for 50 mg/l and the lowest one is 0.17 mg/g at 100 rpm for 5 mg/l antimony concentration.

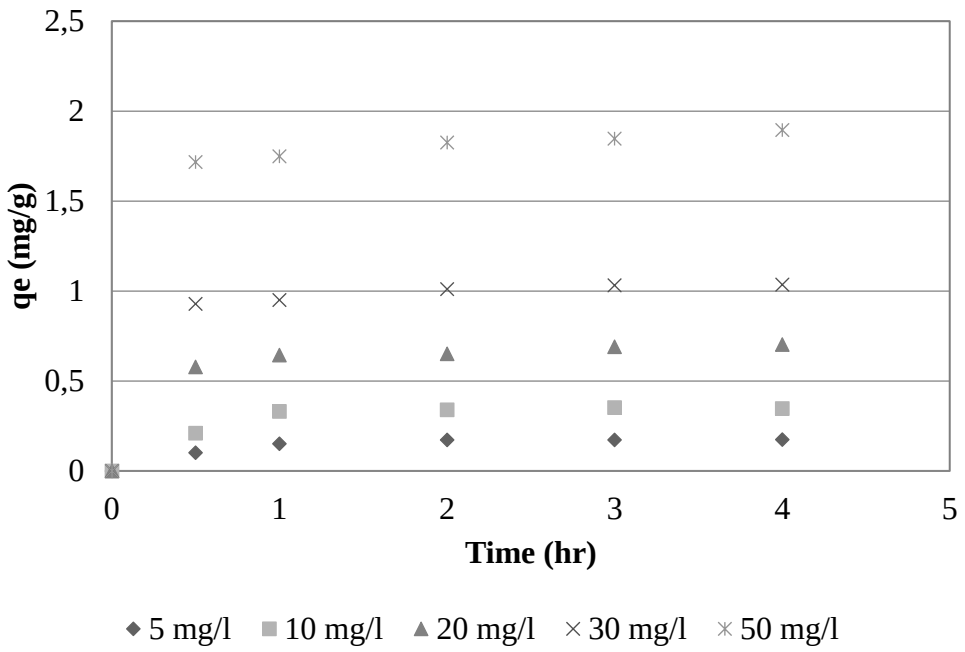

Figure 29. Change of adsorption capacity with time at 100 rpm

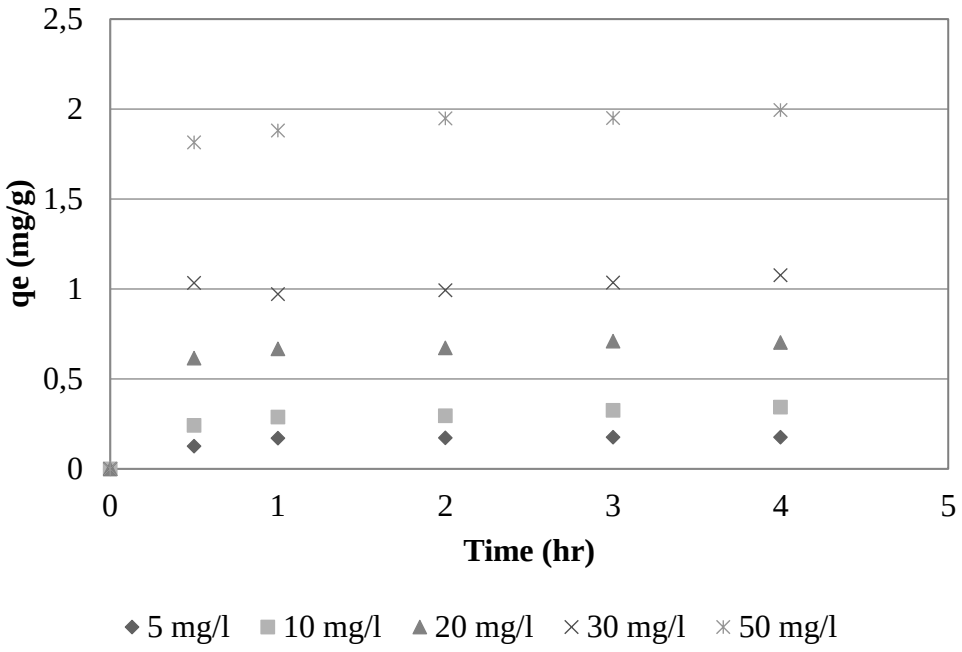

Figure 30. Change of adsorption capacity with time at 120 rpm

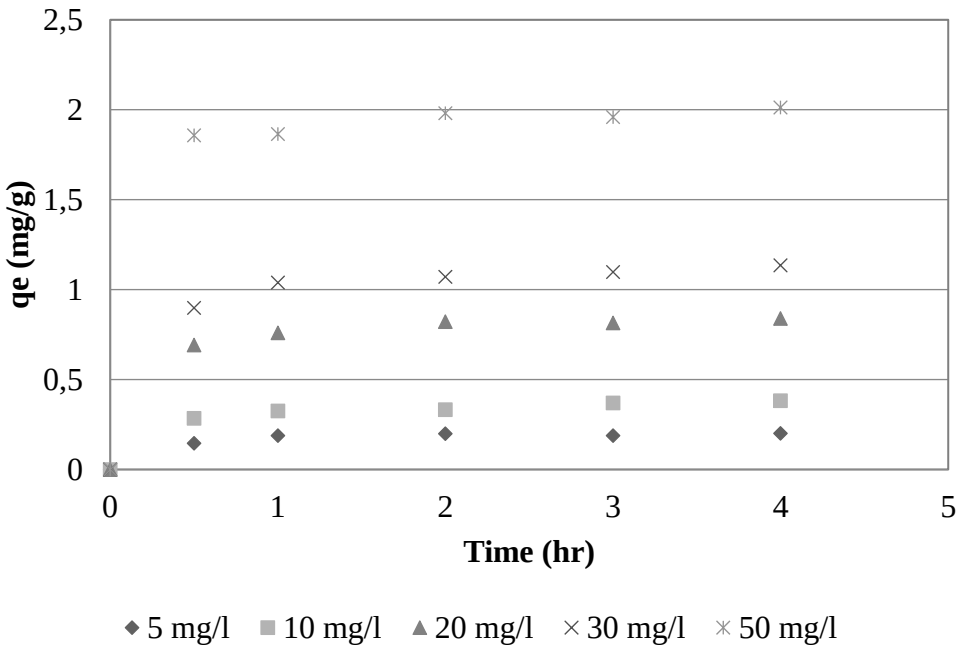

Figure 31. Change of adsorption capacity with time at 140 rpm

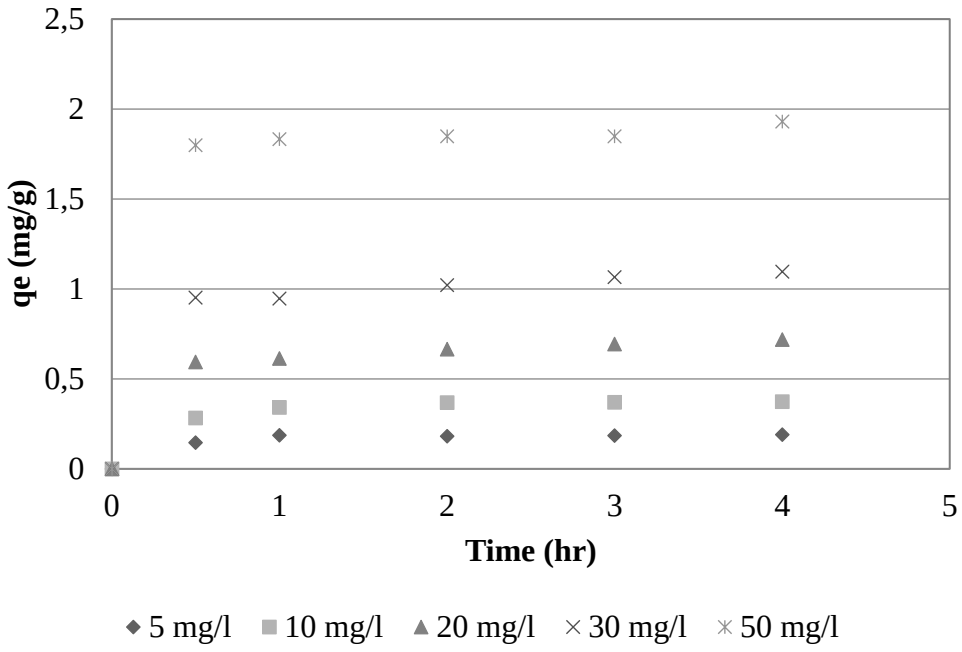

Figure 32. Change of adsorption capacity with time at 180 rpm

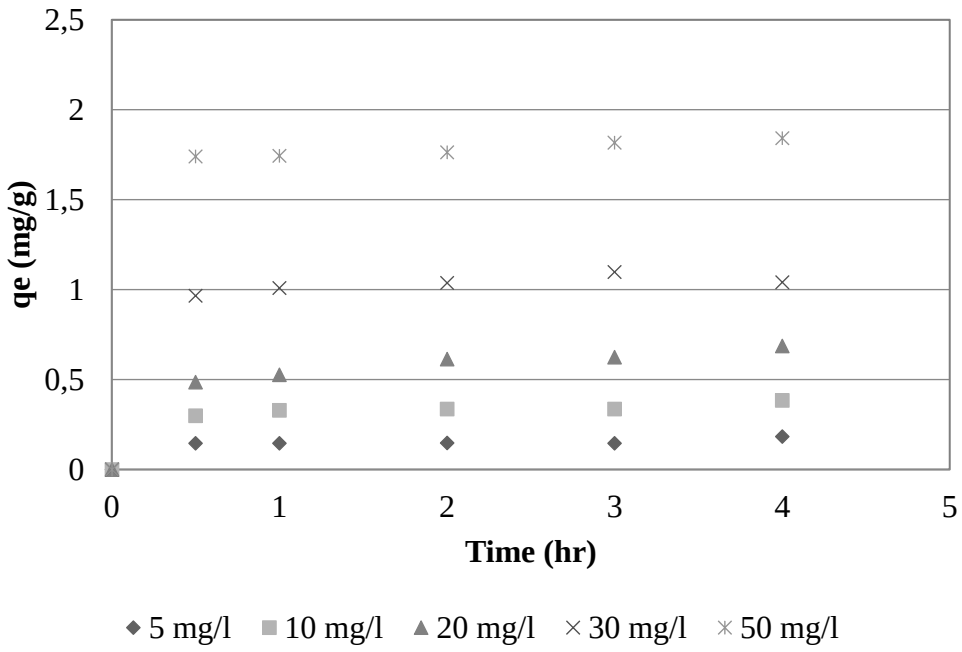

Figure 33. Change of adsorption capacity with time at 200 rpm

Agitation is used to accelerate the adsorption of antimony on zeolite. The results indicated that lower agitation is not favorable for batch experiments. This is probably because at lower agitation speed the adsorbent do not spread in the sample and accumulate in the bottom of the solution. This might decrease to usage of active sites

efficiently and only upper layer of the zeolite active sites would be available to adsorb antimony. So, this situation point outs that agitation speed should be sufficient to ensure that all the surface of the zeolite are readily available for adsorption (Aregawi & Mengistie, 2013).

The equilibrium adsorption capacities are plotted with respect to agitation rate in Figure 34. As it is seen in Figure 34, higher Sb adsorption capacities for all the concentrations were obtained at 140 rpm and lower ones at 100 rpm. The highest capacity is obtained as 2.02 mg/g at 140 rpm for 50 mg/l. At 100 rpm, the capacity decreases to 1.89 mg/g for 50 mg/l. Similar trends are followed by all experiments concentrations. For 5 mg/l, the highest capacity is obtained as 0.20 mg/g at 140 rpm and the lowest one is 0.17 mg/g at 100 rpm. Therefore, According to results of the batch experiments and the explanations on agitation rate, the optimal agitation speed for this study was selected as 140 rpm.

Furthermore, it can be observed that it is sufficient to agitate the solution for 4 hours to ensure that antimony adsorption reaches to equilibrium. According to Figure 34, it is seen that increase of agitation speed promotes to adsorption and increase interaction between zeolite and antimony particles until the certain point which is 140 rpm for this case. However, after that point agitation has negative effect on adsorption process and starts to distribute layer of antimony ions on adsorbent surface and result in decrease of adsorption capacity. Another study on active carbon adsorption also showed that as the agitation speed increases, turbulence in the fluid increases which leads to decrease in boundary layer thickness around the adsorbent particles. As a consequence, the adsorption capacity decreases after a certain agitation rate (Zahoor, 2011).

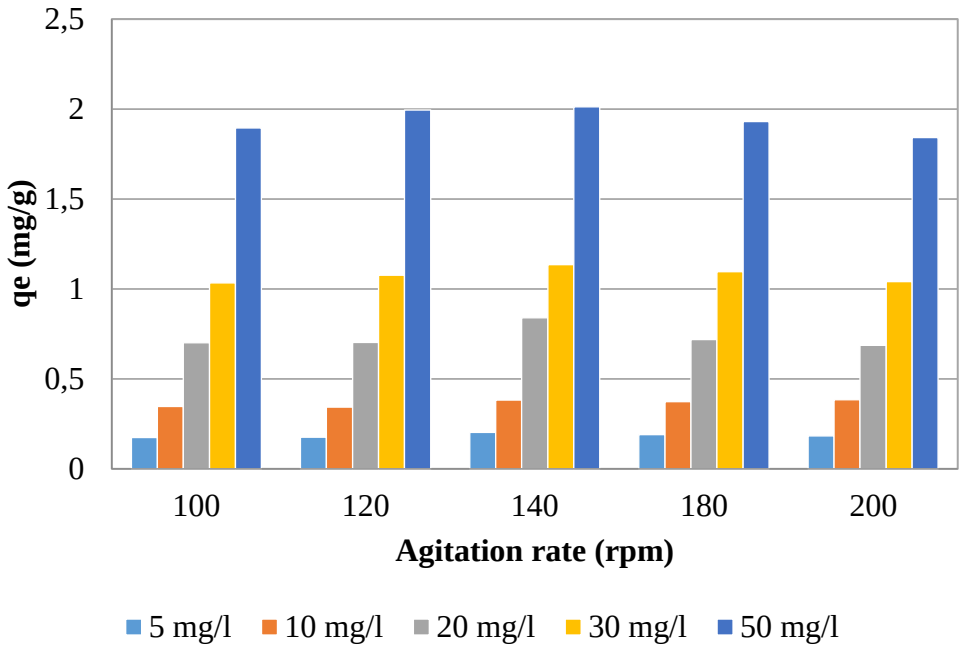

Figure 34. Change of equilibrium adsorption capacity with agitation rate

In addition to previously mentioned explanations, it was observed from pH, temperature and agitation experiments that the adsorption capacity increased as the time increases, and reaches the contact equilibrium at 4 hour. The result suggests that, adsorption takes place rapidly at the initial stage on the external surface of the adsorbent within 1 hour. It is followed by a slower internal diffusion process, which may be the rate determining step and finally attained equilibrium (Aljebori & Alshirifi, 2012).

Moreover, the fast adsorption at the initial stage may be because of the fact that a big number of surface sites are available for adsorption, but after a lapse of time, the remaining surface sites on zeolite particles are difficult to be occupied. This is because of the repulsion between the solute molecules of the solid and bulk phases, hence, make it take long time to reach equilibrium.

Additionally, it was also observed through batch experiments that the adsorption capacities increased with increase of initial antimony concentration. Actually, the ratio of initial antimony amount to available surface area is high at higher concentrations. The initial antimony concentration provides an important driving force to overcome the mass transfer resistance of the antimony between the aqueous and solid phases.

Consequently, at higher antimony concentration, the number of ions competing for the available sites on the surface of zeolite was high, hence, resulting in higher antimony adsorption capacity (Idris et al., 2011).

Equilibrium adsorption capacities of different adsorbents for antimony removal are given in Table 11. According to these results, it can be seen that commonly used adsorbents such as active carbon, carbon nanotubes and the others do not have high antimony adsorption capacities. Result of the study is also given in the comparison table.

Table 11. Sb(III) adsorption capacities of different adsorbents

Adsorbent	**Adsorption capacity**	**Reference**
Multi-walled carbon nanotubes	0.32 mg Sb(III)/g	(Abdel & Mohamed, 2013)
Kaolinite	0.43 mg Sb(III)/g	(Xi et al., 2014)
Granular activated carbon	0.54 mg Sb(III)/g	(Yu et al., 2014)
Bentonite	0.55 mg Sb(III)/g	(Xi, et al., 2011)
Ferric hydroxide	1.55 mg Sb(III)/g	(He et al., 2015)
Natural zeolite	**2.02 mg Sb(III)/g**	**Present study**
$FeCl_3$-modified activated carbons	2.64 mg Sb(III)/g	(Yu et al., 2014)
Graphene	7.46 mg Sb(III)/g	(Leng, et al., 2012)
Synthetic NZVI zeolite	7.65 mg Sb(III)/g	(Zhou et al., 2015)
Synthetic goethite	33.0 mg Sb(III)/g	(Watkins et al., 2006)
Ferrihydrite	35.0 mg Sb(III)/g	(Qi & Pichler, 2016)

4.3.3 Equilibrium Studies

The relationship between the amount of a substance adsorbed and its final concentration in the equilibrium solution is called adsorption isotherm. In order to determine adsorption capacities, equilibrium studies performed with zeolite. The

results of the experiments are given in section 4.3.2. Also, the data obtained from kinetic studies for different pH values, temperature = 25 °C and 140 rpm agitation rate, were nonlinearly fitted to Langmuir and Freundlich isotherm models and were plotted in Figure 35 to Figure 39. Corresponding data for each graph are given in Appendix D.

The value of R^2 (non-linear correlation coefficient) closer to one indicates that the respective equation better fits the experimental data. For all pH experiments, Langmuir model was found to describe adsorption successfully than Freundlich model isotherm with respect to linearity coefficients obtained for both models for antimony. R^2 values for Langmuir model were obtained from 0.810 to 0.951. The Langmuir isotherm assumes a surface with homogeneous binding sites, equivalent sorption energies and no interaction between adsorbed species. Therefore, the favored experimental results suggest that a monolayer of antimony ions is adsorbed on homogeneous adsorption sites on the surface of zeolite. Moreover, theoretical maximum adsorption capacity suggested by Langmuir model decreases as pH goes from 3 to 10. These results are in accordance with the results provided in Figure 23. Langmuir and Freundlich isotherm constants for antimony adsorption onto zeolite are given in Table 12.

Table 12. Langmuir and Freundlich adsorption isotherm model parameters for antimony adsorption by natural zeolite

Isotherm Model	**Parameter**	**pH 3**	**pH 5**	**pH 7**	**pH 9**	**pH 10**
Langmuir	q_m (mg/g)	3.453	3.299	3.137	2.700	2.505
	K_L (l/mg)	0.096	0.091	0.082	0.088	0.076
	R^2	0.949	0.935	0.810	0.872	0.951
Freundlich	K_F (l/mg)	0.500	0.456	0.420	0.408	0.343
	1/n	2.170	2.151	2.163	2.330	2.236
	R^2	0.889	0.851	0.732	0.778	0.877

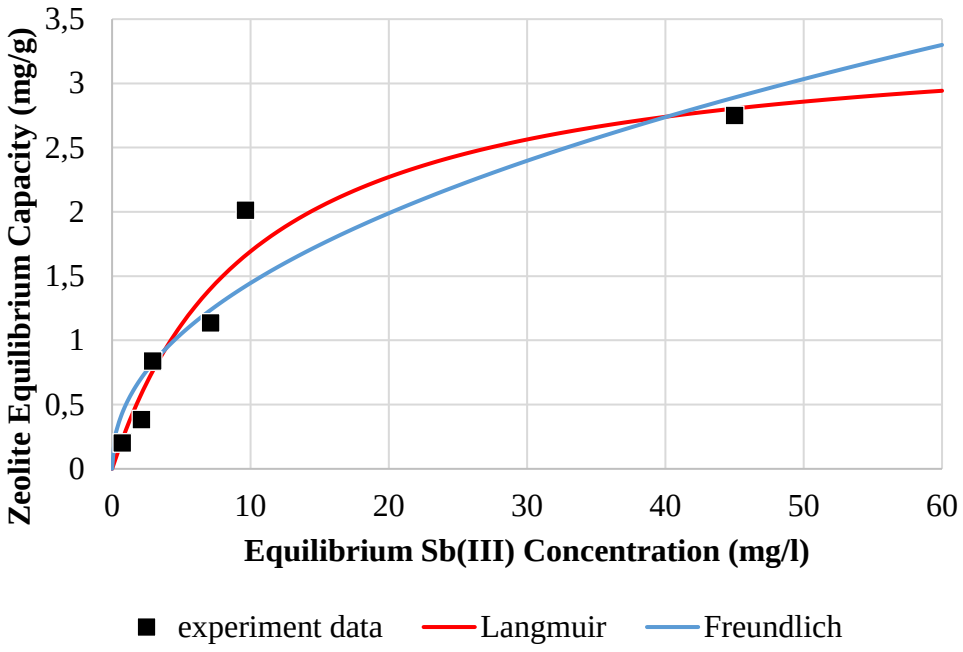

Figure 35. Comparison of Langmuir and Freundlich isotherms in fitting of isothermal data for Sb(III) adsorption on zeolite (pH = 3.0 ± 0.1, T = 25°C, 140 rpm, for contact time = 240 min, and adsorbent dosage = 5 g/(250 ml))

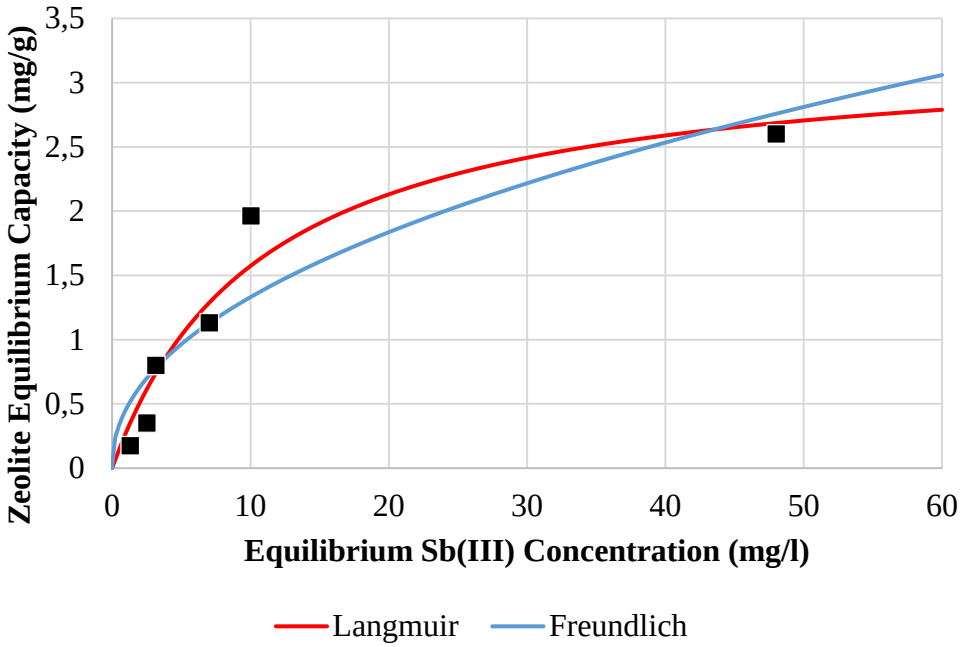

Figure 36. Comparison of Langmuir and Freundlich isotherms in fitting of isothermal data for Sb(III) adsorption on zeolite (pH = 5.0 ± 0.1, T = 25°C, 140 rpm, for contact time = 240 min, and adsorbent dosage = 5 g/(250 ml))

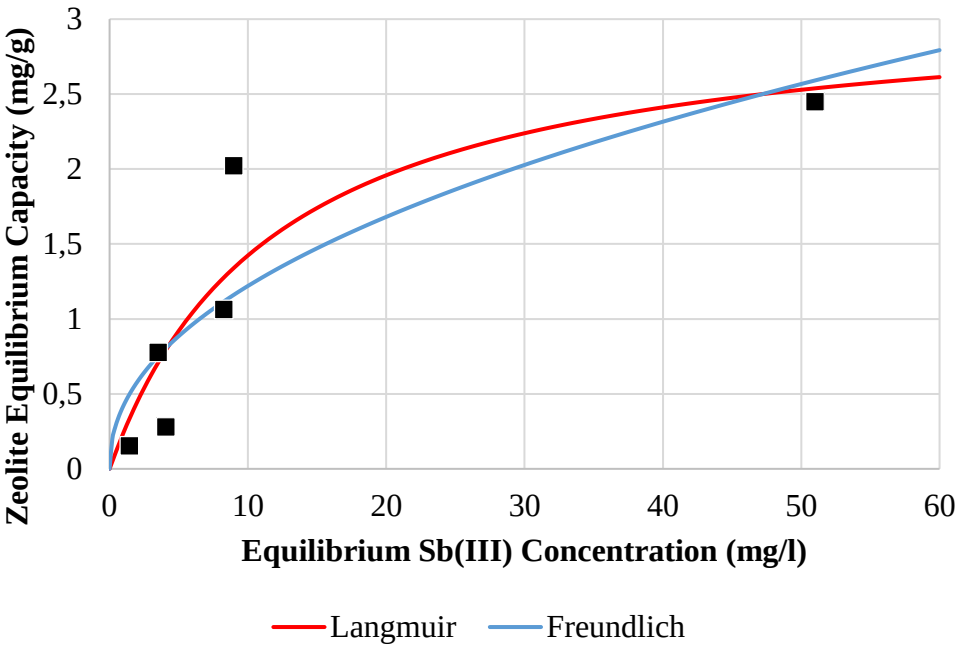

Figure 37. Comparison of Langmuir and Freundlich isotherms in fitting of isothermal data for Sb(III) adsorption on zeolite (pH = 7.0 ± 0.1, T = 25°C, 140 rpm, for contact time = 240 min, and adsorbent dosage = 5 g/(250 ml))

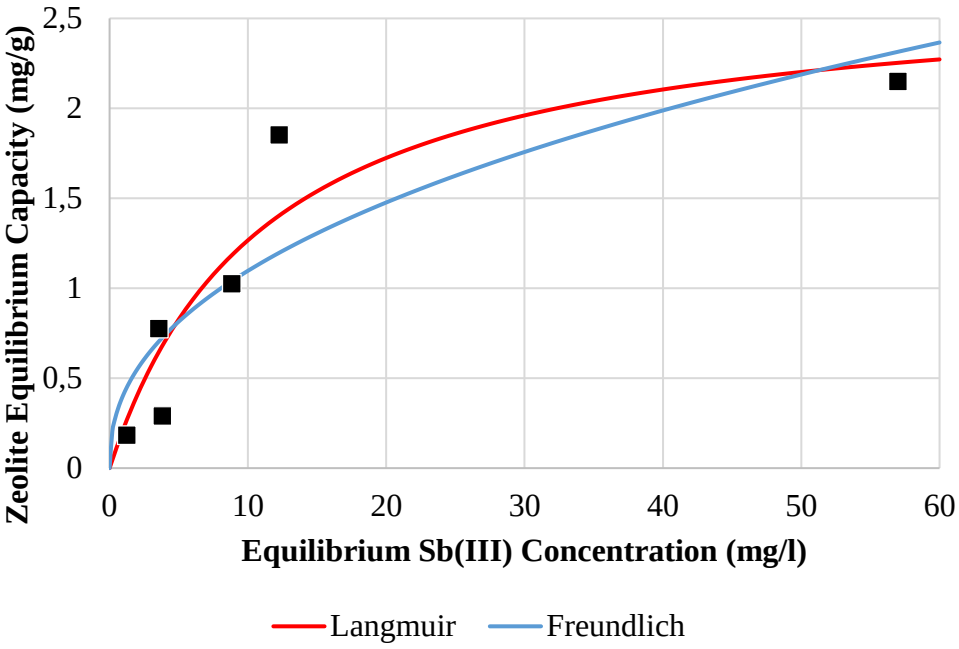

Figure 38. Comparison of Langmuir and Freundlich isotherms in fitting of isothermal data for Sb(III) adsorption on zeolite (pH = 9.0 ± 0.1, T = 25°C, 140 rpm, for contact time = 240 min, and adsorbent dosage = 5 g/(250 ml))

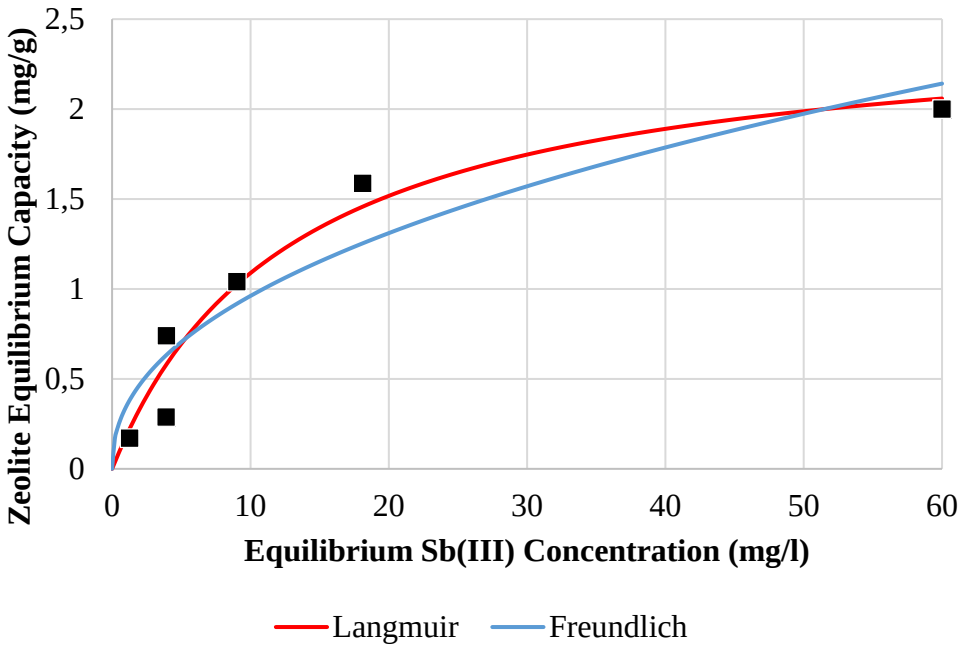

Figure 39. Comparison of Langmuir and Freundlich isotherms in fitting of isothermal data for Sb(III) adsorption on zeolite (pH = 10.0 ± 0.1, T = 25°C, 140 rpm, for contact time = 240 min, and adsorbent dosage = 5 g/(250 ml))

4.4 Treatment of Antimony via Coagulation-Flocculation

The jar test experiments were performed in order to find optimum coagulant dosage and system pH for antimony removal with two common coagulants ferric chloride and aluminum sulfate.

The first jar test experiments were performed by using ferric chloride (FC) as the coagulant. During the experiments three sets of pH; acidic, basic and neutral, for five different initial concentrations were tested. The highest removal efficiencies of antimony for all concentrations were achieved when pH was set to 7. As the FC coagulant dosage increased, the removal efficiencies also increased up to 99 %. The trend in removal efficiencies was similar when pH was set to 10. As it can be seen from Figure 40 to Figure 44, to maintain the same removal efficiency with pH 7, the coagulant dose should be increased in pH 10. The same type and amount of coagulant was used in acidic condition. However, when pH was set to 3, the highest removal efficiency was around 80 %. Moreover, blank samples showed that without ferric chloride addition there was not any antimony removal during jar tests.

The results achieved for antimony removal was in line with previous researchers work. Guo et al. (2009) studied the treatment of antimony by using ferric chloride within the pH range of 3 to 10 with 0.1 mM to 0.3 mM ferric chloride dose. As it can also be seen in this study the lowest removal efficiency which was around 20-40 % was observed at pH 4. In the pH range of 5 to 8 the removal was around 80 %. As the coagulant dose increased the efficiency reached nearly to 99 %. From pH 8 to 10, decrease in antimony removal was observed.

Another study carried out with the same coagulant for Sb(III) removal. It was found that optimum pH range for the highest Sb(III) removal is from 5 to 8. By this method, antimony concentration in effluent was lower than 4 μg/l which is below the drinking water standards of antimony. When the feed water pH was decreased to 9, removal efficiency was declined form 98 % to 94 % (Du et al., 2014).

Our results showed that optimum pH for Sb(III) removal by FC coagulation was determined as 7. This is because of the highest removal efficiency achieved at this point. Moreover, when pH was set to below 7, dissolved iron concentration in the solution intensely increased to high levels (Du et al., 2014). Therefore, if Sb(III) is treated by coagulation in which the ferric chloride is the coagulant, the system should be operated within the pH range of 7 to 10 to obtain considerable removal of Sb(III) and to sustain low dissolved Fe (III) concentration in the solution.

As it is expected, when the ferric chloride dosage is increased, removal of Sb(III) increases. According the below graphs, 200 mg/l FC dosage is found adequate to provide 99 % removal for lower initial Sb concentrations, 5 and 10 mg/l at pH 7 and pH 10. For higher concentration, it is seem that 300 mg/l FC dose can provide above 80 % removal efficiency but for the better removal, 400 mg/l FC dosage are required at optimum pH range 7 and 10. For the highest initial concentration 50 mg/l, 99 % removal is achieved by 400 mg/l coagulant at pH 7 and 500 mg/l coagulant at pH 10. So, it can be concluded that as the initial concentration increases, required coagulant dosage for antimony removal also increases. Moreover, at pH 3, the highest removal efficiency reached with 500 mg/l coagulant dosage is 56 %

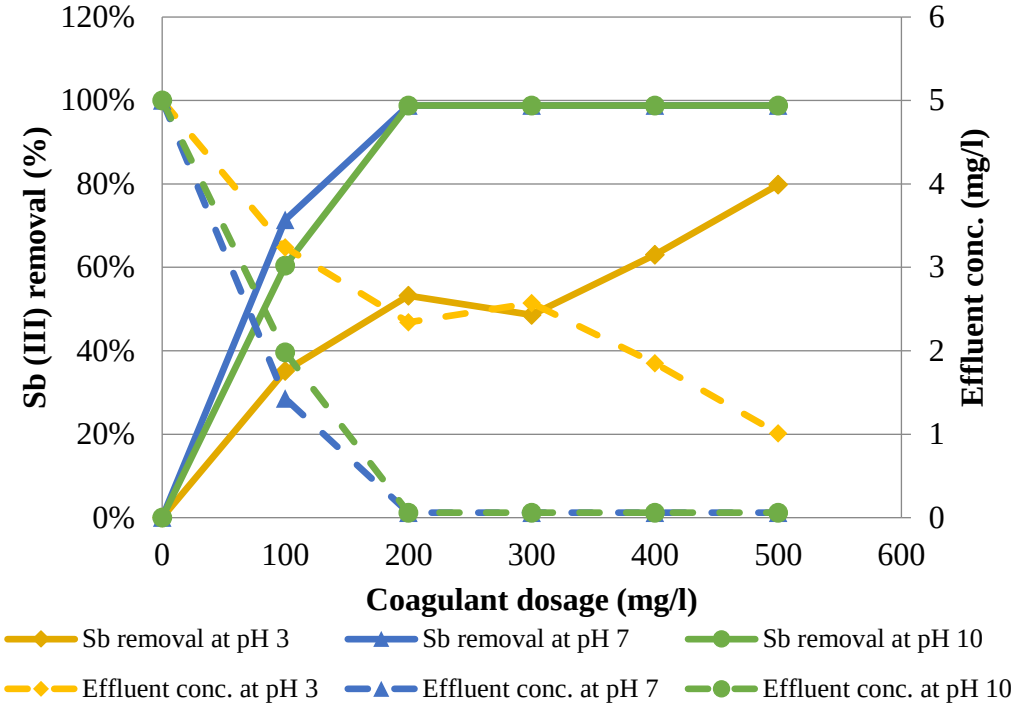

Figure 40. Change of Sb removal percentage and effluent concentration with ferric chloride dosage for 5 mg/l initial Sb concentration at pH 3, 7 and 10

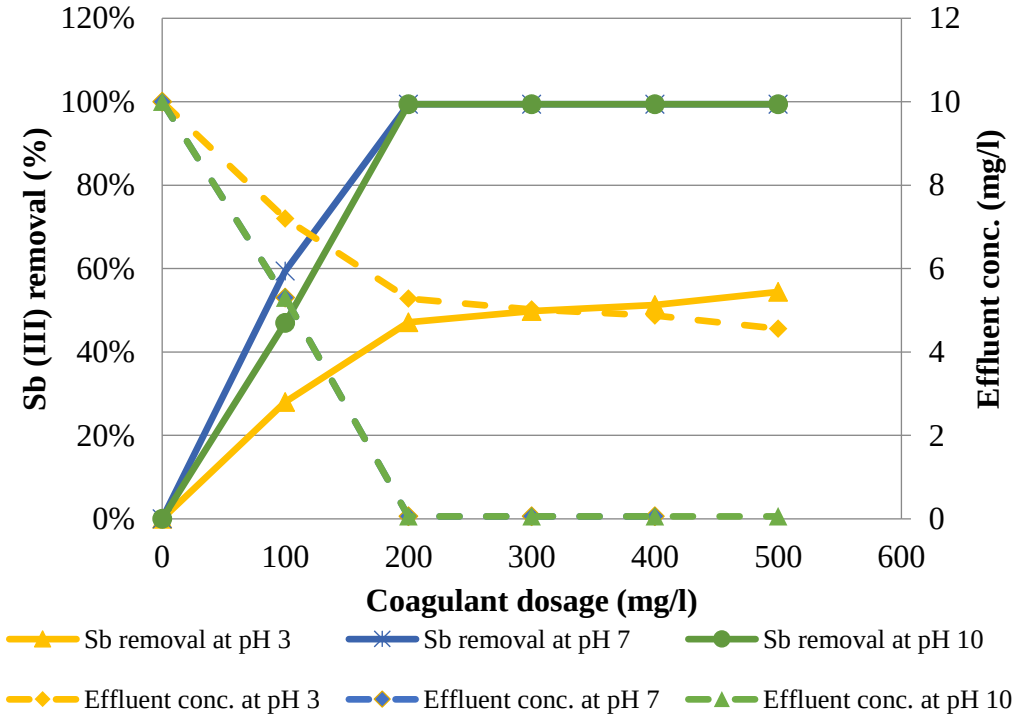

Figure 41. Change of Sb removal percentage and effluent concentration with ferric chloride dosage for 10 mg/l initial Sb concentration at pH 3, 7 and 10

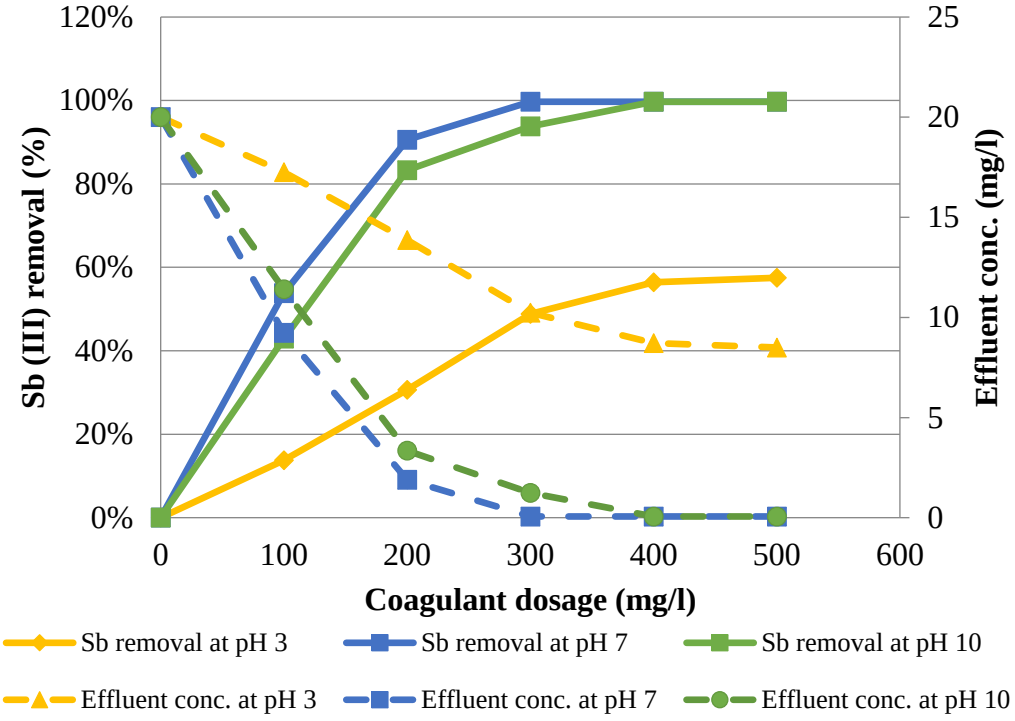

Figure 42. Change of Sb removal percentage and effluent concentration with ferric chloride dosage for 20 mg/l initial Sb concentration at pH 3, 7 and 10

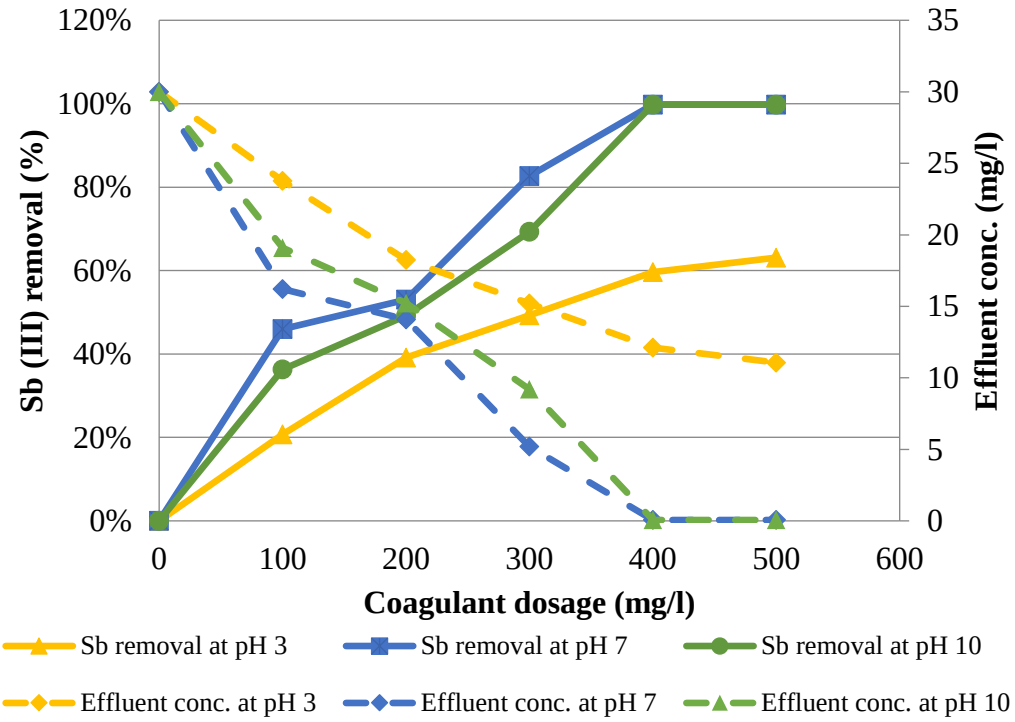

Figure 43. Change of Sb removal percentage and effluent concentration with ferric chloride dosage for 30 mg/l initial Sb concentration at pH 3, 7 and 10

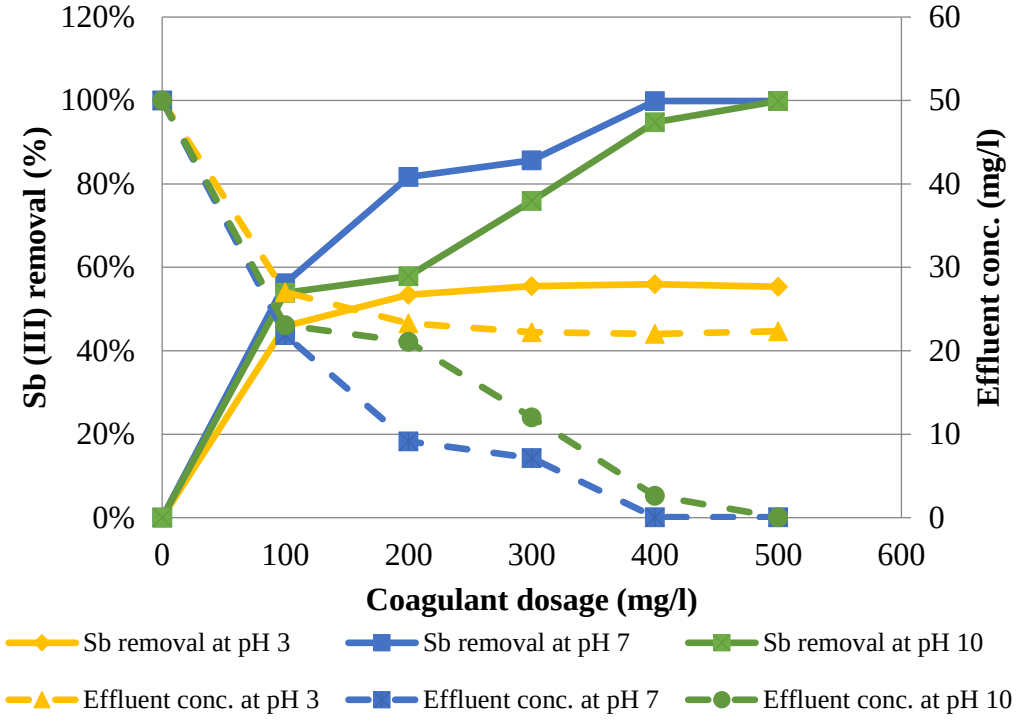

Figure 44. Change of Sb removal percentage and effluent concentration with ferric chloride dosage for 50 mg/l initial Sb concentration at pH 3, 7 and 10

Second set of the jar test experiments were performed by using aluminum sulfate (alum) as the coagulant. During the experiments, three sets of pH; acidic, basic and neutral, for five different initial concentrations were tested. Although high Sb(III) removal was achieved with ferric chloride, Sb(III) was far less efficiently removed by alum. As it can be seen from the Figure 45 - Figure 49, maximum antimony removal with alum was about 40 % which is remarkably lower than ferric chloride efficiency. According to the trends in below graphs, highest removal efficiency was achieved at pH 7. The efficiencies in the pH 10 were also close to pH 7, but at pH 3 the lowest one was observed. Furthermore, blank samples indicated that without alum addition there was not any antimony removal during jar tests. Results also showed that initial antimony concentration does not have significant impact as pH on Sb(III) removal efficiency.

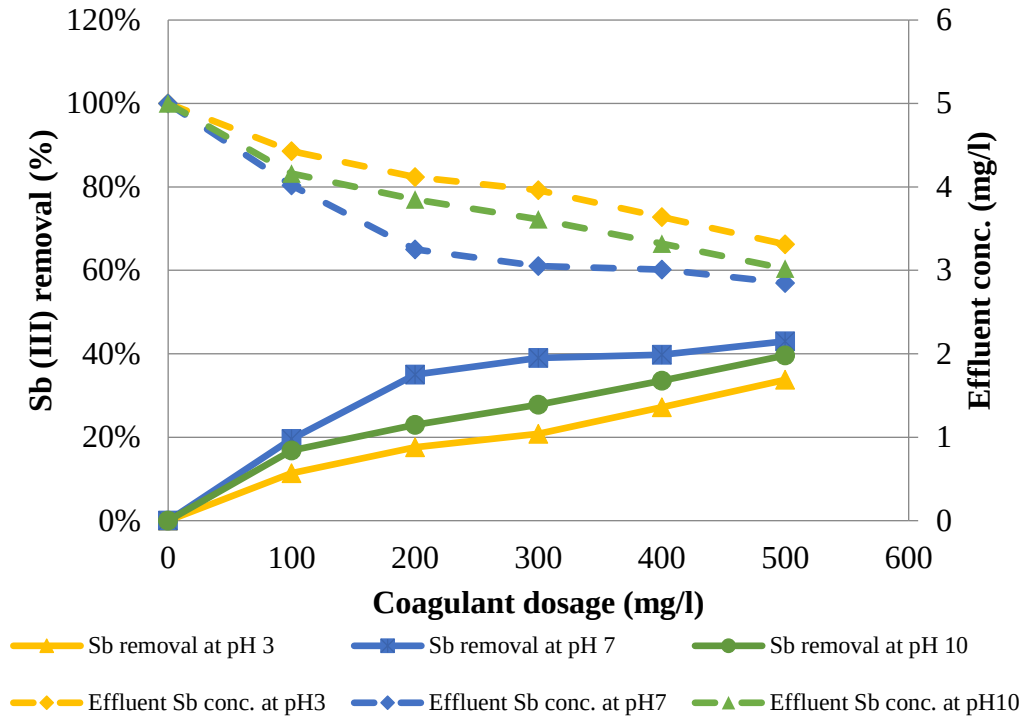

Figure 45. Change of Sb removal percentage and effluent concentration with alum dosage for 5 mg/l initial Sb concentration at pH 3, 7 and 10

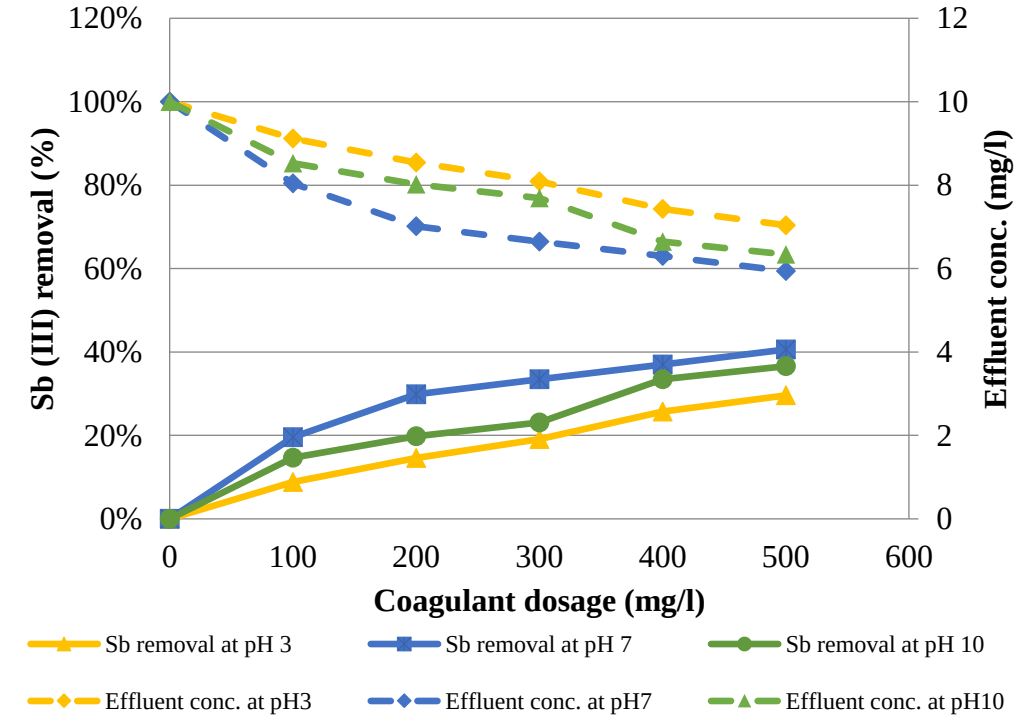

Figure 46. Change of Sb removal percentage and effluent concentration with alum dosage for 10 mg/l initial Sb concentration at pH 3, 7 and 10

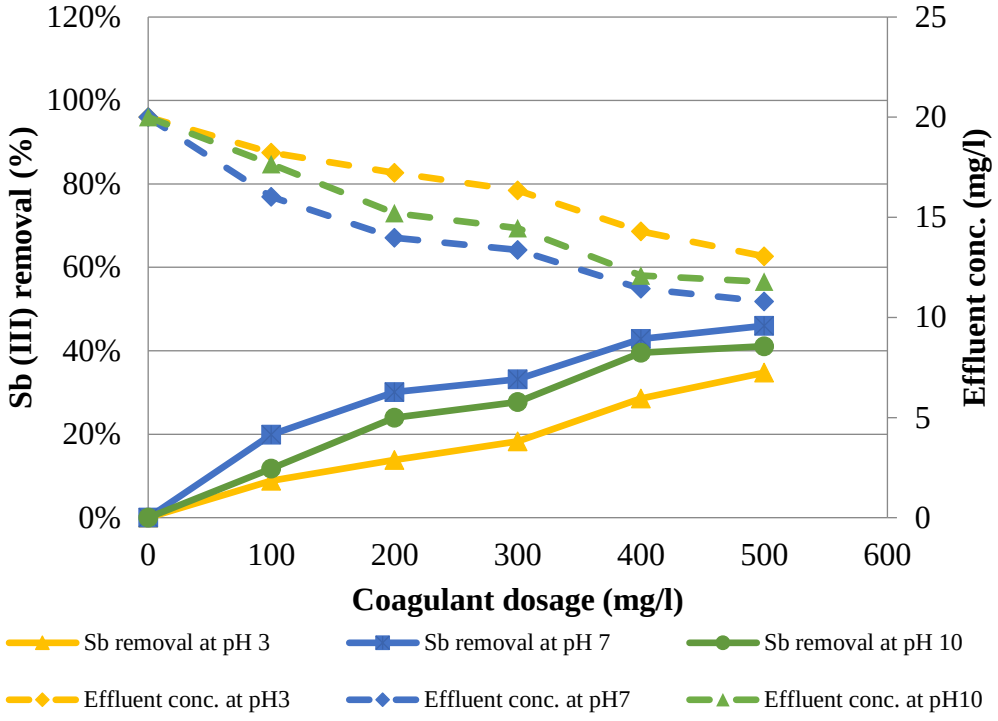

Figure 47. Change of Sb removal percentage and effluent concentration with alum dosage for 20 mg/l initial Sb concentration at pH 3, 7 and 10

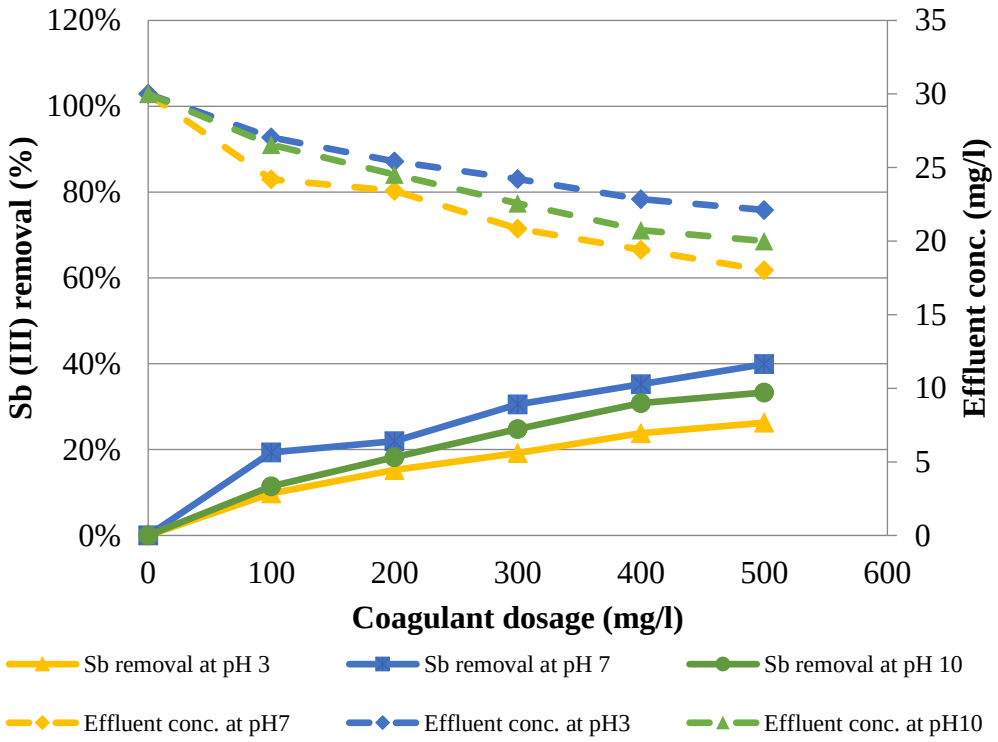

Figure 48. Change of Sb removal percentage and effluent concentration with alum dosage for 30 mg/l initial Sb concentration at pH 3, 7 and 10

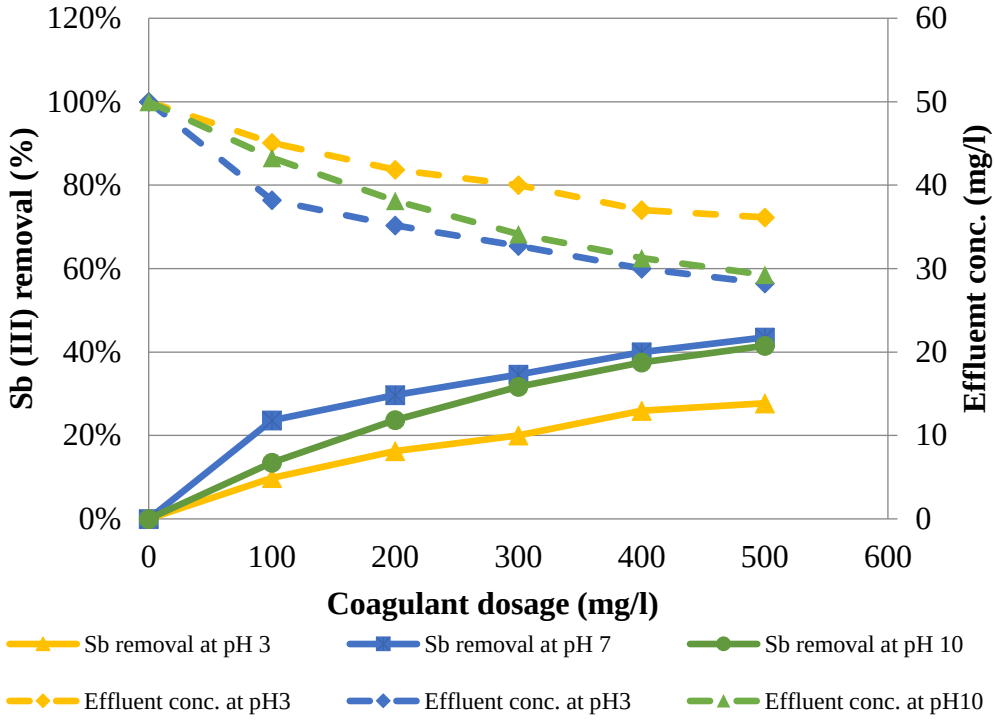

Figure 49. Change of Sb removal percentage and effluent concentration with alum dosage for 50 mg/l initial Sb concentration at pH 3, 7 and 10

According the graphs given in Figure 45 Figure 49, the highest antimony removal efficiency was achieved as 44 % for 50 mg/l initial concentration with 500 mg/l alum dosage at pH 7. For the same conditions removal efficiencies were found as 42 % and 28 % at pH 10 and pH 3, respectively. It is quite below the efficiencies that achieved with the same condition by using ferric chloride.

For alum, theoretic effective hydrolyzing pH range is between 5.5 and 7.7. At the optimum pH 6, alum solubility is the lowest and hence amount of coagulant converted to floc form is maximum (Pernitsky & Edzwald, 2006). This fact supports the results of pH effect on alum coagulation.

Guo et al. (2009) also compared efficiencies of ferric chloride and alum for antimony removal at the pH range 4-10 for 50-500 µg/l antimony concentrations. And, results showed that ferric chloride is much more effective than alum. With 0.1 mM and 0.3 mM alum dosage, only 25 % Sb(III) removal was achieved. In another study, Kang et al. (2003) compared polyaluminum chloride (PACl) and ferric chloride for low initial

antimony concentrations (4-6 µg/l). It was found that PACl does not remove efficiently antimony like ferric chloride; about 40 % efficiency was achieved for Sb(III) removal. The results are similar to removal efficiencies achieved in the present study.

The present study and previous studies showed that ferric chloride coagulants are more suitable for Sb(III) removal when considering the impracticability of alum coagulation for antimony removal. Moreover, ferric chloride has a larger pH range where an effective antimony removal can be achieved. Ferric chloride can be used for antimony removal as an applicable and efficient treatment method when antimony contamination is a significant problem. There are not any detailed experiments on the adsorption mechanism of antimony onto ferric oxide. However it was concluded by Kang et al. (2003) that Sb(III) more probably is removed with hydrophobic bonding during precipitation and adsorption by ferric chloride (Kang et al. 2003).

Antimony removal mechanism by coagulation and flocculation is co-precipitation. Co-precipitation occurs when an inorganic pollutant attaches on surface of the coagulant and forms an insoluble complex ("Arsenic Technologies," 2008). In this study, flocs were formed by the attachment of antimony on ferric chloride and alum surface and the flocs precipitated.

4.5 Treatment of Antimony via Membrane Processes

The use of membrane system is now emerging as an attractive technology for wastewater treatment. In this part, after studying conventional methods adsorption and coagulation-flocculation for antimony removal, as an advanced treatment methods membrane filtration was evaluated. As it is stated in section 3.7, membrane processes were studied briefly to get a general idea on the effect of reverse osmosis and nanofiltration membranes on antimony removal.

In this part of the experiments, two different type of membrane systems Reverse Osmosis (RO) and Nanofiltration (NF) with the specifications given in Table 9 were used for Sb(III) removal. Figure 50 and Figure 52 show the change in filtration flux

with time during the RO experiments at 15 bars for the initial antimony concentrations of 30 and 50 mg/l, respectively. Temperature and pH values were kept constant at 25 °C and 4.5, respectively. As it can be seen from the below graphs, filtration flux were measured at intervals of 30 minutes. The fluxes are measured with clean water before and after filtration and during wastewater filtration. As can be seen, it took time to reach steady state when clean water is given to RO membrane.

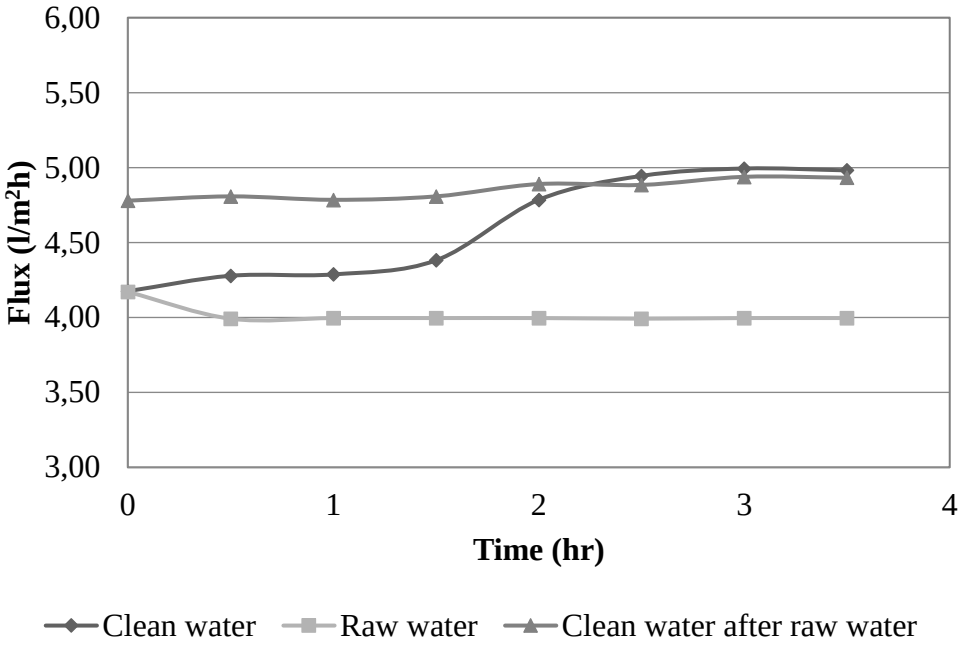

Figure 50. Change of flux with time for 30 mg/l initial antimony concentration

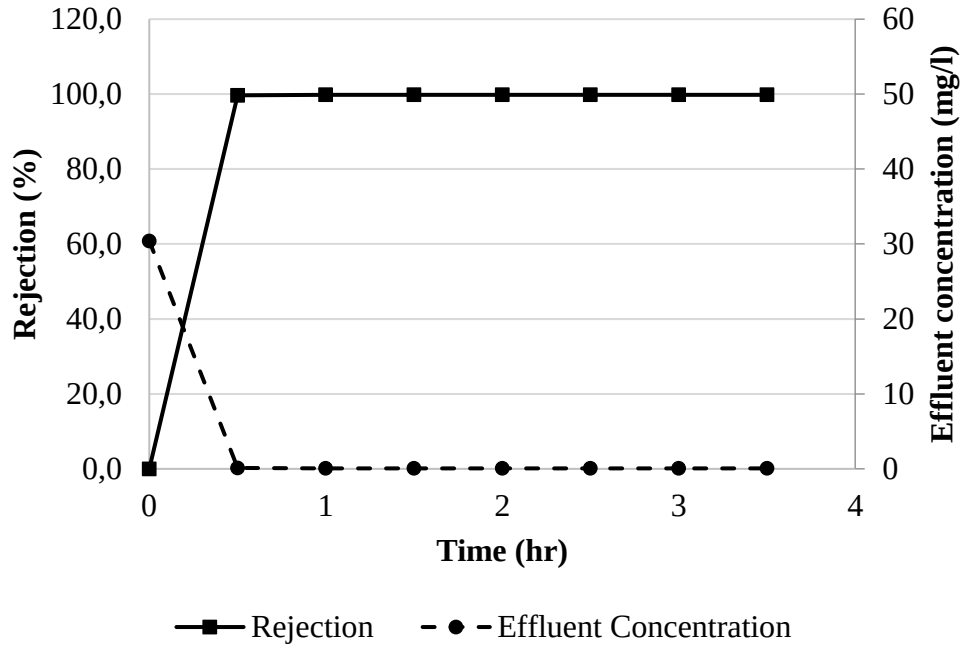

Figure 51. Rejection of antimony with SW30 membrane for 30 mg/l initial antimony concentration

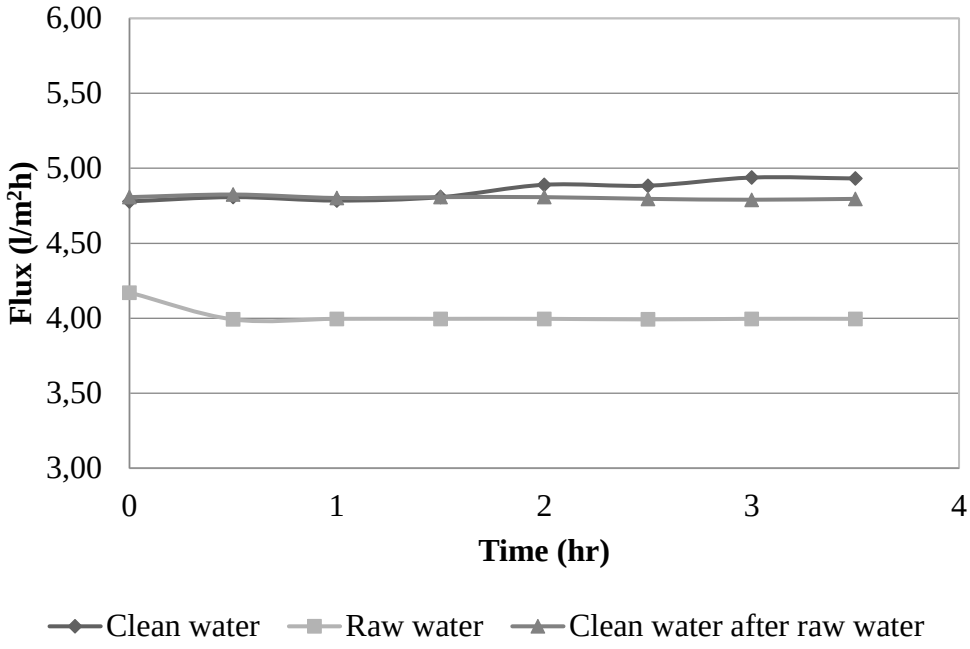

Figure 52. Change of flux with time for 50 mg/l initial antimony concentration

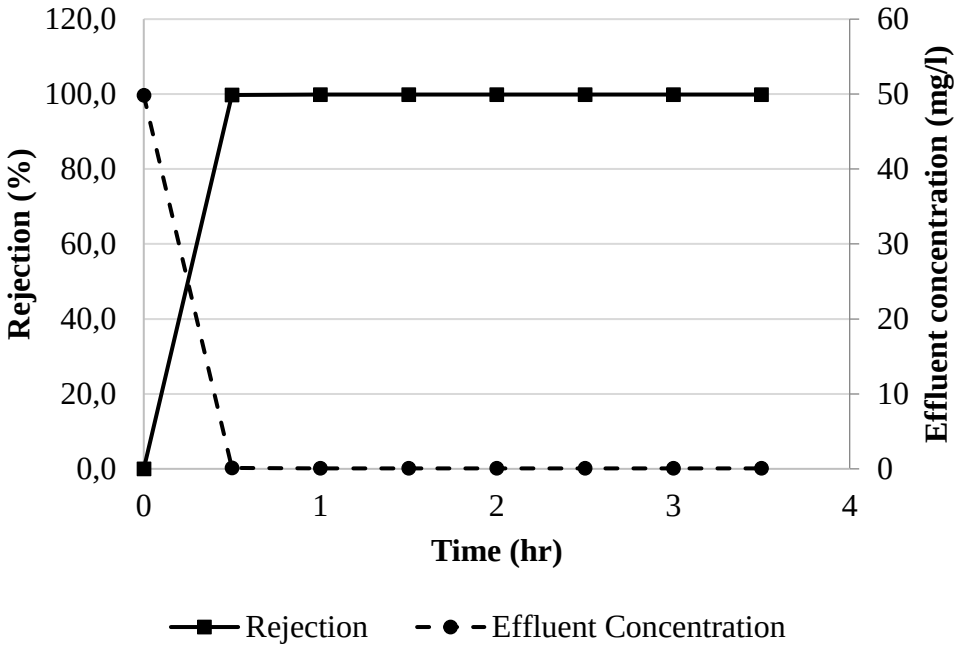

Figure 53. Rejection of antimony with SW30 membrane for 50 mg/l initial antimony concentration

The raw water flux is lower than initial and after filtration fluxes which indicates that there is only slight fouling in RO membrane. The clean water flux measured before filtration was about the same with the flux measured just after filtration. This shows that there is not irreversible fouling. Also, there are not much differences between 30 mg/l and 50 mg/l antimony concentration feed flux, so it can be said that concentration change doesn't have significant effect on process efficiency. In more concentrated feed, again there is not irreversible fouling.

The removal efficiency of membrane was evaluated by the analysis of the feed samples and permeates samples with respect to their antimony concentrations. After system reaches to stability at the end of 30 minutes, high removal efficiency is achieved nearly as 99 %. After the first measurement at 30 minutes, the concentrations of effluents were below the detection limit of AAS which is 60 µg/l (0.06 mg/l). Therefore, the results followed a straight pattern during the remaining measurements. The change of antimony rejection and effluent concentration of antimony with time using SW 30 membrane for the initial antimony concentrations of 30 and 50 mg/l are given in Figure 51 and Figure 53, respectively.

For the study, pH of the feed was set to 4.5. Since other pH values are not studied during the experiments, it is not possible to comment about effect of pH on RO membrane efficiency. However, a study conducted by Kang et al. (2000) showed that removal of antimony compounds doesn't change with pH alterations which was investigated at pH range 3 - 10.

Figure 54 and Figure 56 show the change in filtration flux with time during the NF experiments at 10 bars for the initial antimony concentrations of 30 and 50 mg/l, respectively. Temperature and pH values were constant at 25 °C and 4.5. As it can be seen from the below graphs, filtration flux were measured at intervals of 30 minutes.

The raw water flux is lower than clean water fluxes before and after filtration. The clean water flux before filtration was measured very close to the flux measured just after filtration. The flux decline of NF application was lower than that RO membrane application. It may be due to that RO membranes are tighter than NF. Therefore, RO can retain antimony more than NF and antimony cause more fouling in RO membrane.

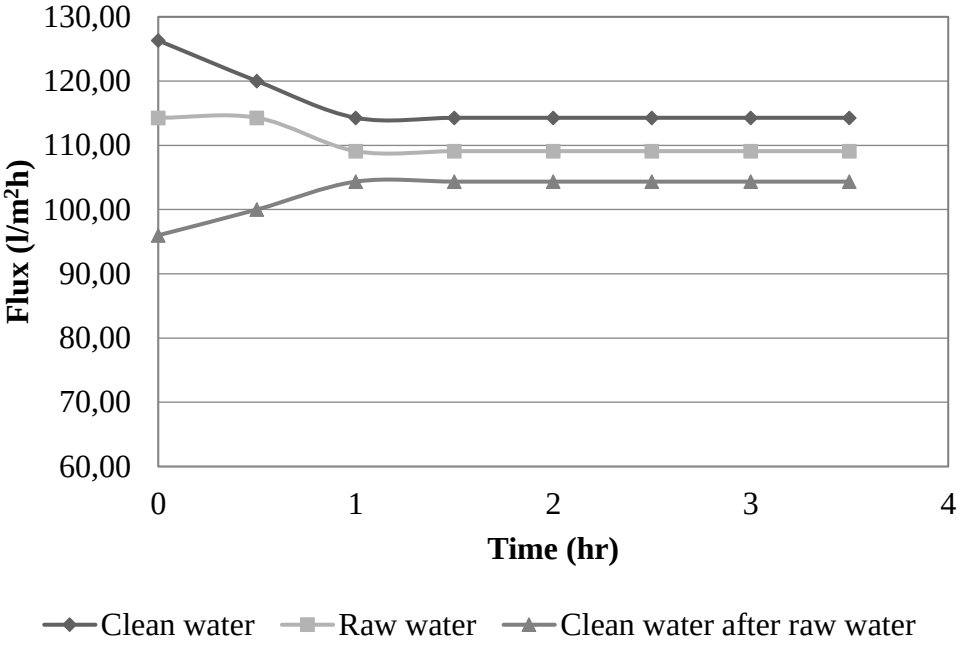

Figure 54. Change of flux with time for 30 mg/l initial antimony concentration for NF270 membrane

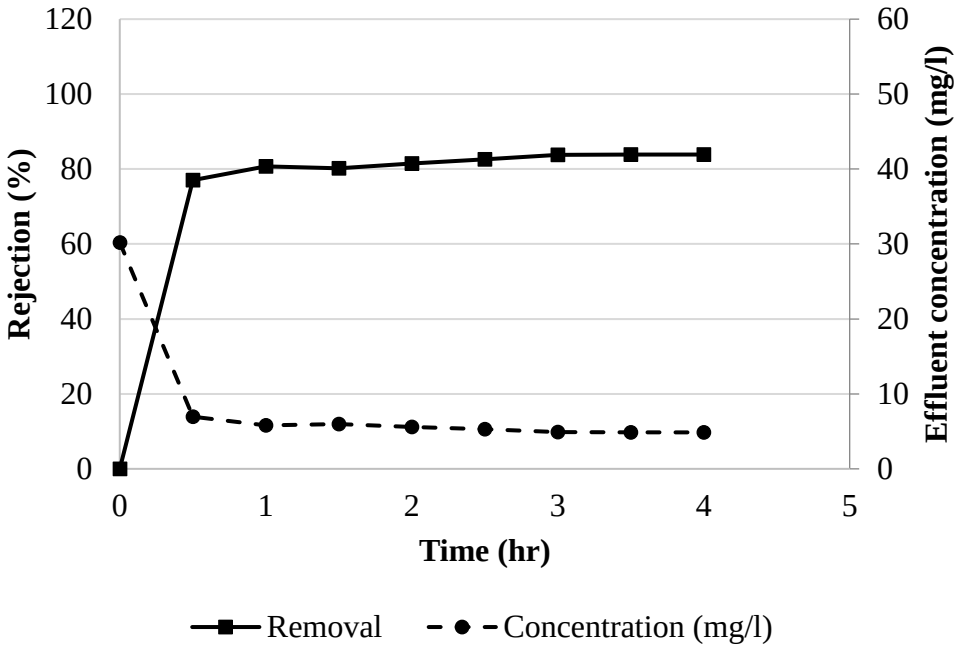

Figure 55. Rejection of antimony with NF270 membrane for 30 mg/l initial antimony concentration

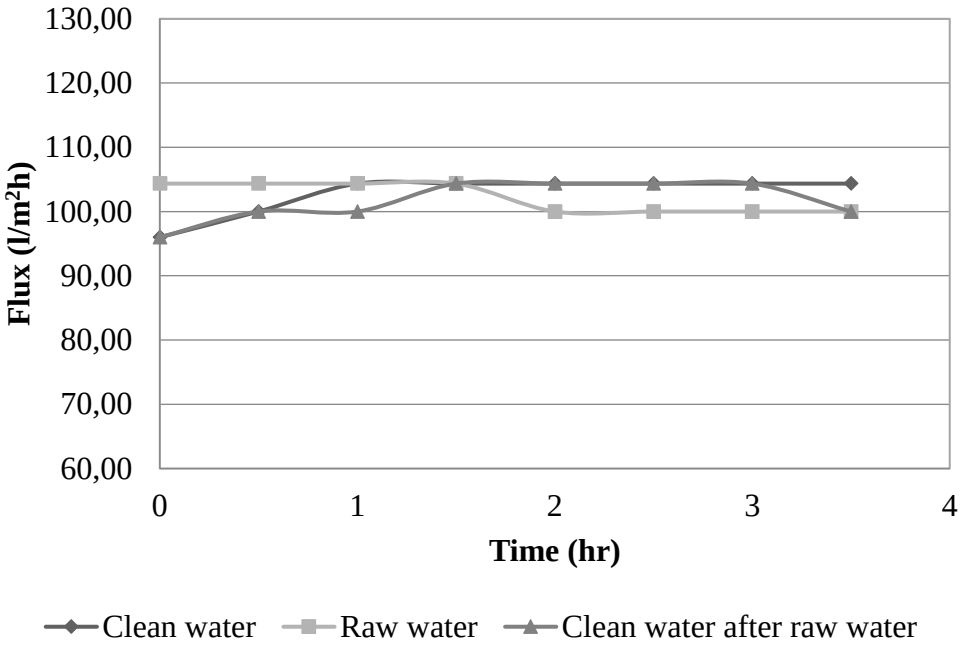

Figure 56. Change of flux with time for 50 mg/l initial antimony concentration for NF270 membrane

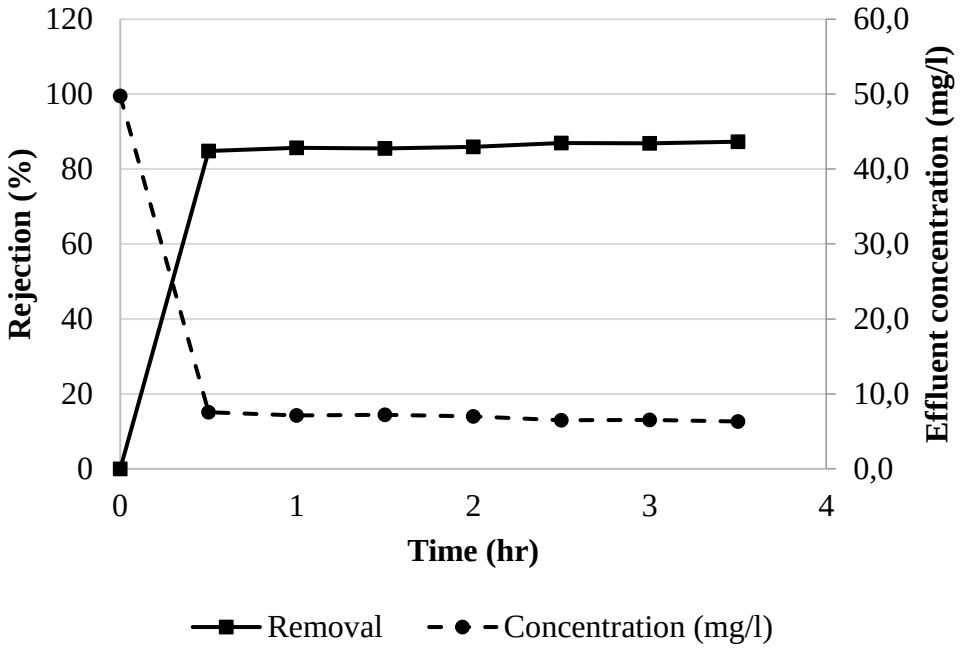

Figure 57. Rejection of antimony with NF270 membrane for 50 mg/l initial antimony concentration

There was no change in filtration flux with time and nearly no irreversible fouling was obtained for both of the RO and NF membrane applications which mean that the fouling was completely reversible. Also, there are not much differences between 30 mg/l and 50 mg/l antimony concentration feed flux, so it can be said that for synthetically prepared antimony solutions, concentration change doesn't have significant effect on process efficiency just as RO process. But for the real wastewater sample, the situation can be different therefore to draw conclusion on this issues same experiments should be performed with real samples.

The removal efficiency of membrane was evaluated by the analysis of the feed samples and permeates samples with respect to their antimony concentrations. Removal efficiencies for both concentrations are found above 80 %. The change of antimony rejection and effluent concentration of antimony with time using NF270 membrane for the initial antimony concentrations of 30 and 50 mg/l are given in Figure 55 and Figure 57, respectively.

This study was conducted at constant temperature 25 °C. But according to literature searches temperature change has an important effect on pore size of the membrane.

Dang et al. (2014) investigated effect of temperature on NF270 membrane pore radius. Results showed that as the feed temperature increased from 20 to 40 °C, the average pore size increased from 0.39 to 0.44 nm. According to results of different studies on different temperature ranges, it is concluded that with increasing temperature, the membrane average pore size increased and this enlargement of the pore size can be result of the thermal expansion of the polyamide skin layer. As a result, increase in temperature could adversely affect rejection of antimony. Therefore, as a result of the study, it was concluded that low temperatures are better in removal of antimony with NF270 membrane (Dang et al., 2014).

The effectiveness of RO and NF membrane were evaluated for antimony removal. According to results, fouling was completely reversible for both membranes. Besides, RO membranes were more satisfactory regarding the permeate quality. In order to give the right decision about membrane performances, more comprehensive study should be implemented and evaluation should be done according the results on the process efficiency and economic feasibility.

4.6 Comparison of Treatment Methods

In this thesis, the conventional methods namely; adsorption, coagulation – flocculation and advanced treatment method membrane filtration were investigated for antimony removal. Results showed that all of three methods have remarkable efficiency on removal of antimony.

Adsorption is a commonly used method due to its effectiveness, simplicity and low cost. Removal of antimony with zeolite was evaluated for different parameters. As a result of batch experiments, optimum conditions for antimony removal were determined as pH 3 and 25 °C. The results of kinetic experiments showed that 85 % removal efficiency was achieved for 5 mg/l initial antimony concentration at optimum conditions. This method seems favorable due to previously mentioned properties of zeolite. Zeolite is very commonly found in Turkey. And also, the location of the zeolite reserves and antimony reserves are very close to each other which can be advantageous as the logistics cost will be minimal.

Coagulation – flocculation was also assessed for different conditions. Results showed that ferric chloride is much more efficient than alum for antimony removal. At ph 7 and 25 °C, with proper ferric coagulant dosage, about 99 % removal can be achieved. Despite its high efficiency and simplicity, adding chemical to remove pollutants should be considered carefully. The correct dosage of chemicals is also very important for the process to work correctly. According to variations in the flux, required chemical amount should be followed regularly.

Lastly, advanced treatment method membrane filtration was applied for antimony removal. As it was expected, high removal efficiencies, about 99 %, was achieved with reverse osmosis and also above 80 % efficiency was achieved with nanofiltration. Results are promising but more comprehensive studies should be performed to evaluate effect of system parameters. When compared with other conventional methods, membrane process is more expensive. Therefore, before application of this method, it should be investigated in all aspects.

As a result, all of the three methods seem as applicable treatment methods for antimony pollution in aquatic environment. According to the need of the treatment and budget of the plant, by evaluating advantages and disadvantages suitable treatment method should be decided for antimony removal. The summary of the removal efficiencies for all the methods are given in Table 13.

Table 13. Comparison of the removal efficiencies

Treatment method	**Details**	**Influent Sb concentration (mg/l)**	**Effluent Sb concentration (mg/l)**	**Highest achieved Sb removal efficiency**
Adsorption	Zeolite as an adsorbent	5	0.75	85 %
Coagulation-Flocculation	Alum as a coagulant	50	28.25	44 %
	Ferric chloride as a coagulant	5-50	<0.06	99 %
Membrane Processes	Nanofiltration	50	6.52	85 %
	Reverse Osmosis	30/50	<0.06	99 %

CHAPTER 5

CONCLUSION

The purpose of this study was to evaluate antimony pollution and to explore antimony removal methods from aquatic environment. In a recent regulation (Yerüstü Su Kalitesi Yönetmeliğinde Değişiklik Yapılmasına Dair Yönetmelik, 2016), antimony has listed among the specific pollutants of Turkey. The initial monitoring results from Yeşilırmak River Basin, where an antimony mining site is located, revealed significant amount of antimony released into the aquatic environment (higher than 200 times of EQS). Furthermore, previous studies also pointed out antimony levels higher than EQS in various regions of Turkey where antimony mining activities take place. Hence, it is expected to observe high levels of antimony in the vicinity of antimony mining sites which are located in seven cities and six different river basins in Turkey. Due to the known reverse effects of antimony on human and environment, the control and removal of antimony in aquatic environment has significant importance.

In order to minimize antimony pollution, easily applicable, efficient, and economical treatment methods that could be integrated in conventional water and wastewater treatment plants were explored. Adsorption due to its convenience, ease of operation and simplicity of design was chosen as a primary alternative. Considering the availability, and cost, zeolite was selected as an adsorbent to examine the removal of antimony via adsorption process. Other two alternatives assessed were coagulation-flocculation and membrane processes.

Efficiency of adsorption process on Sb (III) removal was investigated by using natural zeolite supplied from Gördes region. The main operational parameters; pH, temperature and agitation rate were examined in order to observe the effect on the adsorption capacity of the zeolite. The result of these batch experiments showed that pH is a critical parameter when compared to temperature and agitation. Our results indicated that Sb adsorption with zeolite was favored at acidic pH values. The highest adsorption capacity was achieved at pH 3 and as pH increased adsorption capacity of

zeolite decreased notably. Whereas change in temperature and agitation was not found as critical as pH change. The batch experiments showed that the antimony adsorption increased with time and reached the equilibrium around 4 hours. Highest adsorption capacity was achieved as 2.02 mg/g at pH 3, 25 °C for 50 mg/l initial antimony concentration. As the initial antimony concentration decreased to 5 mg/l, the adsorption capacity of zeolite went down to 0.2 mg/g even at pH 3. Therefore, our results indicated that initial antimony concentration in the environment had major impact on adsorption capacity of the zeolite. Although achieving lowest adsorption capacity for the lowest initial antimony concentration, removal efficiencies were found as the highest for the lowest initial antimony concentration. The highest removal efficiency was achieved as 85 % and 82 % for 5 mg/l and 50 mg/l initial antimony concentration at optimum conditions, respectively. Moreover, experimental data were successfully fitted into Langmuir and Freundlich isotherms and indicated a slightly better fit with the Langmuir model.

Although zeolite was considered as an advantageous adsorbent because of its low cost, availability, user friendly application, non-toxic nature, easy accessibility and abundancy, the antimony adsorption capacity of zeolite was not very high. Due to this reason, other treatment methods, coagulation and flocculation and membrane process, were evaluated. It was possible to reach 99% removal via conventional coagulation and flocculation process with ferric chloride. On the other hand, only 44% removal was achieved with alum. The removal efficiency reached by using membrane processes was remarkable. It was possible to remove 85% of antimony via nanofiltration and 99 % via reverse osmosis membranes.

Conventional treatment methods, adsorption and coagulation-flocculation, and an advanced treatment method, membrane process were investigated and compared between each other in terms of their antimony removal rates. Our results indicated that adsorption, coagulation-flocculation and membrane processes can be evaluated as promising technologies to treat antimony contamination in aquatic environment. Zeolite adsorption could be a cost-effective solution and could be a feasible option where zeolite reserves are in the proximity of antimony mining sites. It is easy of use, simplicity and operational flexibility favors this process over others. As it is seen in the experiments, the initial Sb concentration have significant effect on adsorption

capacity of zeolite. Therefore, this factor should be considered while selecting the appropriate method for antimony removal. On the other hand, coagulation flocculation especially with ferric chloride was found very effective in antimony removal. The cost of chemical and excessive sludge generation would be the main drawback of this process. Remarkably high removal efficiencies were observed from membrane processes. When effluent water is considered for reuse, this process would be a preferred option for antimony removal.

CHAPTER 6

RECOMMENDATIONS

As a future study, pretreatment can be applied to increase adsorption capacity of zeolite. There are some studies on this topic for heavy metal removal but it is very limited for antimony removal. Semmens & Martin (1990) compared raw natural zeolite and zeolite conditioned with sodium chloride solution for heavy metal removal. By conditioning, removal of potassium ions in zeolite increases zeolite capacity and heavy metals selectivity such as copper and cadmium. It is difficult to displace these ions from zeolite structure but it has a significant effect on zeolite ion exchange performance.

This study focused on the samples containing single Sb(III) ions. However, in real aquatic systems, there could be other pollutants as well. Hence, attention should be put on the effect of other coexisting pollutants for the future adsorption process investigations.

In the study, as alternative treatment methods membrane process and coagulation-flocculation process are evaluated briefly. And it is seen that they are promising treatment methods for antimony contamination. In order to evaluate advantages, disadvantages and applicability of these methods for antimony removal in real systems, more comprehensive research and experiments should be performed for future studies.

REFERENCES

A Local Law to Protect Infants And Children From harmful Health Effects Of Unnecessary Exposure To Toxic Chemicals. (2014). *Local Law No. "J" For 2014*. Retrieved from http://app.albanycounty.com/legislature/resolutions/2014/20141208/2014-LL_J.pdf

Abd El Maksod, I. H., Elzaharany, E. A., Kosa, S. A., & Hegazy, E. Z. (2016). Simulation program for zeolite A and X with an active carbon composite as an effective adsorbent for organic and inorganic pollutants. *Microporous and Mesoporous Materials*, *224*, 89–94. http://doi.org/10.1016/j.micromeso.2015.11.020

Abdel, M., & Mohamed, R. M. (2013). Chemical Engineering Research and Design Removal of antimony (III) by multi-walled carbon nanotubes from model solution and environmental samples. *Chemical Engineering Research and Design*, *91*(7), 1352–1360. http://doi.org/10.1016/j.cherd.2013.02.007

Agency for Toxic Substances and Diseases Registry. (2017). Toxicological Profile For Antimony and Compounds. *Agency for Toxic Substances and Disases Registry U.S. Pubblic Health Service*, (September), 136. http://doi.org/10.3109/15569529909037564

Aljebori, A. M. K., & Alshirifi, A. N. (2012). Effect of Different Parameters on the Adsorption of Textile Dye "Maxilon Blue GRL" From Aqueous Solution by Using White Marble. *Asian Journal of Chemistry*, *24*(12), 5813–5816.

An, Y. J., & Kim, M. (2009). Effect of antimony on the microbial growth and the activities of soil enzymes. *Chemosphere*, *74*(5), 654–659. http://doi.org/10.1016/j.chemosphere.2008.10.023

Anderson, C. G. (2012). The metallurgy of antimony. *Chemie Der Erde - Geochemistry*, *72*(SUPPL.4), 3–8. http://doi.org/10.1016/j.chemer.2012.04.001

Aregawi, B. H., & Mengistie, A. A. (2013). Removal of Ni(II) from aqueous solution using leaf, bark and seed of moringa stenopetala adsorbents. *Bulletin of the Chemical Society of Ethiopia*, *27*(1), 35–47. http://doi.org/10.4314/bcse.v27i1.4

Arsenic Technologies. (2008).

Arslan, Ş., & Çelik, M. (2015). Assessment of the pollutants in soils and surface waters around Gümüşköy Silver Mine (Kütahya, Turkey). *Bulletin of Environmental Contamination and Toxicology*, *95*(4), 499–506. http://doi.org/10.1007/s00128-015-1613-6

Barloková, D., Ilavský, J., & Kunštek, M. (2012). Removal of antimony from water by coagulation, *XI*(4).

Basel Convention on the Control of Transboundary Movements of Hazardous Wastes and Their Disposal Adopted By the Conference of the Plenipotentiaries on 22 March 1989. (1992). *Assembly*, (March 1989). Retrieved from http://www.basel.int/portals/4/basel convention/docs/text/baselconventiontext-e.pdf

Ben-noun, L. (2016). *Medical effects of cosmetics*.

Bilgin, O., & Kokturk, U. (n.d.). Raw material properties of gordes zeolite ores.

Biswas, B. K., Inoue, J. ichi, Kawakita, H., Ohto, K., & Inoue, K. (2009). Effective removal and recovery of antimony using metal-loaded saponified orange waste. *Journal of Hazardous Materials*, *172*(2–3), 721–728. http://doi.org/10.1016/j.jhazmat.2009.07.055

Butterman, C., & Carlin, J. F. (2004). Antimony.

Chen, Y. W., Deng, T. L., Filella, M., & Belzile, N. (2003). Distribution and early diagenesis of antimony species in sediments and porewaters of freshwater lakes. *Environmental Science and Technology*, *37*(6), 1163–1168. http://doi.org/10.1021/es025931k

Choi, H., Zhang, K., Dionysiou, D., Oerther, D., & Sorial, G. (2005). *Influence of cross-flow velocity on membrane performance during filtration of biological suspension*. *Journal of Membrane Science* (Vol. 248). http://doi.org/10.1016/j.memsci.2004.08.027

Choubert, J. M., Pomiès, M., Martin Ruel, S., & Coquery, M. (2011). Influent concentrations and removal performances of metals through municipal wastewater treatment processes. *Water Science and Technology*, *63*(9), 1967–1973. http://doi.org/10.2166/wst.2011.126

Cidu, R., Biddau, R., & Dore, E. (2012). Antimony contamination of surface water at abandoned Sardinian mine sites.

Çağın, V. (2006). *Use of Clinoptilolite for Copper and Nickel Removal From Aqueous Solutions*. Middle East Technical University.

Dakovi, A., Rottinghaus, G. E., Kragovi, M., Krajiˇ, D., Mercurio, M., Gennaro, B. De, & Mili, J. (2017). Colloids and Surfaces B : Biointerfaces Adsorption of the mycotoxin zearalenone by clinoptilolite and phillipsite zeolites treated with cetylpyridinium surfactant, *151*, 324–332. http://doi.org/10.1016/j.colsurfb.2016.12.033

Dang, H. Q., Price, W. E., & Nghiem, L. D. (2014). The effects of feed solution temperature on pore size and trace organic contaminant rejection by the nanofiltration membrane NF270. *Separation and Purification Technology*, *125*, 43–51. http://doi.org/10.1016/j.seppur.2013.12.043

Devlet Planlama Teşkilatı. (2001). Sekizinci Beş Yıllık Kalkınma Planı Madencilik Özel İhtisas Komisyonu Raporu Metal Madenler Alt komisyonu Diğer Metal Madenler Çalışma Grubu Raporu. *State Planning Organization*, 46–54.

Du, X., Qu, F., Liang, H., Li, K., Yu, H., Bai, L., & Li, G. (2014). Removal of antimony (III) from polluted surface water using a hybrid coagulation-flocculation-ultrafiltration (CF-UF) process. *Chemical Engineering Journal*, *254*, 293–301. http://doi.org/10.1016/j.cej.2014.05.126

Duran, M., Kara, Y., Akyildiz, G. K., & Ozdemir, A. (2007). Antimony and heavy metals accumulation in some macroinvertebrates in the Yesilirmak River (N Turkey) near the Sb-mining area. *Bulletin of Environmental Contamination and Toxicology*, *78*(5), 395–399. http://doi.org/10.1007/s00128-007-9183-x

Elaiopoulos, K., Perraki, T., & Grigoropoulou, E. (2010). Monitoring the effect of hydrothermal treatments on the structure of a natural zeolite through a combined XRD, FTIR, XRF, SEM and N2-porosimetry analysis. *Microporous and Mesoporous Materials*, *134*(1–3), 29–43. http://doi.org/10.1016/j.micromeso.2010.05.004

Engler, T. W. (n.d.). *Lecture Notes/Reserve Definitions*. Retrieved from http://infohost.nmt.edu/~petro/faculty/Engler472/ReserveDefinitions.pdf

EPA. (2014). Priority Pollutant List. Retrieved from https://www.epa.gov/sites/production/files/2015-09/documents/priority-pollutant-list-epa.pdf

Erdem, E., Karapinar, N., & Donat, R. (2004). The removal of heavy metal cations by natural zeolites. *Journal of Colloid and Interface Science*, *280*(2), 309–314. http://doi.org/10.1016/j.jcis.2004.08.028

European Commission. (1976). Council Directive 76/464/EEC of 4 May 1976 on

pollution caused by certain dangerous substances discharged into the aquatic environment of the Community. Retrieved from http://eur-lex.europa.eu/legal-content/EN/TXT/?uri=CELEX:31976L0464

European Commission. (1998). Council Directive 98/83/EC of 3 November 1998 on the quality of water intended for human consumption. Retrieved from http://eur-lex.europa.eu/legal-content/EN/TXT/?uri=CELEX:31998L0083

European Union. (2008). *Risk Assessment Report-Diantimony Trioxide*.

Fay, M., Brattin, W. J., & Donohue, J. M. (1999). Public Health Statement Antimony. *Toxicology and Industrial Health*, *15*(8), 652–654. http://doi.org/10.1177/074823379901500802

Filella, M., Belzile, N., & Chen, Y. W. (2002a). Antimony in the environment: A review focused on natural waters I. Occurence. *Earth-Science Reviews*, *57*(1–2), 125–176. http://doi.org/10.1016/S0012-8252(01)00070-8

Filella, M., Belzile, N., & Chen, Y. W. (2002b). Antimony in the environment: A review focused on natural waters II. Relevant solution chemistry. *Earth-Science Reviews*, *59*(1–4), 265–285. http://doi.org/10.1016/S0012-8252(02)00089-2

Flakova, R., Zenisova, Z., & Sracek, O. (2012). The behavior of arsenic and antimony at Pezinok mining site , southwestern part of the Slovak Republic, 1043–1057. http://doi.org/10.1007/s12665-011-1310-7

Fu, Z., Wu, F., Amarasiriwardena, D., Mo, C., Liu, B., Zhu, J., … Liao, H. (2010). Antimony, arsenic and mercury in the aquatic environment and fish in a large antimony mining area in Hunan, China. *Science of The Total Environment*, *408*(16), 3403–3410. http://doi.org/10.1016/j.scitotenv.2010.04.031

Gemici, Ü., & Tarcan, G. (2007). Assessment of the pollutants in farming soils and waters around untreated abandoned Türkönü mercury mine (Turkey). *Bulletin of Environmental Contamination and Toxicology*, *79*(1), 20–24. http://doi.org/10.1007/s00128-007-9087-9

Gevorkyan, R. G., Sargsyan, H. H., Karamyan, G. G., Keheyan, Y. M., Yeritsyan, H. N., Hovhannesyan, a. S., & Sahakyan, a. a. (2002). Study of Absorption Properties of Modified Zeolites. *Chemie Der Erde - Geochemistry*, *62*(3), 237–242. http://doi.org/10.1078/0009-2819-00014

Guo, X., Wu, Z., & He, M. (2009). Removal of antimony(V) and antimony(III) from drinking water by coagulation-flocculation-sedimentation (CFS). *Water Research*, *43*(17), 4327–4335. http://doi.org/10.1016/j.watres.2009.06.033

Hamdaoui, O., & Naffrechoux, E. (2007). Modeling of adsorption isotherms of phenol and chlorophenols onto granular activated carbon. Part I. Two-parameter models and equations allowing determination of thermodynamic parameters. *Journal of Hazardous Materials*, *147*(1–2), 381–394. http://doi.org/10.1016/j.jhazmat.2007.01.021

Hargreaves, A. J., Vale, P., Whelan, J., Constantino, C., Dotro, G., & Cartmell, E. (2016). Mercury and antimony in wastewater: Fate and treatment. *Water, Air, and Soil Pollution*, *227*(3). http://doi.org/10.1007/s11270-016-2756-8

He, Z., Liu, R., Qu, J., & Liu, H. (2015). Adsorption of Sb(III) and Sb(V) on Freshly Prepared Ferric Hydroxide (FeOxHy) Zan, *32*(2), 95–102. http://doi.org/10.1089/ees.2014.0155

Herath, I., Vithanage, M., & Bundschuh, J. (2017). Antimony as a global dilemma: Geochemistry, mobility, fate and transport. *Environmental Pollution*, *223*, 545–559. http://doi.org/10.1016/j.envpol.2017.01.057

Idris, M. N., Ahmad, Z. A., & Ahmad, M. A. (2011). Adsorption equilibrium of malachite green dye onto rubber seed coat based activated carbon. *International Journal of Basic & Applied Sciences*, *11*(February), 38–43.

Ilavsk, J. (2008). Removal of Antimony from water by Sorption Materials, 1–6.

IWA. (n.d.). *Coagulation and Flocculation in Water and Wastewater Treatment*. Retrieved from https://www.iwapublishing.com/news/coagulation-and-flocculation-water-and-wastewater-treatment

Jha, B., & Singh, D. N. (2016). Fly Ash Zeolites, *78*. http://doi.org/10.1007/978-981-10-1404-8

Jia, M., Hu, J. W., Luo, J., Duan, S. M., Li, Z. Bin, & Liu, C. (2013). Comparison Study on Adsorption and Removal of Antimony from Acidic Aqueous Solution by Activated Carbons and Machine-Made Charcoal. *Advanced Materials Research*, *779–780*, 1600–1606. http://doi.org/10.4028/www.scientific.net/AMR.779-780.1600

Kang, M., Kamei, T., & Magara, Y. (2003). Comparing polyaluminum chloride and ferric chloride for antimony removal. *Water Research*, *37*(17), 4171–4179. http://doi.org/10.1016/S0043-1354(03)00351-8

Kang, M., Kawasaki, M., Tamada, S., Kamei, T., & Magara, Y. (2000). Effect of pH on the removal of arsenic and antimony using reverse osmosis membranes. *Desalination*, *131*(1–3), 293–298. http://doi.org/10.1016/S0011-

9164(00)90027-4

Kırşan, İ. H. (2004). Türkiye Zeolit Potansiyeli ve Değerlendirme İmkanları. *5. Endüstriyel Hammaddeler Sempozyumu, İzmir, Türkiye*.

Kjaergaard, L. (1977). The redox potential: Its use and control in biotechnology. *Advances in Biochemical Engineering*, *7*. http://doi.org/https://doi.org/10.1007/BFb0048444

Leng, Y., Guo, W., Su, S., Yi, C., & Xing, L. (2012). Removal of antimony (III) from aqueous solution by graphene as an adsorbent. *Chemical Engineering Journal*, *211–212*, 406–411. http://doi.org/10.1016/j.cej.2012.09.078

Li, L. Y., Grace, J. R., Vivacqua, V., Xu, W., & He, G. (2013). Modeling of zinc adsorption onto clinoptilolite in a slurry bubble column, *100*, 326–331. http://doi.org/10.1016/j.ces.2013.02.053

Li, T. (2011). Antimony and Antimony Alloys. *Kirk-Othmer Encyclopedia of Chemical Technology*, *1*(15).

Lin, H., Liu, Q., Dong, Y., Chen, Y., Huo, H., & Liu, S. (2013). Study on Channel Features and Mechanism of Clinoptilolite Modified by LaCl3. *Journal of Materials Science Research*, *2*(4), 37–44. http://doi.org/10.5539/jmsr.v2n4p37

Local Law-Proposed amendment-Prohibiting the sale of children's products containing certain chemicals. (2015). *LL-2015-8*. Retrieved from http://westchestercountyny.iqm2.com/Citizens/Detail_LegiFile.aspx?ID=7750&highlightTerms=local law

Minceva, M., Fajgar, R., Markovska, L., & Meshko, V. (2008). Comparative Study of Zn2+, Cd2+, and Pb2+ Removal From Water Solution Using Natural Clinoptilolitic Zeolite and Commercial Granulated Activated Carbon. Equilibrium of Adsorption . *Separation Science and Technology*, *43*(8), 2117–2143. http://doi.org/10.1080/01496390801941174

Ministry of Forestry and Water Affairs. (2016). Yerüstü Su Kalitesi Yönetmeliğinde Değişiklik Yapılmasına Dair Yönetmelik. *Official Gazette, Dated 10.08.2016, Numbered 29797*. Retrieved from http://www.resmigazete.gov.tr/eskiler/2016/08/20160810-9.htm

Ministry of Health. (2013). İnsani Tüketim Amaçlı Sular Hakkında Yönetmelikte Değişiklik Yapılmasına Dair Yönetmelik. *Official Gazette, Dated 07.03.2013, Numbered 28580*. Retrieved from http://www.resmigazete.gov.tr/eskiler/2013/03/20130307-7.htm

Mitsunobu, S., Harada, T., & Takahashi, Y. (2006). Comparison of Antimony Behavior with that of Arsenic under Various Soil Redox Conditions. *Environmental Science and Technology*, *40*(23), 7270–7276.

Morali, N. (2006). Investigation of Zinc and Lead Removal From Aqueous Solutions Using Clinoptilolite, (January), 109.

Motsi, T., Rowson, N. A., & Simmons, M. J. H. (2009). Adsorption of heavy metals from acid mine drainage by natural zeolite. *International Journal of Mineral Processing*, *92*(1–2), 42–48. http://doi.org/10.1016/j.minpro.2009.02.005

Moussavi, G., Talebi, S., Farrokhi, M., & Sabouti, R. M. (2011). The investigation of mechanism, kinetic and isotherm of ammonia and humic acid co-adsorption onto natural zeolite. *Chemical Engineering Journal*, *171*(3), 1159–1169. http://doi.org/10.1016/j.cej.2011.05.016

Mubarak, H., Chai, L.-Y., Mirza, N., Yang, Z.-H., Pervez, A., Tariq, M., … Mahmood, Q. (2015). Antimony (Sb) – pollution and removal techniques – critical assessment of technologies. *Toxicological & Environmental Chemistry*, *97*(10), 1296–1318. http://doi.org/10.1080/02772248.2015.1095549

Multani, R. S., Feldmann, T., & Demopoulos, G. P. (2016). Antimony in the metallurgical industry: A review of its chemistry and environmental stabilization options. *Hydrometallurgy*, *164*, 141–153. http://doi.org/10.1016/j.hydromet.2016.06.014

Nam, S. H., Yang, C. Y., & An, Y. J. (2009). Effects of antimony on aquatic organisms (Larva and embryo of Oryzias latipes, Moina macrocopa, Simocephalus mixtus, and Pseudokirchneriella subcapitata). *Chemosphere*, *75*(7), 889–893. http://doi.org/10.1016/j.chemosphere.2009.01.048

Nash, M. J., Maskall, J. E., & Hill, S. J. (2000). Methodologies for determination of antimony in terrestrial environmental samples. *Journal of Environmental Monitoring*, *2*(2), 97–109. http://doi.org/10.1039/a907875d

Pavlovic, J., Milenkovic, J., Stojakovic, D., & Rajic, N. (2013). Surface Modification of the Natural Clinoptilolite for Its Potential Use for the Nitrate Removal From, 112–115.

Pernitsky, D. J., & Edzwald, J. K. (2006). Selection of alum and polyaluminum coagulants: principles and applications. *Journal of Water Supply: Research and Technology - Aqua*, *55*(2), 121 LP-141. Retrieved from http://aqua.iwaponline.com/content/55/2/121.abstract

Qi, P., & Pichler, T. (2016). Sequential and simultaneous adsorption of Sb(III) and Sb(V) on ferrihydrite: Implications for oxidation and competition. *Chemosphere*, *145*, 55–60. http://doi.org/10.1016/j.chemosphere.2015.11.057

Ritchie, V. J., Ilgen, A. G., Mueller, S. H., Trainor, T. P., & Goldfarb, R. J. (2013). Mobility and chemical fate of antimony and arsenic in historic mining environments of the Kantishna Hills district , Denali National Park and Preserve , Alaska. *Chemical Geology*, *335*, 172–188. http://doi.org/10.1016/j.chemgeo.2012.10.016

Sarı, A., Çıtak, D., & Tuzen, M. (2010). Equilibrium, thermodynamic and kinetic studies on adsorption of Sb(III) from aqueous solution using low-cost natural diatomite. *Chemical Engineering Journal*, *162*(2), 521–527. http://doi.org/10.1016/j.cej.2010.05.054

Sari, A., Şahinoğlu, G., & Tüzen, M. (2012). Antimony(III) adsorption from aqueous solution using raw perlite and Mn-modified perlite: Equilibrium, thermodynamic, and kinetic studies. *Industrial and Engineering Chemistry Research*, *51*(19), 6877–6886. http://doi.org/10.1021/ie300243n

Satterfield, Z. (2005). Jar Testing. *Tech Brief*, *5*(1).

Semmens, M. J., & Martin, W. P. (1990). The influence of pretreatment on the capacity and selectivity of clinoptilolite for metal ions, *22*(5), 537–542.

Servos, M. R. (2014). *Nanotechnology for Water Treatment and Purification*.

Sharma, A. (2012). *Adsorption-Lecture Notes*. Retrieved from http://nptel.ac.in/courses/103104045/pdf_version/lecture25.pdf

Shirazi, S., Lin, C. J., & Chen, D. (2010). Inorganic fouling of pressure-driven membrane processes - A critical review. *Desalination*, *250*(1), 236–248. http://doi.org/10.1016/j.desal.2009.02.056

Shortland, A. J. (2002). The use and origin of antimonate colorants in early Egyptian glass. *Archaeometry*, *44*(4), 517–530. http://doi.org/10.1111/1475-4754.t01-1-00083

Shotyk, W., Cheburkin, A. K., Appleby, P. G., Fankhauser, A., & Kramers, J. D. (1996). Two thousand years of atmospheric arsenic, antimony, and lead deposition recorded in an ombrotrophic peat bog profile, Jura Mountains, Switzerland. *Earth and Planetary Science Letters*, *145*(1–4), E1–E7. http://doi.org/10.1016/S0012-821X(96)00197-5

Speakman, S. A. (n.d.). Introduction to X-Ray Powder Diffraction Data Analysis, 20.

Retrieved from http://prism.mit.edu/xray/Introduction to XRPD Data Analysis.pdf

Sprynskyy, M., Buszewski, B., Terzyk, A. P., & Namieśnik, J. (2006). Study of the selection mechanism of heavy metal (Pb2+, Cu2+, Ni2+, and Cd2+) adsorption on clinoptilolite. *Journal of Colloid and Interface Science*, *304*(1), 21–28. http://doi.org/10.1016/j.jcis.2006.07.068

Swapp, S. (2014). Scanning Electron Microscope (SEM). Retrieved from http://serc.carleton.edu/research_education/geochemsheets/techniques/SEM.html

Targan, F., Tirtom, V. N., & G, B. A. (2013). Removal of Antimony (III) from Aqueous Solution by Using Grey and Red Erzurum Clay and Application to the Gediz River Sample, *2013*.

The Water Supply (Water Quality) Regulations. (2016). *2016 No. 614*. Retrieved from http://www.legislation.gov.uk/uksi/2016/614/contents/made

Treacy, M. M. J., & Higgins, J. B. (2001). *Collection of Simulated XRD Powder Patterns for Zeolites*. Retrieved from http://www.iza-structure.org/books/Collection_4ed.pdf

Uluozlu, O. D., Sari, A., & Tuzen, M. (2010). Biosorption of antimony from aqueous solution by lichen (Physcia tribacia) biomass. *Chemical Engineering Journal*, *163*(3), 382–388. http://doi.org/10.1016/j.cej.2010.08.022

Ungureanu, G., Santos, S., Boaventura, R., & Botelho, C. (2015). Arsenic and antimony in water and wastewater: Overview of removal techniques with special reference to latest advances in adsorption. *Journal of Environmental Management*, *151*, 326–342. http://doi.org/10.1016/j.jenvman.2014.12.051

USGS. (2015). *The Mineral Industry of Turkey*. Retrieved from https://minerals.usgs.gov/minerals/pubs/country/2013/myb3-2013-tu.pdf

USGS. (2016a). *Antimony- 2014 Minerals Yearbook*. Retrieved from https://minerals.usgs.gov/minerals/pubs/commodity/antimony/myb1-2014-antim.pdf

USGS. (2016b). *Antimony- 2014 Minerals Yearbook.*

Vaca Mier, M., López Callejas, R., Gehr, R., Jiménez Cisneros, B. E., & Alvarez, P. J. J. (2001). Heavy metal removal with mexican clinoptilolite: Multi-component ionic exchange. *Water Research*, *35*(2), 373–378. http://doi.org/10.1016/S0043-1354(00)00270-0

Walton, K. S., & Snurr, R. Q. (2007). Applicability of the BET method for determining surface areas of microporous metal-organic frameworks. *Journal of the American Chemical Society*, *129*(27), 8552–8556. http://doi.org/10.1021/ja071174k

Wang, L., Lewis, G. M., Chen, A. S. C., & National Risk Management Research Laboratory (U.S.). Office of Research and Development. (2011). Arsenic and antimony removal from drinking water by point-of-entry reverse osmosis coupled with dual plumbing distribution U.S. EPA demonstration project at Carmel Elementary School in Carmel, ME, final performance evaluation report, (March). Retrieved from http://purl.fdlp.gov/GPO/gpo19711

Wang, S., & Peng, Y. (2010). Natural zeolites as effective adsorbents in water and wastewater treatment. *Chemical Engineering Journal*, *156*(1), 11–24. http://doi.org/10.1016/j.cej.2009.10.029

Wang, X., He, M., Xi, J., & Lu, X. (2011). Antimony distribution and mobility in rivers around the world's largest antimony mine of Xikuangshan, Hunan Province, China. *Microchemical Journal*, *97*(1), 4–11. http://doi.org/10.1016/j.microc.2010.05.011

Watkins, R., Weiss, D., Dubbin, W., Peel, K., Coles, B., & Arnold, T. (2006). Investigations into the kinetics and thermodynamics of Sb(III) adsorption on goethite (α-FeOOH). *Journal of Colloid and Interface Science*, *303*(2), 639–646. http://doi.org/10.1016/j.jcis.2006.08.044

Xi, J., He, M., & Lin, C. (2011a). Adsorption of antimony(III) and antimony(V) on bentonite: Kinetics, thermodynamics and anion competition. *Microchemical Journal*, *97*(1), 85–91. http://doi.org/10.1016/j.microc.2010.05.017

Xi, J., He, M., & Lin, C. (2011b). Adsorption of antimony(III) and antimony(V) on bentonite: Kinetics, thermodynamics and anion competition. *Microchemical Journal*, *97*(1), 85–91. http://doi.org/10.1016/j.microc.2010.05.017

Xi, J., He, M., & Zhang, G. (2014). Antimony adsorption on kaolinite in the presence of competitive anions, 2989–2997. http://doi.org/10.1007/s12665-013-2673-8

Yang, X., Shi, Z., Yuan, M., & Liu, L. (2015). Adsorption of Trivalent Antimony from Aqueous Solution Using Graphene Oxide : Kinetic and Thermodynamic Studies. http://doi.org/10.1021/je5009262

Yoshida, H., Christensen, T. H., Guildal, T., & Scheutz, C. (2015). A comprehensive substance flow analysis of a municipal wastewater and sludge treatment plant.

Chemosphere, *138*, 874–882. http://doi.org/10.1016/j.chemosphere.2013.09.045

Yousef, R. I., El-Eswed, B., & Al-Muhtaseb, A. H. (2011). Adsorption characteristics of natural zeolites as solid adsorbents for phenol removal from aqueous solutions: Kinetics, mechanism, and thermodynamics studies. *Chemical Engineering Journal*, *171*(3), 1143–1149. http://doi.org/10.1016/j.cej.2011.05.012

Yu, T., Wang, X., & Li, C. (2014). Removal of Antimony by FeCl 3 -Modified Granular-Activated Carbon in Aqueous Solution. *Journal of Environmental Engineering (United States)*, *140*(9), 3–8. http://doi.org/10.1061/(ASCE)EE.1943-7870.0000736.

Zahoor, M. (2011). Effect of Agitation Speed on Adsorption of Imidacloprid on Activated Carbon. *Journal of the Chemical Society of Pakistan*, *33*(3), 305–312.

Zanin, E., Scapinello, J., de Oliveira, M., Rambo, C. L., Franscescon, F., Freitas, L., … Dal Magro, J. (2017). Adsorption of heavy metals from wastewater graphic industry using clinoptilolite zeolite as adsorbent. *Process Safety and Environmental Protection*, *105*, 194–200. http://doi.org/10.1016/j.psep.2016.11.008

Zhou, Z., Dai, C., & Zhou, X. (2015). The Removal of Antimony by Novel NZVI-Zeolite : the Role of Iron Transformation. http://doi.org/10.1007/s11270-014-2293-2

APPENDICES

A. AAS CALIBRATION CURVE

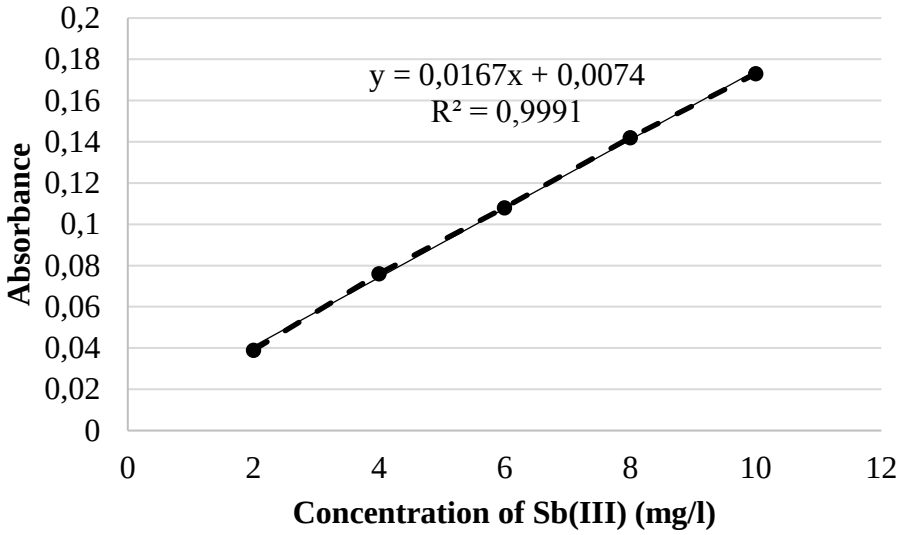

Figure A.1. Calibration Curve of Sb(III)

B. ZEOLITE DATA SHEET

TECHNICAL DATA SHEET

1. GENERAL INFORMATIONS

Chemical name	:	Hydrated sodium-potassium-calcium-alumino-silicate	**CAS No**	:	12173-10-3
Chemical family	:	Natural zeolite	**EINECS No**	:	215-283-8
Chemical abstract name:		Clinoptilolite			
Chemical formula	:	$(Na_{0.5}K_{2.5})\ (Ca_{1.0}Mg_{0.5})(Al_6Si_{30})O_{72}.24H_2O$			

2. MINERAL CONTENT

Clinoptilolite %80-90

* Studies on identification and the origin, petrographic and mineralogical analysis of the rock samples with X-Ray Diffractometer.

3. CHEMICAL CONTENT

SiO_2	64,7	BaO	<0,01	Si / Al	4.9 - 5.3	Mg	0.1 - 0.6
Al_2O_3	11,21	SrO	0,03	Na + K / Ca + Mg	1.4 - 2.2	Ca	0.9 - 1.3
Fe_2O_3	1,38	P_2O_5	0,011	Si	29.4 - 30.1	Na	0.2 - 0.5
MnO	0,02	CaO	2,08	Al	5.6 - 6.1		
TiO_2	0,08	Na_2O	0,38	Fe	0.05 - 0.25		
MgO	0,79	K_2O	3,78	K	1.9 - 2.7		

- Analyzed with XRF spectrophotometry.

4. PHYSICAL CHARACTERISTICS

Appearance	Can be found under granule and powder form.	**Color**	Light cream, beige, almond green.
Particle size	Micronized for animal feed additives	**Moisture content**	< 4 % , < 8 % , < 12 %
	0-1 mm for animal feed additives		
	1-3 mm for soil regulator/conditioner, filter media, animal litter.	**pH**	6,5 – 7,5
	3-5 mm can be produced according to the preferred size for animal litter and filter media applications.	**Solubility in water**	Insoluble
Mineral content	Minimum %85 Clinoptilolite, (up to 99 %). Country rock is clay and mica.	**Water retention capacity**	% 25 – 40
Bulk density	Micronized and 0-1 mm; 1,1 g/cm^3 , 1-3 mm and 3-5 mm 0,8 g/cm^3	**Porosity**	%35 average
Specific gravity	2 g/cm^3	**Melting point**	1.150 °C
Thermal stability	Until 840 °C	**Surface area**	40,79 m^2/g

C. EFFECT OF PH ON KINETIC TESTS

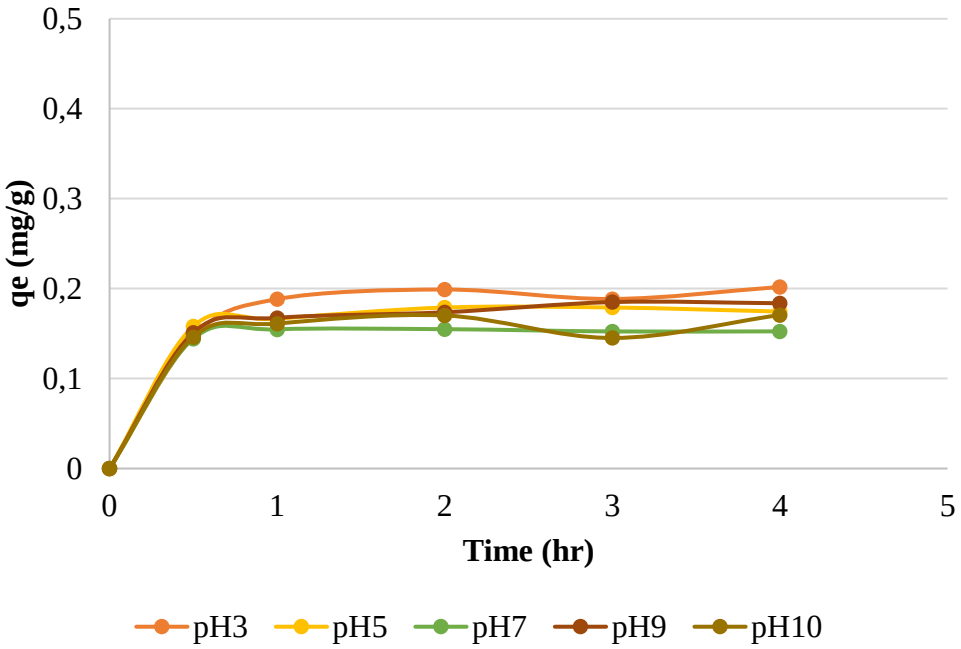

Figure C.1. Change of adsorption capacity with time for 5 mg/l initial Sb concentration

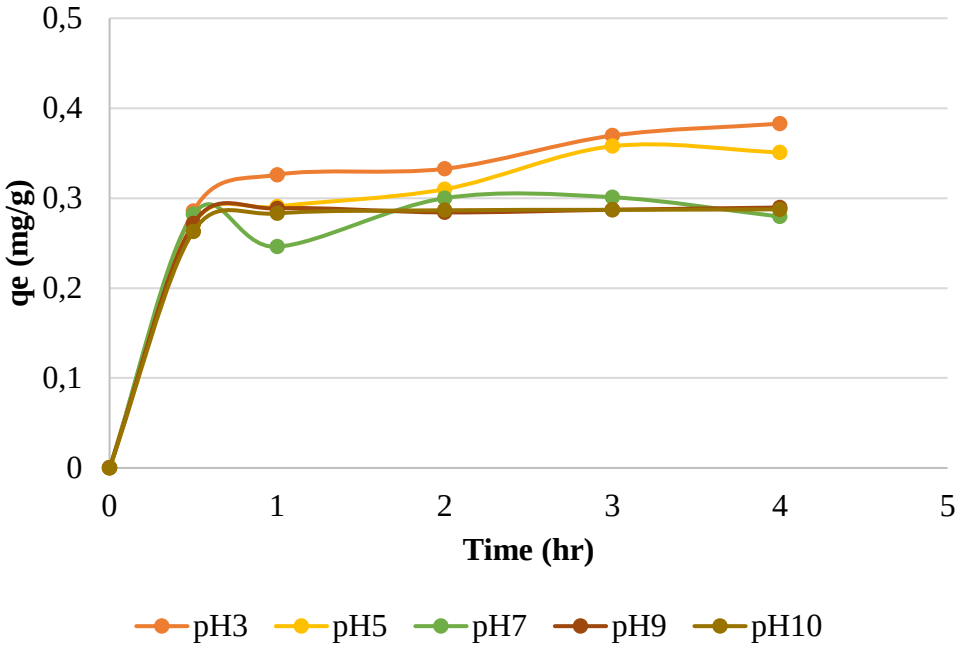

Figure C.2. Change of adsorption capacity with time for 10 mg/l initial Sb concentration

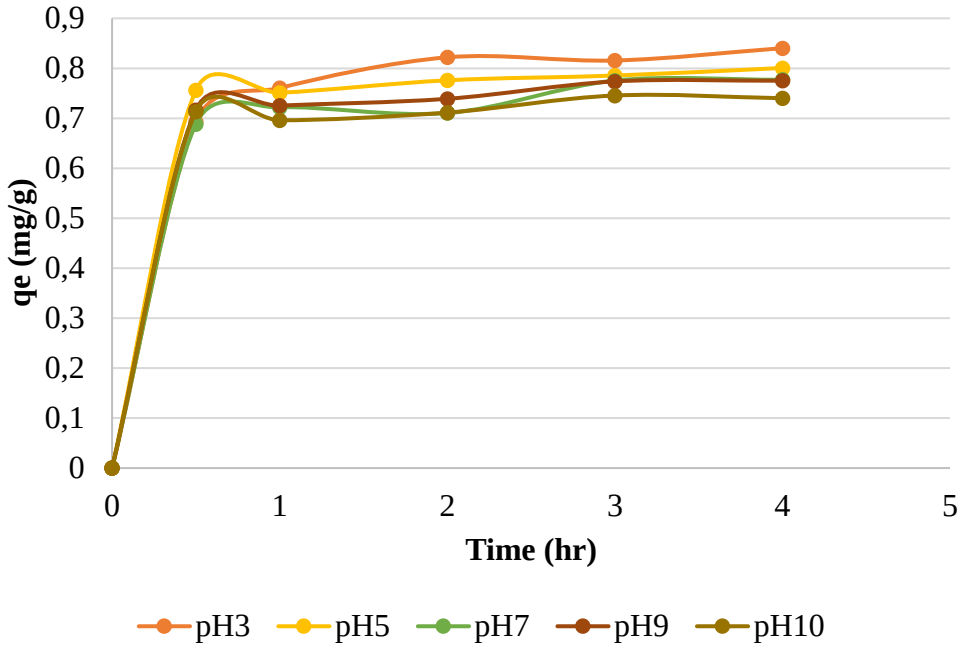

Figure C.3. Change of adsorption capacity with time for 20 mg/l initial Sb concentration

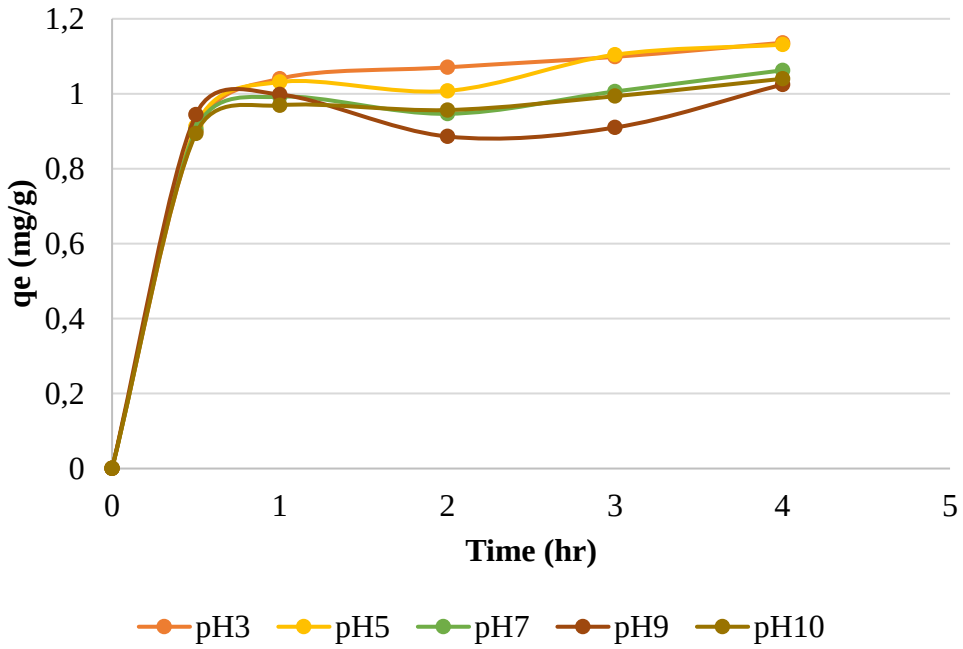

Figure C.4. Change of adsorption capacity with time for 30 mg/l initial Sb concentration

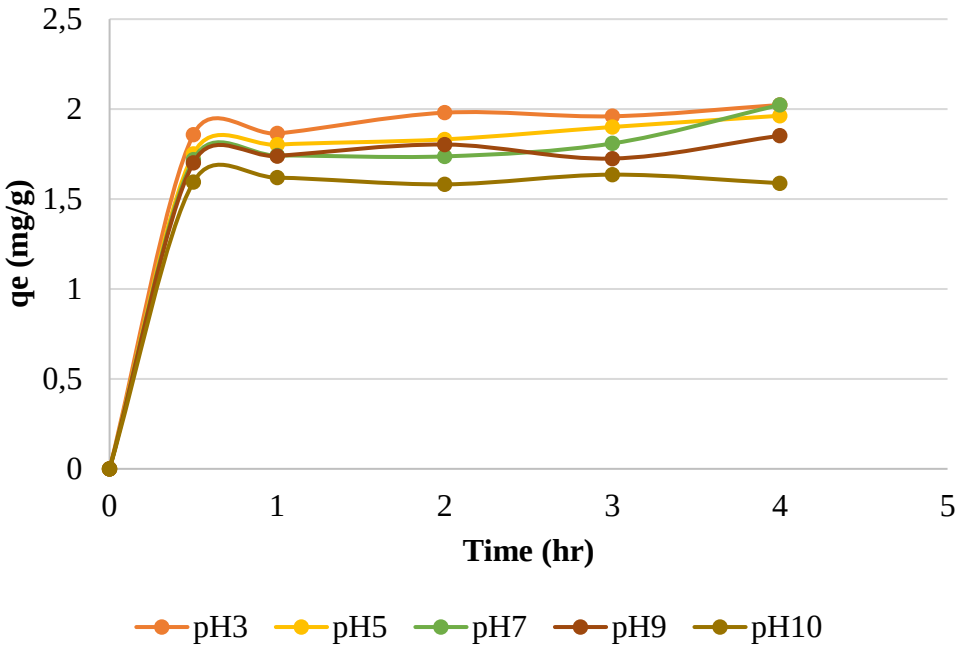

Figure C.5. Change of adsorption capacity with time for 50 mg/l initial Sb concentration

D. EQUILIBRIUM DATA FOR ISOTHERMS

Table D.1. Equilibrium data for zeolite sample at pH = 3.0, T = 25°C, 140 rpm, for contact time = 240 min, and adsorbent dosage = 5 g/250 ml

Equilibrium concentration (Ce) (mg/l)	**Equilibrium capacity (qe) (mg/g)**
0.72	0.20
2.12	0.38
2.92	0.84
7.12	1.14
9.65	2.01
45.01	2.75

Table D.2. Equilibrium data for zeolite sample at pH = 5.0, T = 25°C, 140 rpm, for contact time = 240 min, and adsorbent dosage = 5 g/250 ml

Equilibrium concentration (Ce) (mg/l)	**Equilibrium capacity (qe) (mg/g)**
1.32	0.17
2.52	0.35
3.17	0.80
7.02	1.13
10.03	1.96
48.08	2.60

Table D.3. Equilibrium data for zeolite sample at pH = 7.0, T = 25°C, 140 rpm, for contact time = 240 min, and adsorbent dosage = 5 g/250 ml

Equilibrium concentration (Ce) (mg/l)	**Equilibrium capacity (qe) (mg/g)**
1.43	0.15
4.08	0.28
3.51	0.78
8.26	1.06
8.97	2.02
51.10	2.45

Table D.4. Equilibrium data for zeolite sample at pH = 9.0, T = 25°C, 140 rpm, for contact time = 240 min, and adsorbent dosage = 5 g/250 ml

Equilibrium concentration (Ce) (mg/l)	**Equilibrium capacity (qe) (mg/g)**
1.25	0.18
3.83	0.29
3.56	0.77
8.85	1.02
12.27	1.85
57.04	2.15

Table D.5. Equilibrium data for zeolite sample at pH = 10.0, T = 25°C, 140 rpm, for contact time = 240 min, and adsorbent dosage = 5 g/250 ml

Equilibrium concentration (Ce) (mg/l)	**Equilibrium capacity (qe) (mg/g)**
1.26	0.17
3.90	0.29
3.93	0.74
9.01	1.04
18.12	1.59
59.68	2.02